Earth Flows: Morphology, Mobilization, and Movement

GEOLOGICAL SURVEY PROFESSIONAL PAPER 1264

Earth Flows: Morphology, Mobilization, and Movement

By DAVID K. KEEFER *and* ARVID M. JOHNSON

GEOLOGICAL SURVEY PROFESSIONAL PAPER 1264

A study of the factors controlling earth-flow occurrence and the velocity of an active earth flow

UNITED STATES GOVERNMENT PRINTING OFFICE, WASHINGTON : 1983

UNITED STATES DEPARTMENT OF THE INTERIOR

JAMES G. WATT, *Secretary*

GEOLOGICAL SURVEY

Dallas L. Peck, *Director*

Library of Congress Cataloging in Publication Data

Keefer, David Knight
Earth flows: Morphology, mobilization, and movement.

(Geological Survey professional paper 1264)
Bibliography: p. 53–56
Supt. of Docs. no.: I 19.16:1264
1. Earthflows. 2. Earthflows—California. I. Johnson, Arvid M. II. Title. III. Series: United States. Geological Survey. Professional Paper 1264.
QE599.A2K43 1983 551.3 83–600499

For sale by the Superintendent of Documents, U.S. Government Printing Office
Washington, D.C. 20402

CONTENTS

	Page
Abstract	1
Introduction	1
Previous studies	2
Classification and terminology	4
Acknowledgments	4
Earth-flow morphology, materials, and settings	5
Topography, climate, and geology in areas of earth-flow occurrence	5
San Francisco Bay region	5
Other regions	8
Morphology	8
Idealized earth-flow morphology	10
Subsurface features: Basal shear surfaces, lateral shear surfaces, and associated zones of deformation	13
Earth-flow complexes	16
Materials	17
The Davilla Hill earth-flow complex	22
Description	22
Location and setting	22
Morphology and history of movement	24
Material	27
Subsurface geometry	27
Studies of active earth flows and ground-water conditions, 1974-78	28
Surface displacements	28
Correlations of precipitation with mobilization and rate of movement	29
The Davilla Hill earth-flow complex—Continued	
Studies of active earth flows and ground-water conditions, 1974-78—Continued	
Subsurface displacements	29
Water levels	32
Water contents	32
Unit weights, void ratios, and saturation	33
Laboratory swell tests	33
Piezometric and tensiometric measurements, August 1975-February 1978	36
Analysis of mobilization	38
Measurement of shear-strength parameters, using direct-shear tests	39
Slope-stability analysis of earth flows	40
Discussion	41
A model for earth flow	41
Earth-flow mobilization	43
Model of a moving earth flow	43
Velocity measurements	43
Shear surfaces and adjacent zones of disturbance	46
Distribution of displacements	47
Surges	47
Velocity, boundary slip, and boundary roughness	48
Internal deformation	51
Composite model	51
Conclusions	52
References cited	53

ILLUSTRATIONS

[Plates are in pocket]

PLATE 1. Map showing earth-flow complexes in Eden Canyon and vicinity, Alameda County, California
2. Map and cross section showing the Hidden Valley earth-flow complex, Alameda County, California
3. Maps and cross section showing the Davilla Hill earth-flow complex, Alameda County, California

		Page
FIGURE	1. Location map of part of San Francisco Bay region	3
	2. Photographs of typical earth-flow deposits	5
	3. Bar graphs showing inclinations of slopes on which earth flows occur	6
	4. Block diagrams showing idealized earth flow	8
	5–7. Photographs showing:	
	5. Main scarps and crown cracks of earth-flow complexes	10
	6. Deposits in zones of depletion of earth flows	11
	7. Toe of earth-flow deposit in Bear Valley area	11
	8. Diagram showing cross-section through pressure ridge flanking earth flow at Kirkwood Creek, Mont.	11
	9. Photograph showing lateral ridge in earth flow at Melendy Ranch complex	12
	10. Block diagrams showing formation of lateral ridges	12
	11. Photograph of lateral ridge in earth-flow deposit in Cordelia, Calif., area	13
	12. Photograph of slickensided lateral shear surface on inner flank of lateral ridge at Melendy Ranch complex	13

Page

FIGURE 13. Diagram showing multiple basal shear surfaces underlying earth-flow toe at Beltinge, England ---- 13
14–16. Photographs showing:
14. Types of cracks disrupting earth flows ---- 14
15. Slickensided shear surfaces ---- 14
16. Lateral shear surfaces in zones of depletion of earth flows at Davilla Hill complex ---- 15
17. Block diagram and map of trench cut through earth-flow deposit in Cordelia, Calif., area ---- 15
18. Photograph of convoluted contact between materials in trench cut through earth-flow deposit in Cordelia, Calif., area ---- 15
19. Diagram showing earth-flow deposits exposed in wall of gully near Davilla Hill complex ---- 16
20. Photograph of earth-flow complexes occupying long narrow channels ---- 16
21. Aerial view of two earth-flow complexes in Cordelia, Calif., area ---- 16
22. Photograph of hummocky earth-flow complex near Pleasanton, Calif. ---- 17
23. Chart showing plasticity indexes and liquid limits of earth-flow materials ---- 22
24. Geologic map of Eden Canyon area, showing location of Davilla Hill earth-flow complex ---- 23
25. Chart showing daily precipitation in Eden Canyon, July 1974-February 1978 ---- 25
26. Photographs showing Davilla Hill earth-flow complex ---- 26
27–28. Graphs showing:
27. Cumulative displacements of survey stakes on earth flows ---- 30
28. Displacement of survey stakes on earth flows of Davilla Hill complex ---- 31
29. Photograph and graph showing measurement of subsurface displacements on earth flow 1 of Davilla Hill complex ---- 32
30–33. Graphs showing:
30. Water levels in boreholes ---- 33
31. Natural water contents in boreholes ---- 34
32. Natural water contents in pit 1 ---- 35
33. Piezometric measurements ---- 36
34. Sketch illustrating forces acting on block on inclined plane ---- 39
35. Graphs showing Mohr-Coulomb failure envelopes for direct-shear tests on samples from basal shear surface ---- 40
36. Graphs showing factors of safety as functions of water-table depths ---- 42
37. Graphs showing movement patterns of earth flows monitored with continuous-recording devices ---- 47
38. Diagram showing subsurface displacement profile of earth flow at Beltinge, England ---- 48
39. Graphs and diagrams showing surface-displacement profiles of earth flows ---- 50
40. Graph showing shear resistance as a function of velocity in direct-shear tests on basal-shear-surface material ---- 52

TABLES

Page

TABLE 1. Bedrock in areas containing abundant earth-flow deposits in the San Francisco Bay region ---- 7
2. Bedrock in areas containing abundant earth-flow deposits outside the San Francisco Bay region ---- 9
3. Composition of earth-flow materials ---- 18
4. Clay-mineral content of materials from the Davilla Hill earth-flow complex ---- 28
5. Unit weights, void ratios, and saturation of Davilla Hill earth-flow material ---- 35
6. Laboratory swell tests on Davilla Hill earth-flow material ---- 35
7. Earth-flow velocities ---- 44

EARTH FLOWS: MORPHOLOGY, MOBILIZATION, AND MOVEMENT

By DAVID K. KEEFER and ARVID M. JOHNSON

ABSTRACT

The terms "earthflow" and "earth flow" (after Varnes, 1978) have been applied by previous investigators to several mass-movement phenomena involving fine soils. In this report we describe studies on one type of earth flow—a type characterized by movement at velocities of a few meters or less per day that persists for several days, months, or years. These studies were conducted to determine what morphologic and material properties characterize earth flows of this type, to analyze how such earth flows are mobilized, and to determine what mechanisms control their movement.

During our studies, we examined numerous earth flows and earth-flow deposits in the Coast Ranges of central California; monitored earth-flow movements at three sites; and conducted detailed field, laboratory, and analytical studies at one site—Davilla Hill, near Hayward, Calif. Using information from these studies and from published descriptions of other earth flows, we analyze earth-flow mobilization and propose a model to explain what controls the velocity of an active earth flow.

Our studies show that earth flows are commonly tongue or teardrop shaped. They have rounded, bulging toes and sinusoidal longitudinal profiles, concave upward near the head of the earth flow and convex upward near the toe. Many earth flows are flanked by lateral ridges composed of immobile earth-flow material. Earth flows are bounded by discrete slickensided shear surfaces. Materials in earth flows consist primarily of silt and (or) clay and smaller amounts of sand-size and larger particles; these materials are pervasively fissured and contain a significant amount of entrained water.

At some sites, earth-flow deposits blanket areas of several square kilometers. These large masses of earth-flow material are rarely deposited by a single episode of movement but, rather, are complexes built up over several years by many individual earth flows. Earth flows making up these complexes are mobilized out of older earth-flow material, out of material previously deposited by other types of mass movement, or out of material not previously disturbed by mass movements.

We studied the earth-flow process over a 4-year period at Davilla Hill. Mapping of earth-flow features and monitoring of active earth flows showed that the Davilla Hill earth-flow complex is made up of at least 34 individual earth-flow deposits. The earth flows active during the study period were formed out of older earth-flow material. When active, these earth flows moved several centimeters per day, and most movement took place by shearing along boundary shear surfaces. The earth flows were mobilized by increases in pore-water pressure caused by infiltration of water into the soil during and after rainstorms. Mobilization was accompanied by softening of the material and by an increase in water content due to saturation; no significant volume change or remolding of the material occurred.

Analyses of earth flows elsewhere show that they also are generally mobilized by increases in pore-water pressure. Although short high-velocity surges occur on some earth flows, most are characterized by persistent movement at velocities ranging from less than a millimeter to several meters per day. Most movement takes place by displacement on or immediately adjacent to the boundary shear surfaces. We conclude that the general absence of sustained acceleration in earth flows is due to boundary roughness. Factors controlling earth-flow velocity are: pore-water pressure, the characteristics of asperities on the shear surfaces, and the properties of material on and adjacent to the shear surfaces.

INTRODUCTION

Earth flows are among the most common mass-movement phenomena in nature; they occur in many of the world's hilly and mountainous areas. In parts of the California Coast Ranges near San Francisco Bay, where our field studies were carried out, thousands of earth flows and earth-flow deposits[1] are present: they are identified by dish-shaped scars, by bulging toes, and by long narrow tongue- or teardrop-shaped forms. Some features, such as bulging toes and smooth surface profiles, suggest that earth-flow movement involves a component of fluidlike flow; other features, however, such as slickensided shear surfaces, suggest that earth flows behave more like rigid bodies that move by boundary shear.

Earth-flow activity has been recognized as a distinctive type of mass movement since at least the early 20th century (Howe, 1909; Blackwelder, 1912). Since then, numerous individual earth flows have been described, and detailed investigations have been carried out on a few. Using data from these descriptions and investigations and from our own field and laboratory studies, we have analyzed several aspects of the earth-flow process. In this report we discuss our studies, undertaken to answer the following questions: What morphologic features and material properties characterize earth flows? How are earth flows mobilized? What causes them to stop moving? At what velocities and how

[1]In this report, the term "earth flow" refers to a moving body of earth and water; once movement has stopped, the material displaced by an earth flow is called an "earth-flow deposit."

long do earth flows move? What are the patterns of internal deformation within moving earth flows? What factors control their velocities?

Our investigation was conducted in three stages. At the outset, we identified areas in the San Francisco Bay region of California that contain abundant earth-flow deposits, from reconnaissance in a small airplane (fig. 1). We examined several tens of earth-flow deposits on the ground in those areas to identify the morphologic features, material properties, and topographic and geologic settings characteristic of these deposits. We then combined information from these field studies with information from published studies to formulate a general description of earth-flow morphology, materials, and settings.

During the second stage of our investigation, we monitored movement of earth flows at three sites—Melendy Ranch, Cycle Park, and Davilla Hill (fig. 1)—and conducted more detailed field, laboratory, and analytical studies of the earth flows at Davilla Hill. These more detailed studies included: mapping of morphologic features; augering and subsurface sampling; measurements of ground-water level, pore-water pressure, shear strength and other material properties, and rates and distribution of movement; and slope-stability analyses of mobilization.

In the third stage of the investigation, we formulated general models to explain earth-flow mobilization and the observed velocities and displacement distributions in earth flows.

PREVIOUS STUDIES

Previous investigations include descriptions of numerous earth flows and earth-flow deposits, measurements of displacement on several earth flows, and analyses of mobilization of a few earth flows.

In the San Francisco Bay region, Krauskopf and others (1939) described the geologic setting, movement, and morphology of an earth flow in the Lomerias Muertas area (fig. 1). Other earth flows and earth-flow deposits in part of the Lomerias Muertas area were mapped and described by Oberste-Lehn (1976), who also measured displacement of one earth flow. Radbruch and Weiler (1963) mapped and described earth-flow deposits and tabulated the angles of slopes on which earth flows occurred in several square kilometers of the central Orinda, Calif., area (fig. 1); a similar study was conducted by Turnbull (1976) in an area of about 6 km^2 around Davilla Hill (pl. 1; fig. 1). Nilsen and Turner (1975) studied the relations between landslide occurrence, amount and temporal distribution of precipitation, and position of old landslide deposits in a region that included part of the Orinda area. Earth-flow complexes near Davilla Hill were mapped by Aboim-Costa and Stein (1976) (pl. 2) and Spain and Upp (1976). Ellen and others (1979) and Peterson (1979) discussed the relation between soil and bedrock type and earth-flow occurrence in part of the Hicks Valley area (fig. 1). Our investigation was previously discussed in the reports by Keefer (1976, 1977a, b, c) and Keefer and Johnson (1978).

Earth flows are also abundant in parts of the Coast Ranges north of the San Francisco Bay region. Cooksley (1964) described the morphology and geologic setting of one earth-flow complex[2] near the Eel River. Kelsey (1977, 1978) described earth flows and monitored movement on one earth-flow complex along the Van Duzen River. Descriptions of and movement data on several earth flows in the Redwood Creek basin are included in the reports by Harden and others (1978), Nolan and others (1979), and Janda and others (1980).

Swanson and James (1975), Swanson and Swanston (1977), and Swanson and others (1980) described and measured movement and ground-water level on an earth-flow complex in the western Cascade Range of Oregon. Earth-flow movements in the Oregon Coast Ranges and the Cascade Range were also discussed by Swanston (1980).

A regional study of earth-flow occurrence in several thousand square kilometers of northwestern Wyoming and adjacent areas of Idaho and Montana was presented by Bailey (1972). Individual earth-flow complexes in this region were described by Blackwelder (1912), Waldrop and Hyden (1962), Hadley (1964), Fraser and others (1969), and Bailey (1972). Blackwelder's description of the Gros Ventre earth-flow complex in this region is one of the earliest and clearest in the literature; this earth-flow complex was used by Sharpe (1938) as a type example of the earth-flow process.

Elsewhere in the United States, earth flows in western Pennsylvania, West Virginia, eastern Kentucky, and eastern Ohio were described by Sharpe and Dosch (1942). The Slumgullion earth-flow complex in Colorado was described by Howe (1909) and Crandell and Varnes (1961); Crandell and Varnes (1961) also monitored movement there. Two other earth-flow complexes in Colorado were described by Varnes (1949).

Outside the United States, earth-flow complexes have been described at sites in New Zealand (Benson, 1940), England (Ward, 1948; Hutchinson and Bhandari, 1971; Barton, 1973; Hawkins, 1973; Brunsden and Jones, 1976; Bromhead, 1978), the islands of Barbados (Prior and Ho, 1972) and Vestspitzbergen (Chandler, 1972),

[2]An "earth-flow complex" contains several earth-flow deposits and associated features; it may also contain one or more active earth flows.

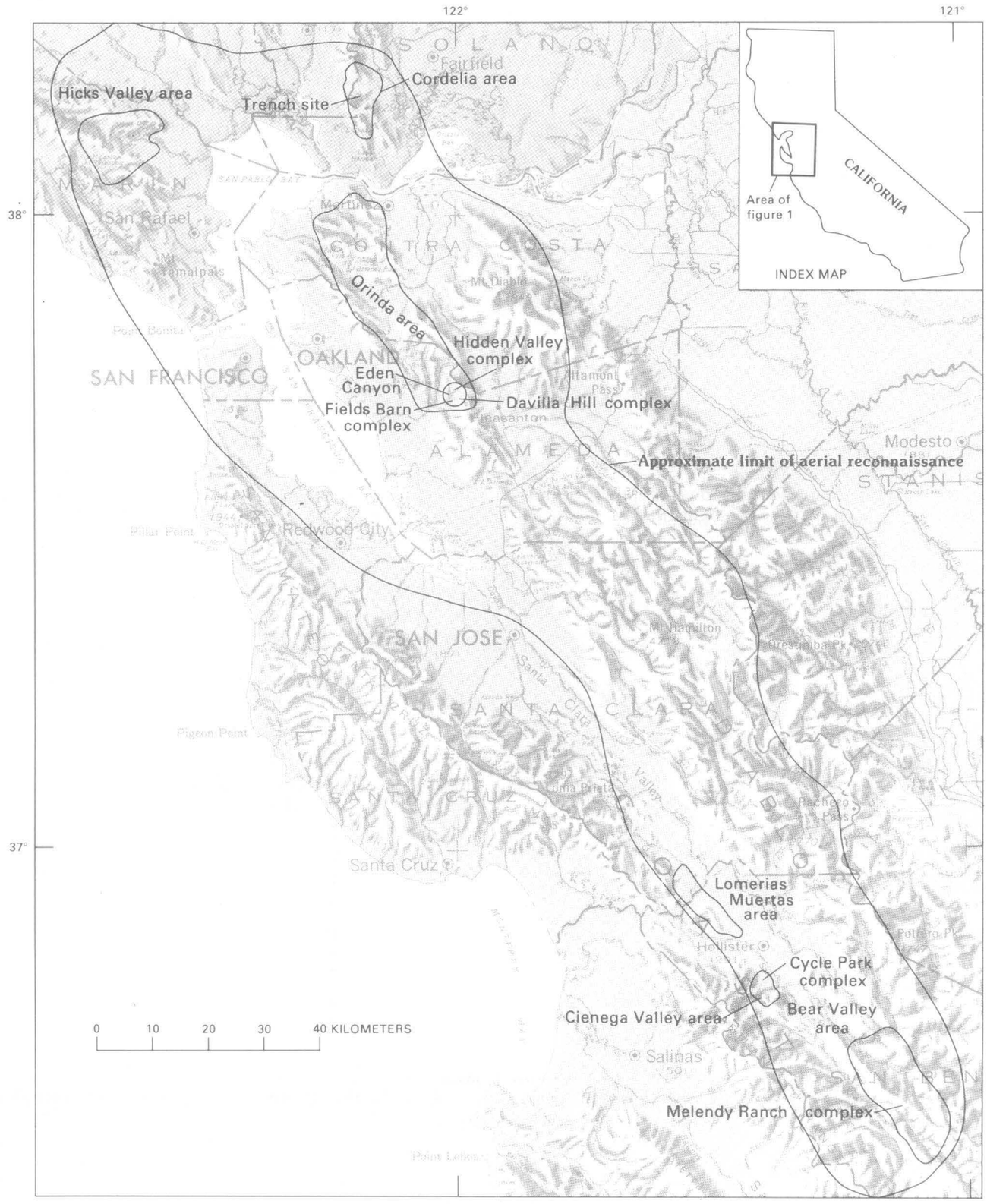

FIGURE 1.—San Francisco Bay region, showing limit of aerial reconnaissance, areas where earth-flow deposits are abundant, and sites discussed in text. Base from U.S. Geological Survey, 1971, California Shaded Relief Map, scale 1:1,000,000.

Australia (Pilgrim and Conacher, 1974; Dunkerley, 1976), Czechoslovakia (Fussgänger and Jadroň, 1977), and Scandinavia (Rapp, 1960; Prior, 1977). Descriptions and movement data have been reported for earth flows in the Panama Canal Zone (Cross, 1924), New Zealand (Campbell, 1966), the U.S.S.R. (Ter-Stepanian, 1967; Ter-Stepanian and Ter-Stepanian, 1971), England, Japan, and Switzerland (Skempton and Hutchinson, 1969), and Czechoslovakia (Záruba and Mencl, 1969). Hutchinson and Bhandari (1971), Chandler (1972), Dunkerley (1976), Fussgänger and Jadroň (1977), and Prior (1977) performed slope-stability analyses of earth-flow mobilization.

In addition to these studies, comprehensive site studies of earth flows have been carried out at Beltinge, England (Hutchinson, 1970), and Minnis North, northern Ireland (Prior and others, 1968, 1971; Prior and Stephens, 1971, 1972; Hutchinson and others, 1974). These studies included descriptions of morphology, monitoring of movement, measurement of several material properties and of ground-water level or pore-water pressure, and analyses of mobilization.

CLASSIFICATION AND TERMINOLOGY

The term "earth flow," as used in this report, refers to the "drier and slower" type of earth flow described in the mass-movement classification of Varnes (1978, p. 19-20, fig. 2.lr3). This type of mass movement is called "earthflow" in the classification of Sharpe (1938) and "slow earthflow" in the classification of Varnes (1958). Most other previous investigators in North America have applied the term "earthflow" to this type of mass movement; the term "earthflow" was used in our previous reports (Keefer, 1976, 1977a, b, c; Keefer and Johnson, 1978).

Our definition of the term "earth flow" encompasses both "earthflows" and "mudflows" as defined in the mass-movement classification of Skempton and Hutchinson (1969), which has been widely used in the United Kingdom.[3] In more recent publications in the United Kingdom (Chandler, 1972; Hutchinson and others, 1974; Bromhead, 1978), the term "mudslide" has been used for the type of mass movement discussed in our report.

Some semantic confusion in the use of the unmodified term "earthflow" stems from Sharpe's (1938) use of the term to refer to two different types of mass movement. Our use of "earth flow" refers to the slower moving type described by Sharpe (1938, p. 53-55) and illustrated by the Gros Ventre earth-flow complex of Blackwelder (1912). The other type of mass movement (Sharpe, 1938, p. 50-53) commonly takes place in glacial sediment and involves very rapidly moving bodies of liquefied material. In more recent classifications, this type of mass movement has been called "rapid earthflow" (Varnes, 1958), "rapid earth flow" or "quick clay flow" (Varnes, 1978, p. 19, fig. 2.lr2), or "retrogressive quick clay sliding" (Skempton and Hutchinson, 1969).

"Debris flow" is another kind of mass movement commonly confused with earth flow. A debris flow, however, differs from an earth flow in several respects. In a debris flow, granular soils that generally are admixed with only small amounts of clay, entrained water, and air are mobilized into materials that move very rapidly on gentle slopes. Debris flows are not bounded by discrete shear surfaces, and most movement takes place by distributed internal shear. Debris-flow material is coarser grained than earth-flow material. In addition, debris-flow deposits generally form during a single episode of activity, so that, within a few minutes or hours, a typical debris flow mobilizes, flows through a channel to the surface of an alluvial fan, forms a deposit, and dries. Such deposits are rarely remobilized. More detailed descriptions of the debris-flow process were given by Johnson (1965, 1970).

In our report, the term "soil" refers to any uncemented or poorly cemented aggregate of mineral grains, with or without organic constituents. This usage conforms to the definitions of Peck and others (1974) and Varnes (1978). Following the definitions of Varnes (1978), "earth" is soil in which 80 percent or more of the grains are smaller than 2 mm in diameter, and "debris" is soil in which 20 to 80 percent of the grains are larger than 2 mm in diameter.

ACKNOWLEDGMENTS

This work was funded by the U.S. Geological Survey and was carried out in cooperation with Stanford University, Stanford, Calif.; we gratefully acknowledge the assistance of numerous people from both institutions. In particular, Edwin L. Harp of the U.S. Geological Survey aided in many aspects of the research, including the initial fieldwork and modification of some field and laboratory equipment. Deane Oberste-Lehn, Richard Turnbull, and Douglas Yadon, all formerly of Stanford University, showed us many interesting earthflow deposits in the field, and Douglas Yadon made arrangements for digging the trench in the Cordelia, Calif., area. Clay-mineral determinations were made by John Sarmiento, and Atterberg-limit and grain-size determinations were made by John Sarmiento, Michael Bennett, and Joseph Heffern, all of the U.S. Geological Survey. The manuscript was read by G. Wayne Clough,

[3]The distinction between "earthflow" and "mudflow," as defined by Skempton and Hutchinson (1969), is based on the amount of internal disruption: mudflows are more disrupted than earthflows.

Bernard Hallet, Richard H. Jahns, and Ernest I. Rich of Stanford University and by Robert W. Fleming, Edwin L. Harp, and David J. Varnes of the U.S. Geological Survey; their reviews and constructive criticisms led to numerous improvements. Seena N. Hoose, Gerald F. Wieczorek, Raymond C. Wilson, and T. Leslie Youd, all of the U.S. Geological Survey, provided helpful insights during many stimulating discussions.

Ralph Azevedo, Charlotte Berberick, Mr. and Mrs. Perry Davilla, Mr. and Mrs. A. A. Fields, the Paul Hudner family, and Carl Leberer kindly gave permission for field studies on their land; without their generous cooperation this work would not have been possible. We are particularly indebted to Mr. and Mrs. Perry Davilla and Mr. and Mrs. A. A. Fields for permission to conduct extensive studies on their property, and to Mr. and Mrs. A. A. Fields for providing records from their rain gage.

We especially thank Karen H. Keefer, who assisted with the fieldwork on numerous occasions, drafted most of the original figures, and contributed many helpful suggestions and insights.

EARTH-FLOW MORPHOLOGY, MATERIALS, AND SETTINGS

In parts of the California Coast Ranges near San Francisco Bay the hillsides are dotted by thousands of earth-flow deposits (fig. 2). Similar earth-flow deposits occur in many parts of the world, and, in some regions, earth flow is the dominant mass-movement process (Radbruch and Weiler, 1963; Bailey, 1972; Dunkerley, 1976; Turnbull, 1976).

TOPOGRAPHY, CLIMATE, AND GEOLOGY IN AREAS OF EARTH-FLOW OCCURRENCE

SAN FRANCISCO BAY REGION

In the San Francisco Bay region, earth flows occur within a belt of northwest-southeast-trending mountain ranges collectively called the "California Coast Ranges." Topography in these mountains ranges from gently rolling hills to steep rugged ridges separated by narrow canyons; elevations range from sea level to about 1,200 m.

Within the Coast Ranges, we identify six areas where earth-flow deposits are abundant (fig. 1). In these areas, the topography is characterized by rolling hills or by ridges with broad rounded crests and moderately steep flanks. Earth flows in these areas commonly come to rest on or at the bases of the hillsides or ridges; few travel more than a few meters on the gentle valley floors. Many earth flows come to rest part way down apparently uniform slopes.

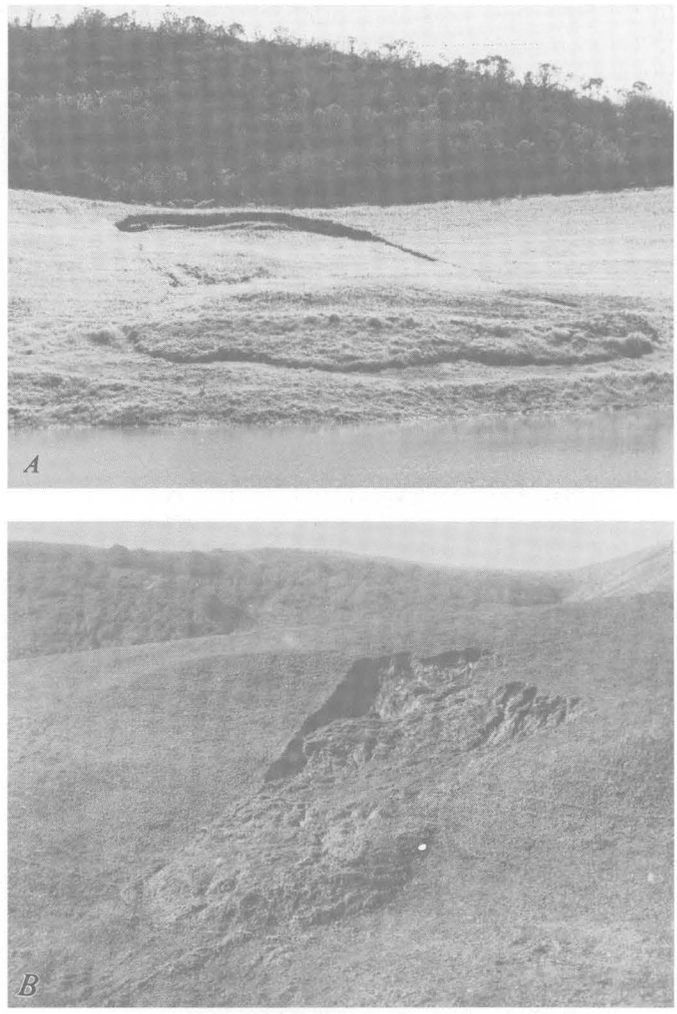

FIGURE 2.—Typical earth-flow deposits. *A*, Near La Honda, Calif. Photograph by G. F. Wieczorek, U.S. Geological Survey. *B*, Near Berkeley, Calif. Photograph by G. K. Gilbert, U.S. Geological Survey.

Inclinations of the slopes on which earth flows occur have been systematically measured in two parts of the Orinda, Calif., area (fig. 1). In the central Orinda area, earth flows occur only on slopes of 10° or steeper, and 99 percent of all earth-flow complexes are on slopes of 15° or steeper (fig. 3A). In the area around Davilla Hill, earth flows occur only on slopes of 8° or steeper, 99 percent of earth-flow complexes are on slopes of 12° or steeper (fig. 3B), and all earth-flow complexes on slopes of less than 14° are associated with such locally steep slopes as roadcuts, gully walls, or streambanks (Turnbull, 1976). Although systematic studies of slope inclination have not been carried out elsewhere in the San Francisco Bay region, the slopes in the other five areas with abundant earth flows appear to be comparable to those in the Orinda area.

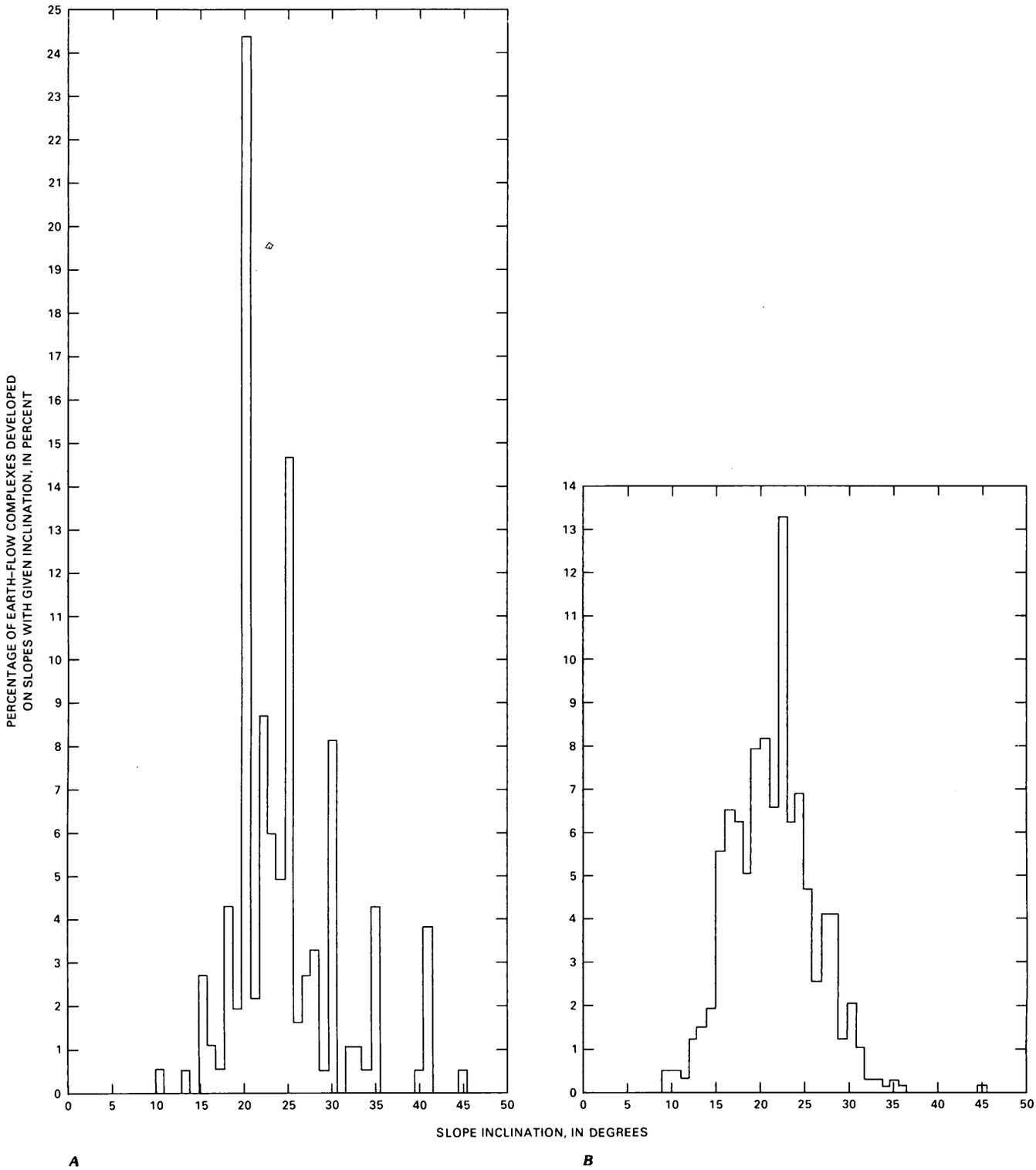

FIGURE 3.—Inclinations of slopes on which earth flows occur. Locations of areas shown in figure 1. *A*, Central Orinda, Calif., area. Total number of earth-flow complexes included in study, 185. Data from Radbruch and Weiler (1963). *B*, Eden Canyon and vicinity. Total number of earth-flow complexes included in study, 582. Data from Turnbull (1976).

The San Francisco Bay region has a Mediterranean-type climate with warm dry summers and cool rainy winters. Annual precipitation varies greatly from place to place; in the six areas containing abundant earth-flow deposits, average annual precipitation ranges from 36 cm (in parts of the Bear Valley area) to 101 cm (in parts of the Hicks Valley area) (Rantz, 1971). Nearly all precipitation falls as rain in the months October through April, when storms generated over the Pacific Ocean pass through the region; the amount and distribution of precipitation during any given year depend on the number and intensity of these storms. Thus, the annual precipitation at any one place also varies considerably from year to year. For example, in the 125-year period from 1851 to 1976, annual precipitation in downtown San Francisco ranged from 18 to 125 cm (San Francisco Chronicle, 1976, p. 1). Severe storms can drop a large proportion of the average annual precipitation within a few hours or days. Temperatures in the San Francisco Bay region rarely fall below freezing, and snow accounts for a negligible amount of the total precipitation.

In the San Francisco Bay region, most or all earth flows move only during the rainy, winter months; most earth flows are mobilized during winters having above-average precipitation; and earth flows are especially common after severe, late-winter rains (Radbruch and Weiler, 1963; Nilson and Turner, 1975; Oberste-Lehn, 1976; Turnbull, 1976; Keefer, 1977a). During the warm dry summers in the San Francisco Bay region, most hillside materials, including earth-flow deposits, are thoroughly desiccated.

Table 1 lists bedrock types in the six areas containing abundant earth-flow deposits. Five of these six areas are underlain primarily by poorly consolidated Tertiary shale, mudstone, sandstone, and conglomerate. Parts of the Hicks Valley area (fig. 1) are underlain by heterogeneous tectonic melange with a matrix of highly sheared shale; other parts of this area are underlain by relatively unsheared sandstone and shale or by blueschist-facies metamorphic rocks.

Within each of these six areas, both the abundance of earth-flow deposits and the bedrock lithology vary. Detailed mapping in parts of the Orinda area (Radbruch and Weiler, 1963; Turnbull, 1976), the Lomerias Muertas area (Oberste-Lehn, 1976), the Cordelia area (Douglas Yadon, unpub. data, 1976) and the Hicks Valley area

TABLE 1.—*Bedrock in areas containing abundant earth-flow deposits in the San Francisco Bay region*

[See figure 1 for locations]

Area	Bedrock	Reference
Orinda----------	Orinda Formation (Miocene): Freshwater conglomerate, sandstone, siltstone, and shale containing minor amounts of volcanic tuff, limestone, and lignite. All the rocks are soft, poorly consolidated, and closely jointed; all the clastic rocks have a clay matrix.	Ham (1952), Hall (1956), Robinson (1956), Radbruch and Weiler (1963), Turnbull (1976).
Cordelia----------	Kreyenhagen Formation (Eocene): Silty clay-shale and poorly consolidated micaceous feldspathic sandstone.	Sims and others (1973), Douglas Yadon (unpub. data, 1976).
	Unnamed formation (Jurassic or Cretaceous): Mudstone and shale containing minor amounts of conglomerate and sandstone.	
Bear Valley-------	Etchegoin group (Miocene and Pliocene): Poorly consolidated conglomerate, sandstone, siltstone, and shale.	Wilson (1943).
	Serpentinite (Jurassic or younger): Green, bluish-green, and bluish-gray; pervasively sheared.	
Cienega Valley----	Etchegoin Formation (Miocene and Pliocene): Thick-bedded sandstone containing minor amounts of micaceous siltstone, brackish-marine and marine.	Dibblee (1975).
	Nonmarine sedimentary rocks (Pliocene): Claystone, siltstone, and interbedded friable sandstone.	
Lomerias Muertas--	Purisima(?) Formation (Pliocene): Shale, claystone, siltstone, and friable sandstone containing minor amounts of conglomerate and tuff.	Oberste-Lehn (1976).
Hicks Valley------	Franciscan assemblage (Jurassic and Cretaceous): Blueschist-facies metamorphic rocks; tectonic melange with matrix of pervasively sheared shale and sandstone; relatively unsheared shale and sandstone. Earth-flow deposits are most abundant in clayey soils developed on melange.	Blake and others (1974), Ellen and others (1979), Peterson (1979).

(Ellen and others, 1979; Peterson, 1979) showed that most earth flows occur where the bedrock contains a large proportion of clay.

OTHER REGIONS

In two areas outside the San Francisco Bay region, the minimum inclinations of slopes on which earth flows occur are rather low. In the Gros Ventre Mountains of Wyoming, the minimum inclination is 2° (Bailey, 1972); along the coast of southeastern England, the minimum inclination is 4° (Hutchinson and Bhandari, 1971). Elsewhere, slopes on which earth flows occur were reported to range from 6° (Hadley, 1964) to 35° (Harden and others, 1978). Minimum slope inclinations have been determined from systematic studies in two areas: in the Redwood Creek basin in northern California, where the minimum inclination is 9° (Harden and others, 1978); and in the Razorback Range in Australia, where the minimum inclination is 10° (Dunkerley, 1976). Thus, the inclinations of slopes on which earth flows occur in most other areas are comparable to those in the San Francisco Bay region.

Earth flows occur in areas where precipitation or ground-water flow is sufficient to saturate surficial hillside materials at least intermittently. Previous studies have shown that earth flows mobilize during periods of high precipitation (Campbell, 1966; Prior and Stephens, 1972; Hutchinson and others, 1974; Harden and others, 1978; Swanson and others, 1980) or during periods with a surplus of precipitation over evapotranspiration (Hutchinson, 1970).

Outside the San Francisco Bay area, earth flows also occur in areas where the bedrock contains a large proportion of clay. Bedrock types in areas of earth-flow occurrence include stiff fissured clays, flysch, altered and weathered volcanic rocks, tectonic melange, glacial till, and poorly consolidated shale, mudstone, and sandstone (table 2).

MORPHOLOGY

Figures 4*A* and 4*B* illustrate an idealized earth flow, a model synthesized from our field observations

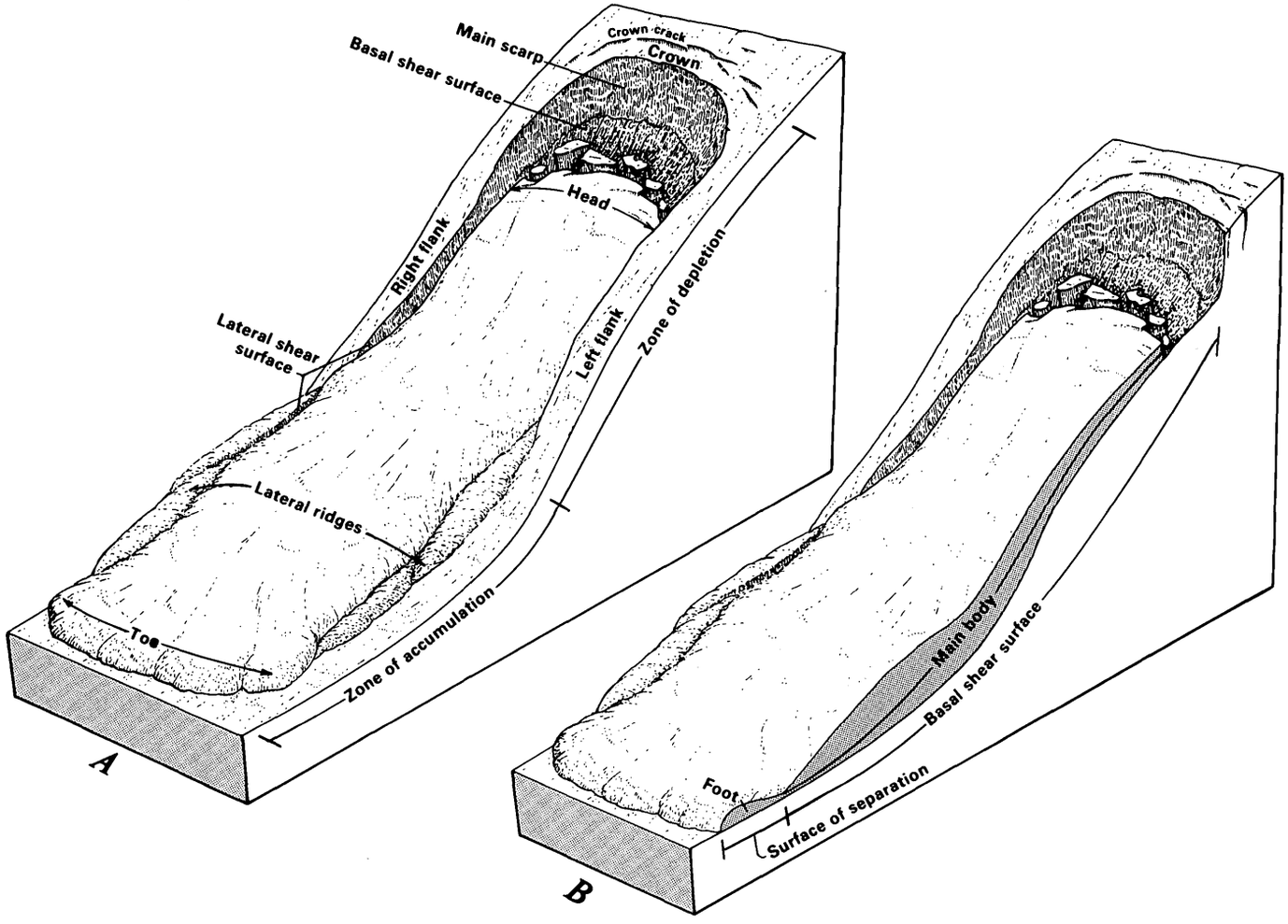

FIGURE 4.—Idealized earth flows, showing features described in text. *A*, Surface features. *B*, Subsurface features.

TABLE 2.—*Bedrock in areas containing abundant earth-flow deposits outside the San Francisco Bay region*

Area	Bedrock	Reference
Redwood Creek basin, northern California.	Franciscan assemblage (upper Mesozoic): Unmetamorphosed argillaceous rocks and slightly metamorphosed highly sheared sedimentary rocks.	Harden and others (1978).
Van Duzen River basin, northern California.	Franciscan melange (Mesozoic and early Cenozoic): Highly sheared clayey siltstone.	Kelsey (1977).
Eel River basin, northern California.	Franciscan Group of Cooksley (1964) (upper Mesozoic): Interbedded black shale, graywacke, and conglomerate; folded, faulted, and locally intruded by serpentinite; deeply weathered to abundant clay.	Cooksley (1964).
Western Cascade Range, Oregon.	Volcaniclastic rocks, lava flows, ash flows, and intrusive rocks (Tertiary), highly altered to form clay and saprolite; earth flows are particularly common where soft volcaniclastic rocks are capped by harder lava flows and (or) ash flows.	Swanson and James (1975), Swanson and Swanston (1977), Swanson and others (1980).
Northwestern Wyoming and adjacent parts of Montana and Idaho.	Soft shale and claystone (upper Mesozoic to Eocene) with interbedded sandstone and siltstone containing minor amounts of conglomerate, limestone, and coal; much of the shale and claystone is highly plastic and bentonitic. Glacial till (Quaternary)	Bailey (1972).
Gardiner area, Montana.	Dacite breccia (Eocene) containing abundant highly plastic bentonite---------- Landslide Creek Formation (Upper Cretaceous): Conglomeratic sandstone interbedded with bentonitic mudstone and claystone.	Fraser and others (1969).
Upper Ohio River Valley; Ohio, West Virginia, Pennsylvania, and Kentucky.	Clay, clay-shale, and coal (Pennsylvanian and Permian): Earth flows are particularly abundant where rock creep has formed impermeable layers with dips parallel to slopes; many earth flows form at sags in impermeable layers.	Sharpe and Dosch (1942).
Barbados----------	Shale, mudstone, and sandstone (Tertiary)----------	Prior and Ho (1972).
Panama Canal Zone.	Cucaracha Formation (early Miocene): Sandy claystone, very poorly cemented and very closely fractured, deeply weathered to soil containing abundant kaolin, mica, chlorite, and iron oxides; rock disintegrates after oven drying at 100°C and reexposure to water.	National Academy of Sciences (1924).
Dunedin district, New Zealand.	Abbotsford mudstone (Cretaceous): Glauconitic mudstone----------	Benson (1940).
Razorback Range, Australia.	Wianamatta Group (Triassic): Shale interbedded with lithic sandstone----------	Dunkerley (1976).
Antrim coast, northern Ireland.	Decomposed claystone, chalk, basalt, marl (Triassic), and glacial till (Quaternary): Earth flows occur only where Triassic strata dip steeply inland owing to disturbance by rotational slumping; steep dip allows ground water to percolate along bedding planes.	Prior and others (1968).
Coastal cliffs in southeastern England.	London clay (Eocene), Barton clay (Eocene), and Hamstead beds (Oligocene): Stiff fissured overconsolidated clay with interbedded silt and fine sand.	Ward (1948), Hutchinson (1970), Hutchinson and Bhandari (1971), Barton (1973), Bromhead (1978).
Coastal cliffs in Denmark.	Mo clay and Lille Baelt clay (Eocene): Stiff fissured overconsolidated clay containing some volcanic tuff and diatomaceous beds.	Prior (1977).
Okoličné area, Czechoslovakia	Flyschoid strata of Zakopane facies (Paleogene): Claystone containing lesser amounts of sandstone; earth flows form where confined aquifers occur.	Fussgänger and Jadrǒn (1977).
Carpathian Mountains, Czechoslovakia.	Soft tectonically disturbed flysch, sandstone, and pelitic and argillaceous shale (Paleogene). Tuff, agglomerate, coal, and poorly consolidated clay, silt, sand, and gravel (Neogene).	Záruba and Mencl (1969).

and from descriptions by other investigators. The model shows the characteristic features of earth-flow morphology; examples of these features are shown in figures 5 through 19. Not all earth flows contain every feature in this model. Individual earth flows may also differ from the model in shape: some have irregular boundaries that conform to the local topography. Earth flows range in size from bodies a few meters long, a few meters wide, and less than 1 m deep to bodies more than 1 km long, several hundred meters wide, and more than 10 m deep. Many earth flows also occur as parts of larger earth-flow complexes.

IDEALIZED EARTH-FLOW MORPHOLOGY

On the hillside above an earth flow, a *main scarp* and a zone of *crown cracks* mark the upslope boundary of the area disturbed by mass movement. The crown cracks break the earth in the *crown* region into blocks (fig. 5*A*, *B*); from time to time, blocks become detached and fall, slide, or slump down the main scarp. The main scarp is steep; it is linear (fig. 5*B*) or arcuate (fig. 5*C*) in plan view. Main scarps associated with some large earth flows are higher than 100 m. The main scarp bounds a natural amphitheatre, called the *zone of depletion*. The zone of depletion comprises the *head* and proximal part of an earth flow as well as deposits of blocks that have become detached from the crown. In some zones of depletion, these deposits are slices of earth that have slid on curved failure surfaces and rotated backward to form slump deposits (figs. 5*C*, 6*A*); in other zones of depletion, the deposits are irregular blocks that result from earth falls or earth block slides[4] (fig. 6*B*). Still other zones of depletion are relatively free of fall, slide, or slump deposits. The head of an earth flow can be adjacent to the main scarp or at some distance downslope, in which case part of the *basal shear surface* is exposed on the floor of the zone of depletion.

An earth flow itself is tongue or teardrop shaped (fig. 2). The length of an earth flow, measured from head to *toe*, is greater than its width, measured from *flank* to flank; and its width is greater than its depth. The flanks are parallel or diverge slightly downslope. The average surface slope of an earth flow is gentler than the slope of the adjacent, undisturbed part of the hillside. In the zone of depletion, the earth-flow surface is at a lower elevation than the ground on either flank. Farther downslope, in the *zone of accumulation*, the surface of an earth flow bulges above the undisturbed ground on either flank. The distal margin of an earth flow is a rounded, bulging toe (fig. 7).

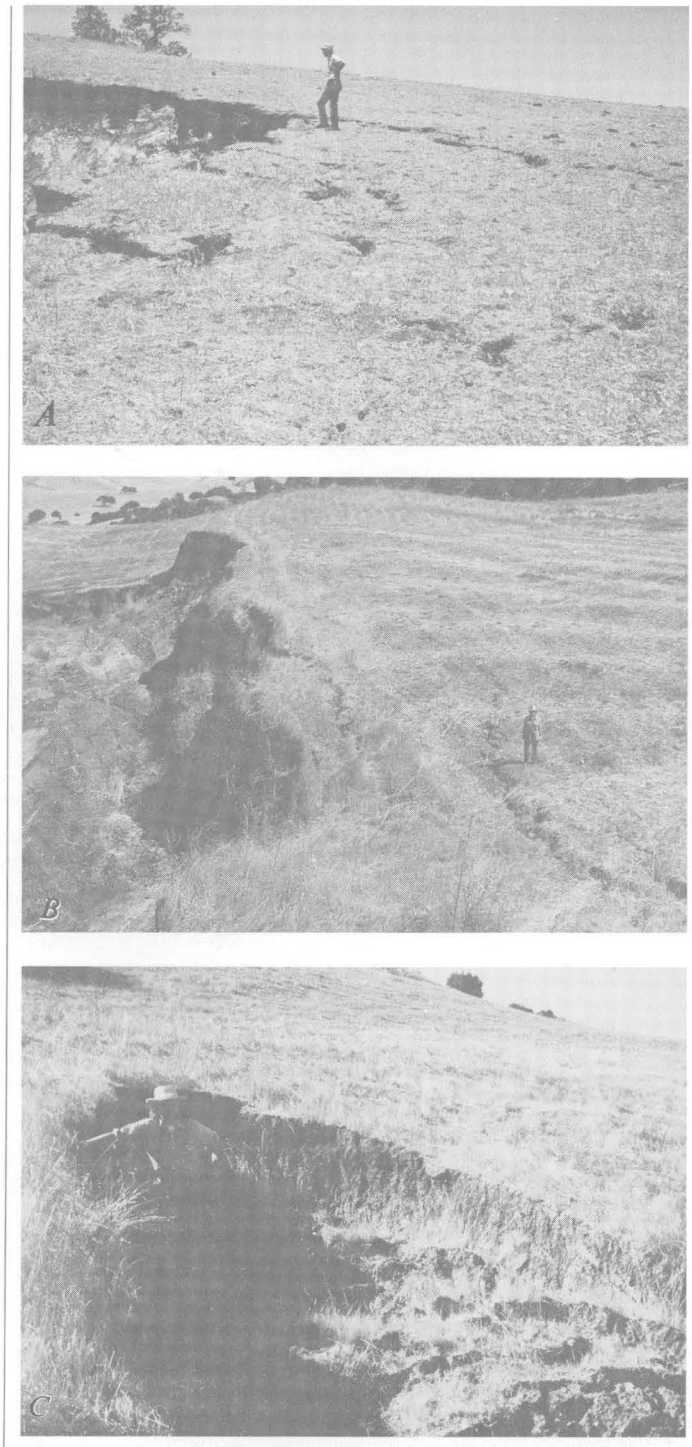

FIGURE 5.—Main scarps and crown cracks of earth-flow complexes. Crown cracks break earth upslope from crown into angular blocks. From time to time, blocks become detached and fall, slide, or slump from crown, so that scarp retreats upslope. *A*, Crown cracks adjacent to main scarp (upper left) of earth-flow complex in Bear Valley area. *B*, Linear main scarp and crown cracks of earth-flow complex in Bear Valley area. *C*, Arcuate main scarp of earth-flow deposit near Fields Barn complex. In zone of depletion at base of scarp are several blocks of earth that have slumped from main scarp. Photograph by E. L. Harp, U.S. Geological Survey.

[4]In *earth falls*, grains or coherent blocks of earth descend slopes by free fall, bounding, leaping, or rolling. In *earth block slides*, blocks of earth move downslope translationally along distinct failure surfaces.

FIGURE 6.—Deposits in zones of depletion of earth flows. *A*, Slump deposits in complex in Bear Valley area. *B*, Small sod-covered blocks are deposits of earth block slides in Fields Barn complex.

FIGURE 7.—Toe of earth-flow deposit in Bear Valley area. In plan view, toe is rounded and curved concave sourceward; in profile, toe has steep frontal slope. Toe has overriden former ground surface and is underlain by a surface of separation. Field notebook on toe is 22 by 30 cm.

In longitudinal profile, an earth flow is concave upward in the zone of depletion and convex upward in the zone of accumulation; in overall profile it resembles a single sinusoidal wave. On some earth flows, this concavity and convexity are so pronounced that a closed topographic depression is formed near the head; on other earth flows, the longitudinal profile is nearly linear except for a steepening of slope associated with the toe. Small local irregularities may be superimposed on this profile, but the sinusoidal form itself appears to be nearly universal among earth flows. The near-universality of this form indicates that it is not due to local site conditions but is characteristic of earth-flow movement. The sinusoidal profile probably results from thinning of the earth flow near the head and thickening near the toe during movement.

In the zone of accumulation, an earth flow is flanked by lateral ridges that form in three different ways. One type of lateral ridge is pushed up as a pressure ridge (fig. 8); these pressure ridges have slickensided shear surfaces on their outer flanks. A second type of lateral ridge forms by overflow of earth-flow material onto the adjacent ground surface (fig. 9). Ridges of a third type form where a toe overrides the former ground surface and the earth flow then stops moving, forming an earth-flow deposit. If a later earth flow remobilizes part of this deposit, some material adjacent to the flanks may be left in place and form lateral ridges (figs. 10, 11). Lateral

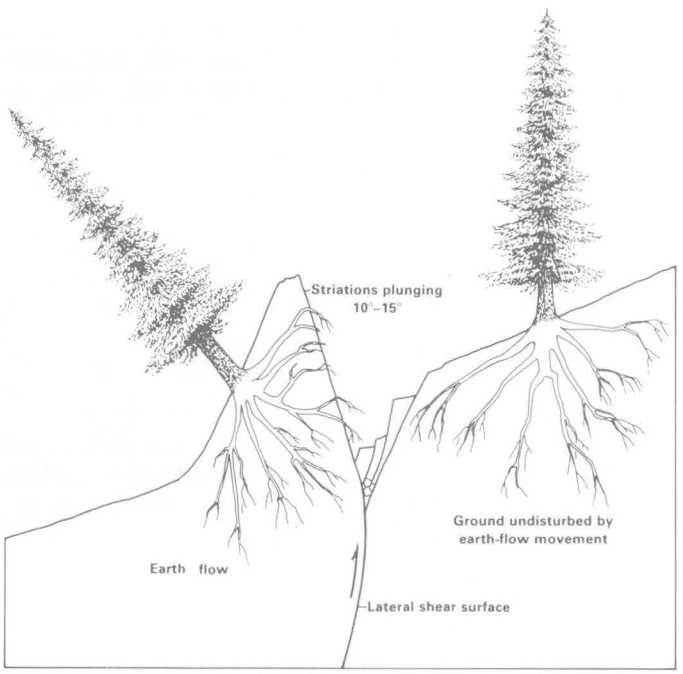

FIGURE 8.—Cross section through pressure ridge flanking earth flow at Kirkwood Creek, Mont. (after Hadley, 1964). Note lateral shear surface on outer flank.

FIGURE 9.—Lateral ridge (between arrows) formed by local overflow of material from earth flow at Melendy Ranch complex. Earth-flow surface is light area to left of lateral ridge.

ridges of the second and third types have slickensided shear surfaces on their inner flanks (fig. 12). The lateral ridges flanking many earth flows are composite features, made up of several segments of one or the other of these types.

The distal margin of an earth flow is a steep, bulging, rounded toe (fig. 7). Even though this toe is not confined laterally, it is only slightly wider than those parts of an earth flow that are so laterally confined; only minor spreading of the material near the toe occurs. Some earth-flow toes override the ground surfaces downslope from them (fig. 7); the boundaries between the distal parts, or *feet*, of these earth flows and the former ground surfaces are called *surfaces of separation*. Some toes contain recumbent folds (Blackwelder, 1912; Krauskopf and others, 1939); other toes are underlain by multiple shear surfaces arranged like imbricate thrust faults (fig. 13). Both the folds and the multiple shear surfaces indicate thickening and shortening in the zones of accumulation.

Although an earth flow moves as a generally coherent body, it is disrupted by numerous cracks. One type of crack, which occurs throughout the earth flow, is caused by differential movement (fig. 14*A*). A second type, which occurs in echelon sets adjacent to the flanks, is caused by drag along the flanks (fig. 14*B*). A third type of crack is caused by desiccation (fig. 14*C*); these desiccation cracks resemble the cracks formed by differential movement.

The *main body* of an earth flow is bounded by slickensided *basal* and *lateral shear surfaces* (figs. 12, 15). In the zone of depletion, the surface traces of lateral shear surfaces are scarps connecting with the main

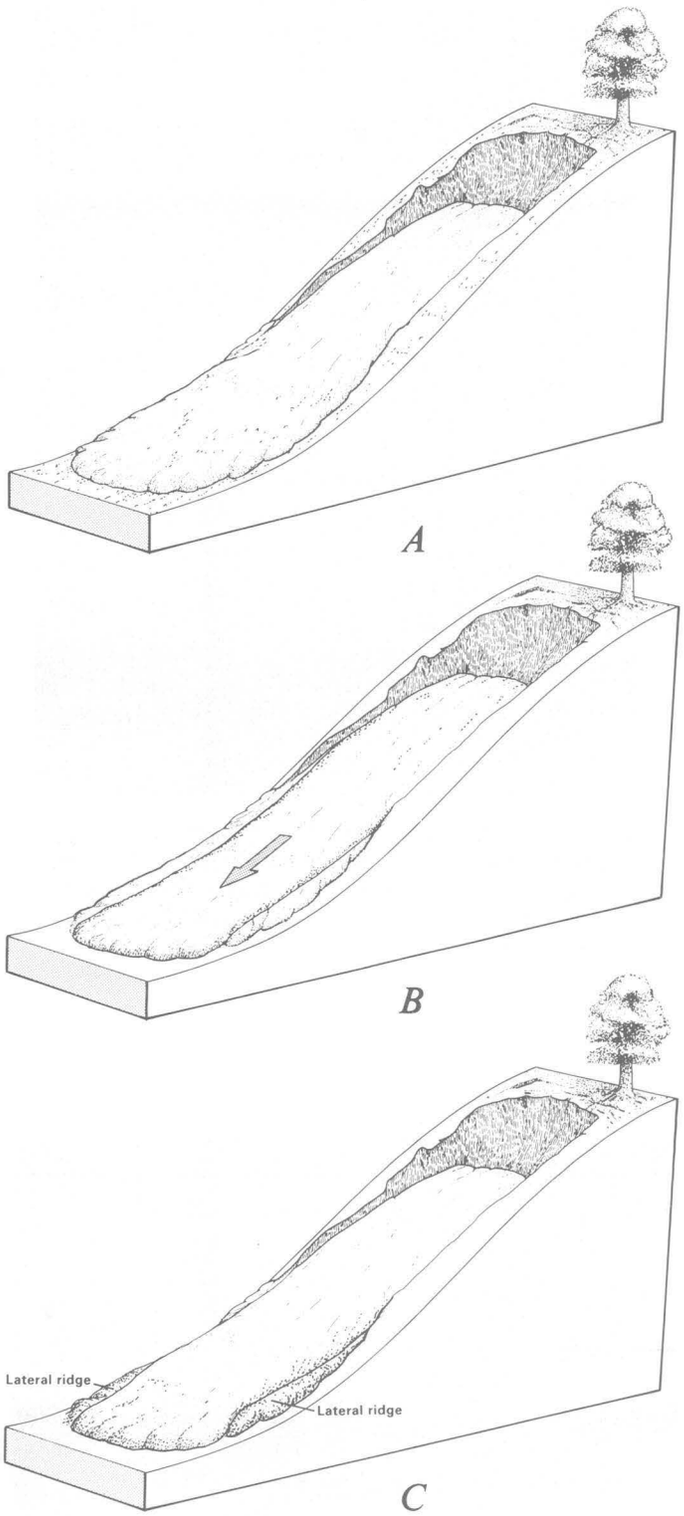

FIGURE 10.—Formation of lateral ridges when toe overrides former ground surface and is later remobilized (third type mentioned in text). *A*, Earth flow toe overrides former ground surface; earth flow becomes inactive and forms an earth-flow deposit. *B*, Part of earth-flow deposit is remobilized by another earth flow. *C*, As second earth flow advances, part of deposit that was not remobilized is left in place to form a pair of lateral ridges.

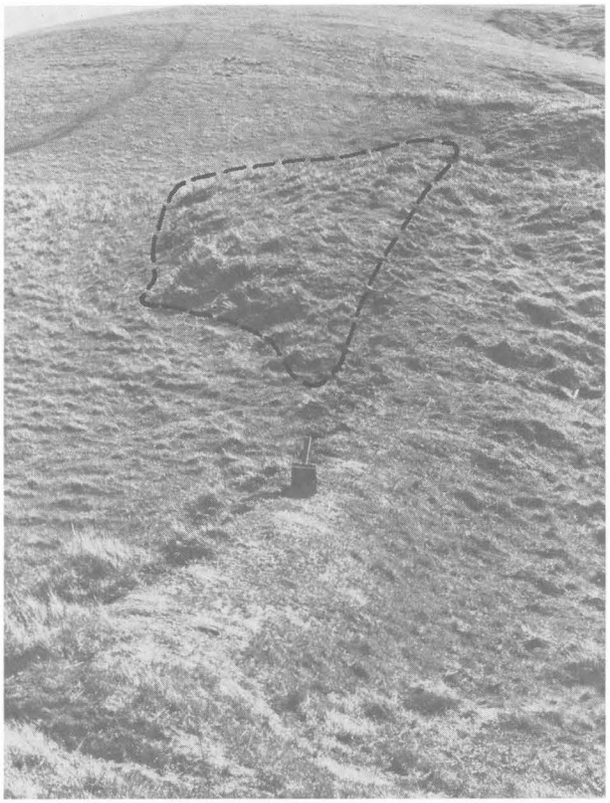

FIGURE 11.—Earth-flow deposit in Cordelia, Calif., area, showing lateral ridge (dashed outline) formed as illustrated in figure 10. Deposit is to right of lateral ridge. Ground to left of lateral ridge is undisturbed by earth-flow movement. Notebook is 22 by 30 cm.

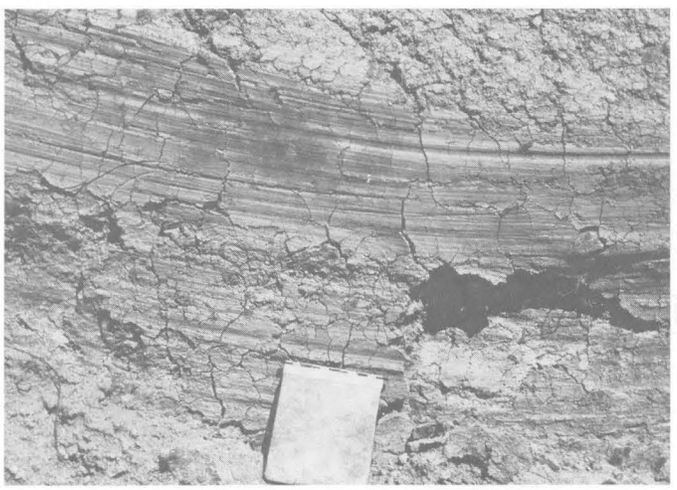

FIGURE 12.—Slickensided lateral shear surface on inner flank of lateral ridge at Melendy Ranch complex. Notebook is 22 by 30 cm.

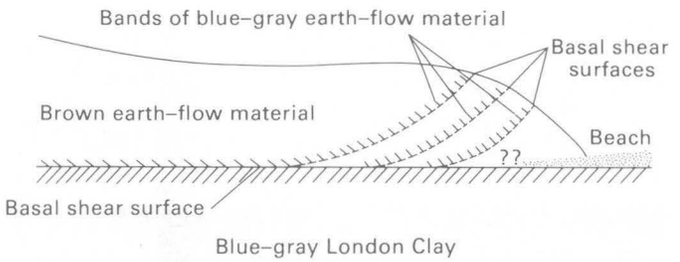

FIGURE 13.—Multiple basal shear surfaces underlying earth-flow toe at Beltinge, England (after Hutchinson, 1970), indicating thickening and shortening in zone of accumulation. Reprinted with permission of J. N. Hutchinson.

scarp (fig. 16*A*), or open cracks within the amphitheatre (fig. 16*B*). In the zone of accumulation, lateral shear surfaces are commonly scarps bounding lateral ridges (figs. 8, 12). Subsurface geometries of basal and lateral shear surfaces are described in the next section.

SUBSURFACE FEATURES: BASAL SHEAR SURFACES, LATERAL SHEAR SURFACES, AND ASSOCIATED ZONES OF DEFORMATION

During our study, we examined basal and lateral shear surfaces and associated features in a trench into an earth-flow deposit in the Cordelia, Calif., area, in a gully eroded through an earth-flow complex near Davilla Hill, and in two pits excavated into the Davilla Hill earth-flow complex.

The trench in the Cordelia area was excavated through a lateral ridge and part of the zone of accumulation of the earth-flow deposit. The long axis of the trench was perpendicular to the direction of movement of the earth flow; thus, the trench provided a transverse cross section through the deposit (fig. 17*A*). Figure 17*B* is a map of the trench wall, showing traces of the shear surfaces and associated features. The basal shear surface is pervasively slickensided (fig. 15*A*). The trace of this shear surface, though generally linear, contains one major asperity (B, fig. 17*B*) and two subsidiary shear surfaces (A and B, fig. 17*B*). The basal shear surface is underlain by a poorly consolidated yellowish-brown mudstone broken by fractures spaced a few millimeters apart. Whereas most of the earth-flow deposit is composed of dark-brown silty clay, the layer immediately above the basal shear surface is composed of softened yellowish-brown mudstone. The boundary between the mudstone and the clay, though distinct, is highly convoluted (fig. 18); the softened-mudstone layer also contains rounded lumps of the clay. The convoluted boundary and the inclusion of lumps of the clay in the softened mudstone indicate that significant internal deformation had taken place in the zone adjacent to the shear surface.

FIGURE 14.—Types of cracks disrupting earth flows. *A*, Cracks caused by differential movement at Melendy Ranch complex. Such cracks occur throughout most or all earth flows and earth-flow deposits. Photograph by E. L. Harp, U.S. Geological Survey. *B*, Echelon cracks along flank of earth flow at Davilla Hill complex. Such cracks are caused by drag along flanks. Lens cap is 5 cm in diameter. *C*, Dessication cracks in earth-flow deposit at Davilla Hill complex. Cloth flag in center foreground (arrow) is 5 by 10 cm.

A steeply dipping lateral shear surface joins the basal shear surface at a sharp bend (C, fig. 17*B*); in transverse cross section, therefore, this earth-flow deposit is approximately rectangular. Near the ground surface, the lateral shear surface splits into two branches. One branch forms the outer flank of a lateral ridge (D, fig. 17*B*); the other branch may form the inner flank of this lateral ridge, but this relation could not be determined because most of the lateral ridge was covered by spoil from the trench. No slickensides were observed on the lateral shear surface.

In a gully near Davilla Hill, two earth-flow deposits, one on top of the other, are exposed in longitudinal cross section (fig. 19). The basal shear surface underlying the upper deposit is broadly planar. The apparent dip of the shear surface decreases gradually from 17°

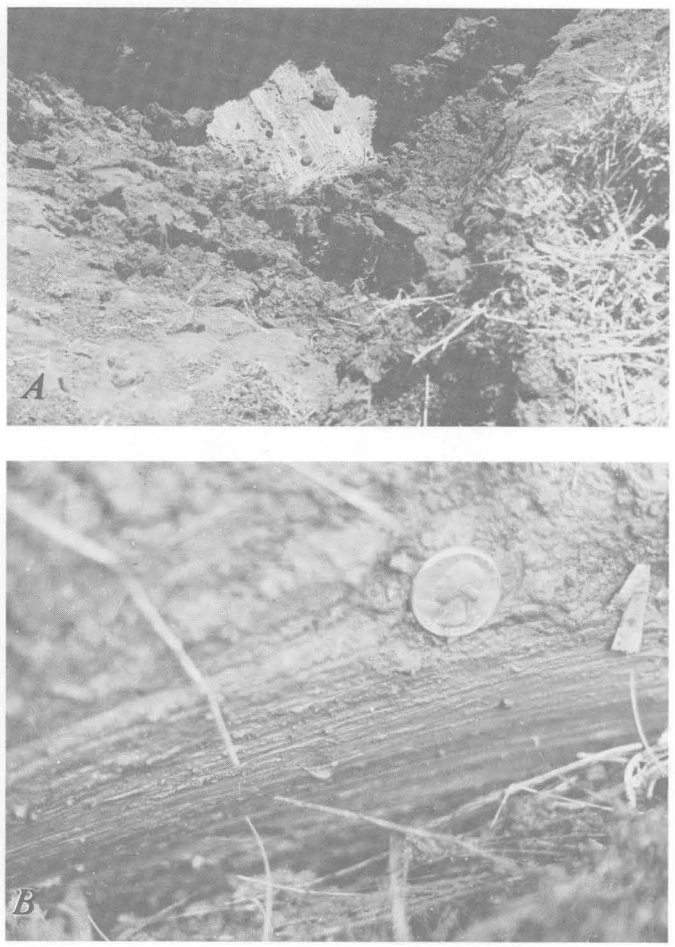

FIGURE 15.—Slickensided shear surfaces. *A*, Basal shear surface exposed on floor of trench in Cordelia, Calif. area. Slickensides trend parallel to inferred direction of earth-flow movement. Slickensided area is approximately 50 cm on a side. View vertically downward. *B*, Lateral shear surface at Davilla Hill site. Direction of earth-flow movement is toward left. Slickensides are on margin of earth flow which is raised above adjacent, immobile material visible along lower edge of photograph. View obliquely downward.

under the head to horizontal at a point about 1 m upslope from the toe; downslope from there, the dip reverses, and, under the toe itself, the shear surface dips upslope about 15°. This shear surface is underlain by a layer, 20 to 30 mm thick, of very soft sheared silty clay. The shear surface underlying the lower deposit is underlain by a zone of sheared material, 3 mm thick. Both shear surfaces are slickensided.

Two pits dug at the Davilla Hill site exposed areas, a few centimeters on a side, of the slickensided basal shear surface of one earth-flow deposit. We did not observe any structures indicative of deformation in material adjacent to this shear surface.

FIGURE 16.—Lateral shear surfaces in zones of depletion of earth flows at Davilla Hill complex. *A*, Scarp forming lateral shear surface. Fresh crack (between arrows) at base of scarp is boundary between active earth flow and immobile material. Scarp is approximately 0.5 m high. *B*, Trace of lateral shear surface as an open crack. Lateral shear surface is parallel to and approximately 20 cm from base of scarp bounding zone of depletion. Scarp is visible on other side of lens cap (5 cm in diameter) from lateral shear surface. Direction of earth-flow movement is toward right. View obliquely downward.

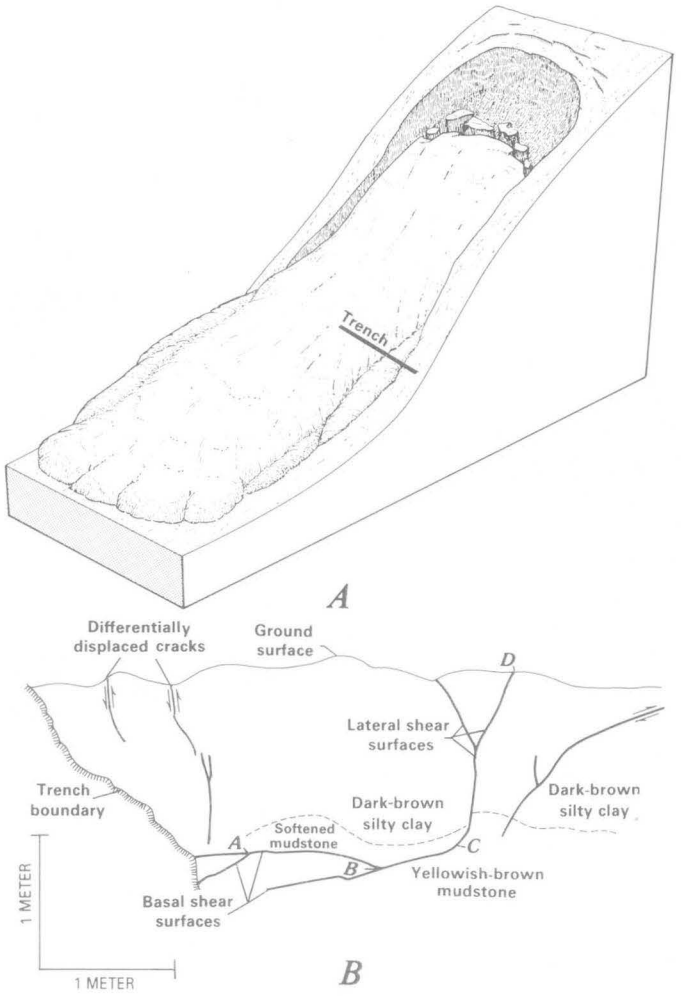

FIGURE 17.—Trench cut through earth-flow deposit in Cordelia, Calif., area. *A*, Location and orientation of trench in relation to earth-flow features. *B*, Trench wall, showing earth-flow basal and lateral shear surfaces, boundaries between different materials, and differentially displaced cracks (sense of displacement indicated by arrows). View upslope.

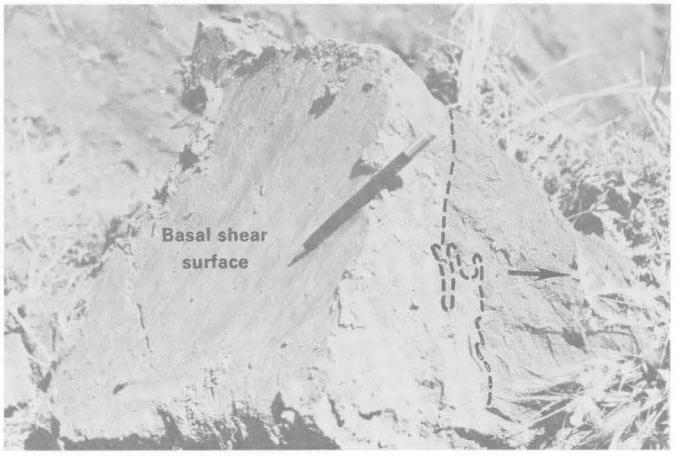

FIGURE 18.—Convoluted contact (dashed line) between softened yellow-brown mudstone (lighter material) and dark-brown silty clay (darker material) in sample taken from trench in Cordelia, Calif., area (see fig. 17). Slickensided basal shear surface is visible on left boundary of sample. Arrow points toward original top of sample. Pencil is 15 cm long. Photograph by G. F. Wieczorek, U.S. Geological Survey.

EARTH-FLOW COMPLEXES

On many hillsides, earth-flow deposits occur in long narrow channels (pls. 2, 3; fig. 20; earth-flow complex 1 in fig. 21). At the upslope margin of each channel is a scarp, and at the downslope margin is at least one earth-flow toe. Within the channels, the topography appears to be a chaotic jumble of bulges, depressions, and blocks separated by scarps and cracks. Such topography led Blackwelder (1912, p. 490-491) to describe a feature of this kind as a "long glacier-like tongue" with a surface composed of "orderless humps and hollows."

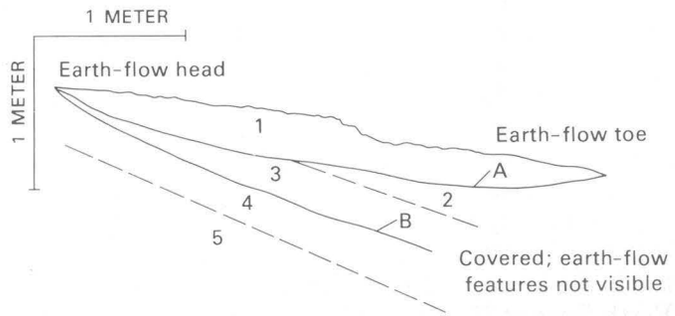

FIGURE 19.—Wall of gully near Davilla Hill complex. Two earth-flow deposits, underlain by basal shear surfaces, are exposed in longitudinal cross section. Dashed lines indicate contacts between different materials; solid lines indicate basal shear surfaces. 1, earth-flow deposit 1, dark-yellowish-brown silty sand; 2, earth-flow deposit 2, dark-yellowish-brown silty sand; 3, earth-flow deposit 2, light-olive-gray silty sand; 4, dark-yellowish-brown silty sand; 5, moderate-brown silty sand; A, basal shear surface underlain by 20 to 30 mm of very soft silty clay; B, basal shear surface underlain by 3-mm-thick shear zone.

This and many other published descriptions imply that all the material in a channel is part of a single large earth-flow deposit. Our examination of several tens of these channels and detailed mapping of these features at three sites, however, show that most such channels contain several smaller earth-flow deposits (see section entitled "The Davilla Hill Earth-Flow Complex"; pls. 2, 3; Aboim-Costa and Stein, 1976; Keefer, 1976; 1977a; Spain and Upp, 1976). The Hidden Valley earth-flow complex (pl. 2) contains at least 13 distinct earth-flow deposits, and the Davilla Hill earth-flow complex (pl. 3) at least 34. Alternating zones of depletion and accumulation, formed by numerous individual earth flows, are shown on the cross section in plate 2. Deposits that are completely preserved are similar in form to those shown in figures 2 and 4. Many deposits, however, are highly disrupted by cracks or are partially destroyed by erosion, by renewed earth-flow movement, or by other mass-movement processes. In some channels, earth-flow deposits are piled one on top of another, piggyback fashion; in others, they are separated by zones containing the deposits of other types of mass movement.

Most earth-flow deposits, therefore, occur as parts of earth-flow complexes. A given earth-flow complex may contain several earth-flow deposits, as well as other types of mass-movement deposits. Some earth-flow complexes consist of a single sinuous channel (pls. 2, 3), others of several coalescing channels (fig. 20; earth-flow

FIGURE 20.—Earth-flow complexes occupying long narrow channels on a hillside near Davilla Hill complex. Arrows mark upslope margins of channels, each of which contains several earth-flow deposits.

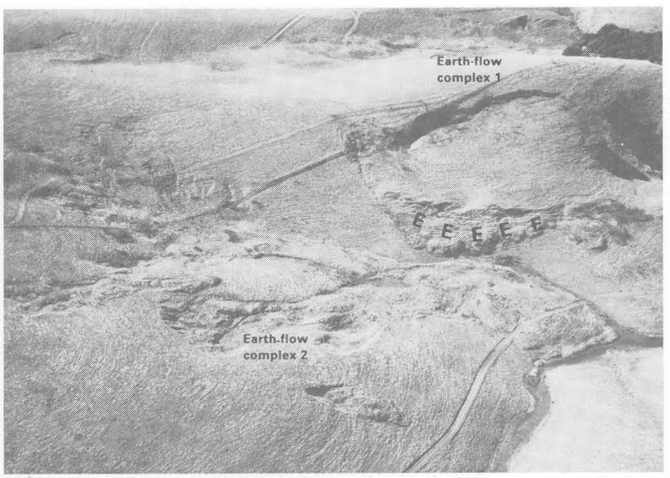

FIGURE 21.—Two earth-flow complexes in Cordelia, Calif., area. Earth-flow complex 1 consists of several earth-flow deposits in a network of sinuous coalescing channels. Earth-flow complex 2 consists of a broad slump deposit (S) and several earth-flow deposits (E) adjoining slump deposit. Note road near base of hillside for scale.

complex 1 in fig. 21); still others are irregular in outline and blanket broad areas with hummocky, disrupted topography (earth-flow complex 2 in fig. 21; fig. 22). Some earth flow complexes have surface areas of several tens of square kilometers (Bailey, 1972).

The channels of earth-flow complexes are flanked by a combination of scarps and lateral ridges. In many places, the lateral ridges are made up of several segments arranged in echelon. These echelon patterns document the passage of several earth flows through each channel; each subsequent earth flow came to rest farther downslope, as illustrated in figure 10.

At any given time, an earth-flow complex may contain one or more active earth flows moving through any part of the complex. In many earth-flow complexes, earth flows are intermittently active for several years (Radbruch and Weiler, 1963; Campbell, 1966; Hutchinson, 1970; Hutchinson and others, 1974) or even several centuries (Crandell and Varnes, 1961; Swanson and Swanston, 1977). Within complexes, earth flows commonly are formed out of older earth-flow deposits; the younger earth flows, however, do not have the same boundaries as the older deposits. New scarps and lateral shear surfaces commonly cut across the older boundaries, and earth flows formed out of older earth-flow material leave behind irregular remnants of the older deposits.

MATERIALS

Earth flows occur in various fine materials, including residual soils, colluvial soils, old earth-flow deposits, and deposits of other types of landslides. Sand-, silt-, and clay-size grains predominate in earth-flow materials, and, in most earth flows, silt and clay make up more than 50 percent of the matrix (table 3). Some earth flows also incorporate larger rock fragments, lumps of stiff clay, or such miscellaneous debris as tin cans or sheep carcasses. The earth flows and earth-flow deposits that we examined in the San Francisco Bay region are composed of silty clay, clayey silt, or silty sand (table 3). The silty sand of the Melendy Ranch earth-flow complex is the coarsest material we observed, and the silty clay of the Cycle Park earth-flow complex is the finest (table 3).

The clay mineralogy of earth-flow materials varies from site to site (table 3). In the Davilla Hill and Fields Barn earth-flow complexes in the Orinda, Calif., area, illite and chlorite are the predominant clay minerals, and in the Cycle Park earth-flow complex montmorillonite and illite; in the Melendy Ranch earth-flow complex, talc and serpentine are the only clay minerals present. Montmorillonite predominates in the clay of earth flows at Slumgullion, Colo. (Crandell and Varnes, 1961), in the Gros Ventre Mountains of Wyoming (Bailey, 1972), and in the Lomerias Muertas area (Oberste-Lehn, 1976). Earth flows at Minnis North, northern Ireland, contain large proportions of montmorillonite and illite and minor amounts of kaolinite (Prior and others, 1971). Earth flows on the Caribbean island of Barbados contain a mixture of kaolinite, illite, chlorite, and montmorillonite (Prior and Ho, 1972).

The wide range in the plasticity of earth-flow materials, as measured by the Atterberg liquid and plastic limits and plasticity index, reflects variations in both clay-mineral content and grain-size distribution (fig. 23; table 3). On the plasticity chart of the Unified Soil Classification System, most earth-flow materials plot near the A-line, which separates plastic from nonplastic soils (fig. 23). Of the 19 earth-flow materials plotted (fig. 23), 8 are CH soils (clays with high plasticity), 5 are CL soils (clays with low plasticity), 5 are MH soils (silts with high plasticity), and one is a CL–ML soil.

Active earth flows contain a significant amount of entrained water; reported water contents[5] range from 27 to about 60 percent (table 3). Earth-flow mobilization is accompanied by an increase in water content (Hutchinson, 1970; Prior and others, 1971; Keefer, 1977a) and, at many sites, by softening of the material (Ward, 1948; Prior and others, 1968; Hutchinson, 1970; Hutchinson and Bhandari, 1971; Prior and others, 1971; Hutchinson and others, 1974; Keefer, 1977a). Most active earth flows are so soft that they will not support a person's weight; others contain a stiff crust over a soft interior, and still others are relatively stiff throughout. Earth

FIGURE 22.—Earth-flow complex near Pleasanton, Calif., showing hummocky topography typical of large earth-flow complexes.

[5]Water content = 100(weight of water)/(weight of dry soil).

TABLE 3.—*Composition of earth-flow materials*

[Natural water content of fine-grained matrix is listed for active earth flows only; natural water content = 100(weight of water)/(weight of solids). Liquidity index = (natural water content - Atterberg plastic limit)/(Atterberg liquid limit - Atterberg plastic limit). Strength parameters: ϕ_p, peak angle of internal friction; ϕ_{rem}, angle of internal friction of remolded material; ϕ_f, angle of internal friction on plane of cracks in soil; ϕ_{ss}, angle of internal friction on shear surface; ϕ_r, residual angle of internal friction; c_p, peak cohesion; c_{rem}, cohesion of remolded material; c_f, cohesion on plane of cracks in soil; c_{ss}, cohesion on shear surface; c_r, residual cohesion; $s_{u,p}$, peak undrained shear strength measured with field or laboratory vane; $s_{u,rem}$, undrained shear strength of remolded material measured with field or laboratory vane; s_u, undrained strength, whether peak or remolded not specified; $S_t = s_{u,p}/s_{u,rem}$, sensitivity. Except where noted, values of ϕ and c are from drained direct-shear tests. n.d., not determined]

Site	Description of material	Clay minerals (percent)	Grain size (percent)			Atterberg limits (percent)		Natural water content (percent)	Liquidity index	Strength parameters	Reference
			Clay (<2 μm)	Silt	Sand and coarser (>62 μm)	Plastic	Liquid				
Davilla Hill, Orinda area[1].	Clayey silt containing sandstone and shale pebbles and varying amounts of organic material; soft and wet when earth flows are active, stiff to crumbly when desiccated; pervasively fissured.	Illite (49), chlorite (26), kaolinite (20), montmorillonite (4).	44	51	5	30	56	38.4	0.32	ϕ_p=25.4°, c_p=5.0 kN/m^2, ϕ_{ss}=15.5°, c_r=0.525 kN/m^2, $s_{u,p}$=11 kN/m^2, $s_{u,rem}$=4.9 kN/m^2, S_t=2.2.	Keefer (1976, 1977a).
Fields Barn, Orinda area[1].	Clayey silt; medium-stiff when wet, very stiff when desiccated.	Illite (69), chlorite (16), kaolinite (13), montmorillonite (2).	30	57	13	19	38	27	.42	---	Keefer (1977a).
Melendy Ranch, Bear Valley area[1].	Silty sand, bluish-green; soft and sticky when earth flow is active, loose and powdery when desiccated.	Talc, serpentine--	12	38	50	n.d.	n.d.	29	--	---	Keefer (1976), (1977a).
Cycle Park, Cienega Valley area[1].	Alternating lenses of brown to black silty clay and tan to light-brown clayey silt; sticky but firm enough to walk on when earth flow is active, stiff when desiccated.	Montmorillonite (36), illite (24), chlorite (20), kaolinite (20).	49	42	9 (Silty clay)	30	74	37	.16	---	Keefer (1976, 1977a).
			29	62	9 (Clayey silt)	25	48	29	.17		
Earth-flow deposits in Gros Ventre Valley, northwestern Wyoming.	Heterogeneous assortment of shale, sandstone, conglomerate, volcanic breccia, and basalt; grains range in size from clay to 3-m boulders; much of fine matrix weathers to "popcorn" texture characteristic of bentonitic shale; much of material is unstratified and resembles glacial till.	---	28	47	25 (Sample 1)	25	48	--	--	---	Bailey (1972).
			20	60	20 (Sample 2)	17	28	--	--	---	
			32	63	5 (Sample 3)	16	36	--	--	---	

Beltinge, England.	Soft clay matrix containing lumps of overconsolidated argillaceous debris. Earth flow is generally too soft to support a person's weight when active; stiff crust present at times.	---	66	--	--	30	85	38-49	.15-0.35	$s_{u_p} = s_{u,rem} = 4.8\text{-}7.2$ kN/m^2, $S_t = 1.0$.	Hutchinson (1970).
Bouldnor 1, Isle of Wight, England.	Material derived from stiff fissured Oligocene clay.	---	67	--	--	27-33	67-80	32-55	--	$\phi_r = 13.5°$, $c_r = 0$.	Hutchinson and Bhandari (1971).
Isle of Sheppey, England.	Soft clay derived from overconsolidated stiff fissured Eocene London clay; when active, earth flow will not support a person's weight.	---	--	--	--	28	66	50	.58	---	Hutchinson and Bhandari (1971).
Minnis North, northern Ireland, earth flow 1.	Clay and glacial till containing some boulders; matrix is soft clay containing various-size lumps of stiffer debris.	---	53	--	--	23	59	41-43	.50-.56	$s_u < 4.8$ kN/m^2, $^2\phi_p = 24°\text{-}27°$, $^2c_p = 0\text{-}2$ kN/m^2, $^2\phi_r = 14.5°\text{-}15.0°$, $c_r = 0$.	Prior and Stephens (1972), Hutchinson and others (1974).
Minnis North, northern Ireland, earth flow 2.	Clay and glacial till containing boulders; matrix is soft clay containing various-size lumps of stiffer debris.	Montmorillonite and illite (89), kaolinite (11).	--	--	--	29	65	59	.83	---	Prior and Stephens (1971).
Rojne Klint, Denmark[3].	Stiff fissured overconsolidated Eocene clay, in part reworked by older earth flows.	Kaolinite, montmorillonite, illite.	63	--	--	31	58	--	--	---	Prior (1977).
Rosnaes, Denmark[3].	Weathered stiff fissured overconsolidated Eocene clay.	do----------	59	--	--	32	60	--	--	$\phi_f = 12°$, $c_f = 9.5$ kN/m^2, $\phi_r = 11°$, $c_r = 0$.	Do.
Helgenaes, Denmark[3].	Earth flows developed on rotational slump blocks composed of glacial till and stiff fissured overconsolidated Eocene clay.	do----------	52	--	--	36	61	--	--	---	Do.
Castle Hill, England[3].	Soft wet clay derived from seacliffs composed of stiff fissured overconsolidated Eocene London clay; material will not support a person's weight.	---	--	--	--	27	90	--	--	---	Ward (1948).
Sarsorya, Vestspitsbergen, locality 1.	Gray silt containing siltstone fragments.	---	9	33	58	--	--	--	--	---	Chandler (1972).

TABLE 3.—*Composition of earth-flow materials*—Continued

Site	Description of material	Clay minerals (percent)	Grain size (percent)			Atterberg limits (percent)		Natural water content (percent)	Liquidity index	Strength parameters	Reference
			Clay (<2 μm)	Silt	Sand and coarser (>62 μm)	Plastic	Liquid				
Sarsorya, Vestspitsbergen, locality 2.	Slightly plastic gray silt containing siltstone fragments.	---	18-31	60	9-22	--	--	--	--	$\phi_p \geq 36°$	Do.
Bruce Vale, Barbados.	Clay weathered from Tertiary shale.	Kaolinite, montmorillonite, illite, chlorite.	[4]54	--	--	36	61	--	--	---	Prior and Ho (1972).
Saddleback, Barbados.	do----------	Kaolinite, illite, chlorite.	[4]8	--	--	22	27	--	--	---	Do.
Bathsheba, Barbados.	do----------	Kaolinite, montmorillonite, illite, chlorite.	[4]48	--	--	32	83	--	--	---	Do.
Bellplaine, Barbados.	Clay weathered from Tertiary shale; earth flows form on slopes terraced for soil conservation.	do----------	[3]47	--	--	30	75	--	--	---	Do.
Razorback Range, Australia.	Friable clay loam, stiff clay, clay containing weathered shale fragments.	---	45-55	--	--	--	--	--	--	$r=20°-24.5°$ $c_r=1.9-6.9$ kN/m^2	Dunkerley (1976).
Southern Chittering Valley, Australia.	Colluvium; shear surfaces in impermeable claypan.	---	30-71	--	--	--	--	--	--	---	Pilgrim and Conacher (1974).

Site	Description of material	Reference
"Y" earth flow, Lomerias Muertas area[1].	Shale, low-density, highly fissile, closely fissured; sand, poorly sorted, coarse to fine; claystone, dense, massive, plastic; sandstone, very friable, fine-grained, well-sorted; predominant clay mineral is montmorillonite.	Oberste-Lehn (1976).
Gros Ventre earthflow complex, Wyo. ("Upper Gros Ventre slide")	Soft shale, clay, and old landslide deposits----------	Blackwelder (1912).

Gardiner, Mont---------	Blocks of shale, sandstone, conglomerate, volcanic breccia, and basalt; grains range in size from clay to 3-m boulders; fine-grained matrix is bentonitic.	Waldrop and Hyden (1963).
Kirkwood, Mont---------	Clayey colluvium and soil derived primarily from the Morrison Formation (Upper Jurassic), which is composed of claystone, siltstone, mudstone, and moderately friable sandstone.	Hadley (1964).
Slumgullion, Colo------	Material derived from hydrothermally altered Tertiary volcanic flows and breccia; contains abundant montmorillonite.	Crandell and Varnes (1961).
Redwood Creek basin, Calif.	Residual soils and colluvium derived from argillaceous and (or) highly sheared rocks of the Franciscan assemblage (upper Mesozoic).	Harden and others (1978).
Cedar Creek, Colo------	Very fine grained poorly consolidated mudstone, shale, and clay; material breaks down very rapidly under alternating exposure to water and air.	Varnes (1949).
Ames, Colo-------------	Unconsolidated glacial till composed of clay and rock flour, with less than 2 percent coarser rock fragments as much as 1.5 m in diameter.	Do.
Merecomb Farm, England.	Weathered mudstone derived from fissured Keuper Marl (Triassic)----------	Hawkins (1973).
Fairy Dell, England----	Material from landslide blocks originating in the Upper Greensand (Lower Cretaceous), which is composed of sand and closely jointed chert, and the Gault (Lower Cretaceous), which is composed of sandy clay.	Brunsden and Jones (1976).
Sochi, Black Sea area, U.S.S.R.	Colluvial material derived from Oligocene argillite and sandstone----------	Ter-Stepanian (1967).
Okoličné, Czechoslovakia.	Old landslide deposits derived from tectonically disturbed Paleogene flysch----------	Fussgänger and Jadrŏn (1977).
Žarnovice, Czechoslovakia.	Clay and weathered volcanic-tuff agglomerate----------	Záruba and Mencl (1969).
Handlová, Czechoslovakia	Old landslide deposits composed of agglomerate, andesitic debris, and remolded silty clay.	Do.

[1]See figure 1 for locations of sites.

[2]Values from consolidated-undrained triaxial tests with pore-water-pressure measurements.

[3]Measurements of physical properties were made on parent material from which earth-flow material is derived.

[4]Clay size, <5 μm.

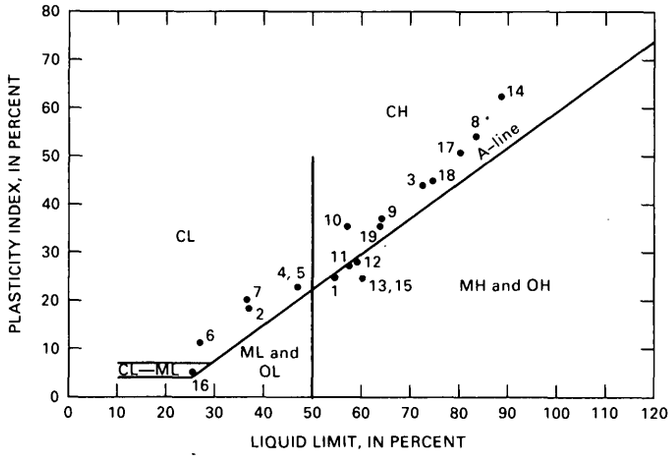

FIGURE 23.—Plasticity indexes and liquid limits of earth-flow materials on plasticity chart used for classification of fine soils according to Unified Soil Classification System. Plasticity index = liquid limit-plastic limit. Data points (see table 3 for references): 1, Davilla Hill; 2, Fields Barn; 3, Cycle Park, silty clay; 4, Cycle Park, clayey silt; 5, Gros Ventre Valley, sample 1; 6, Gros Ventre Valley, sample 2; 7, Gros Ventre Valley, sample 3; 8, Beltinge, England; 9, Isle of Sheppey, England; 10, Minnis North, northern Ireland, earth flow 1; 11, Rojne Klint, Denmark; 12, Rosnaes, Denmark; 13, Helgenaes, Denmark; 14, Castle Hill, England; 15, Bruce Vale, Barbados; 16, Saddleback, Barbados; 17, Bathsheba, Barbados; 18, Bellplaine, Barbados; 19, Minnis North, northern Ireland, earth flow 2. A-line, separates plastic from nonplastic soils; CH, clays with high plasticity; CL, clays with low plasticity; MH, silts with high plasticity; ML, silts with low plasticity; OH, organic soils with high plasticity; OL, organic soils with low plasticity.

flows, in general, are softer and more fluid than material in earth slumps or earth block slides, as defined by Varnes (1978), and stiffer and less fluid than material in debris flows and rapid earth flows such as those described by Johnson (1970) and Varnes (1978), respectively.

The shear strengths[6] of earth-flow materials are affected both by material composition and by the presence of planes of weakness, including cracks and slickensided shear surfaces. Drained[7] shear strength along cracks and shear surfaces is much lower than the peak (upper bound) shear strength of a given earth-flow material (Hutchinson and others, 1974; Keefer, 1977a; Prior, 1977). Shear strengths along many slickensided shear surfaces are nearly equal to the residual (lower bound) strength of the material (Hutchinson and Bhandari, 1971; Fussgänger and Jadroň, 1977; Prior, 1977). Under undrained[7] conditions, field-vane shear strengths measured at two sites—Davilla Hill and Beltinge, England—showed that the earth-flow materials have low sensitivities.[8] At Beltinge, the average sensitivity is only slightly greater than 1.0 (Hutchinson, 1970); and at Davilla Hill, 2.2.

THE DAVILLA HILL EARTH-FLOW COMPLEX

In this section we describe field, laboratory, and analytical investigations of the Davilla Hill earth-flow complex that were undertaken to study the earth-flow process at a representative site. Field studies were conducted from September 1974 to February 1978. During February 1975, four earth flows mobilized within the complex, and movements continued for several weeks. During these several weeks, surface and subsurface movements and ground-water levels were measured, samples were obtained for laboratory testing, and the undrained strength of the earth-flow material was measured with a field vane. Morphologic features of the earth-flow complex were mapped in June and July 1975.

Beginning in August 1975 and continuing through February 1978, pore pressures and ground-water levels were monitored with portable tensiometers and open-standpipe piezometers; sampling also continued during this time. Two earth flows were active in the complex during January and, possibly, February 1978, but no earth flows were active during the exceptionally dry winters of 1975-76 or 1976-77. During January and February 1978, studies consisted of visual observations and of monitoring of water levels and pore-water pressures.

Laboratory tests were carried out to measure strength parameters for use in analysis of mobilization; to measure changes in water content, saturation, and volume associated with mobilization; and to determine grain sizes, Atterberg limits, clay mineralogies, and consolidation properties of the earth-flow material. Earth-flow mobilization at Davilla Hill was analyzed using a modified form of the slope-stability analysis developed by Morgenstern and Price (1965, 1967).

DESCRIPTION

LOCATION AND SETTING

The Davilla Hill earth-flow complex is near the head of Eden Canyon in the southern part of the Orinda,

[6]Soil in an earth flow is assumed to be a Coulomb material, for which Terzaghi's theory of effective stress is valid. Thus

$$\tau = (\sigma_n - u)\tan\bar{\phi} + \bar{c},$$

where τ = the effective shear strength on a plane within the soil, σ_n = the normal stress on the plane, u = the pore-water pressure, $\bar{\phi}$ = the angle of internal friction, $\bar{c}$ = the cohesion.

[7]Under *drained* conditions, excess pore-water pressures generated by strain are allowed to dissipate by free movement of pore water; under *undrained* conditions, these pore-water pressures are not allowed to dissipate.

[8]Sensitivity = (peak undrained shear strength) / (undrained shear strength of remolded material).

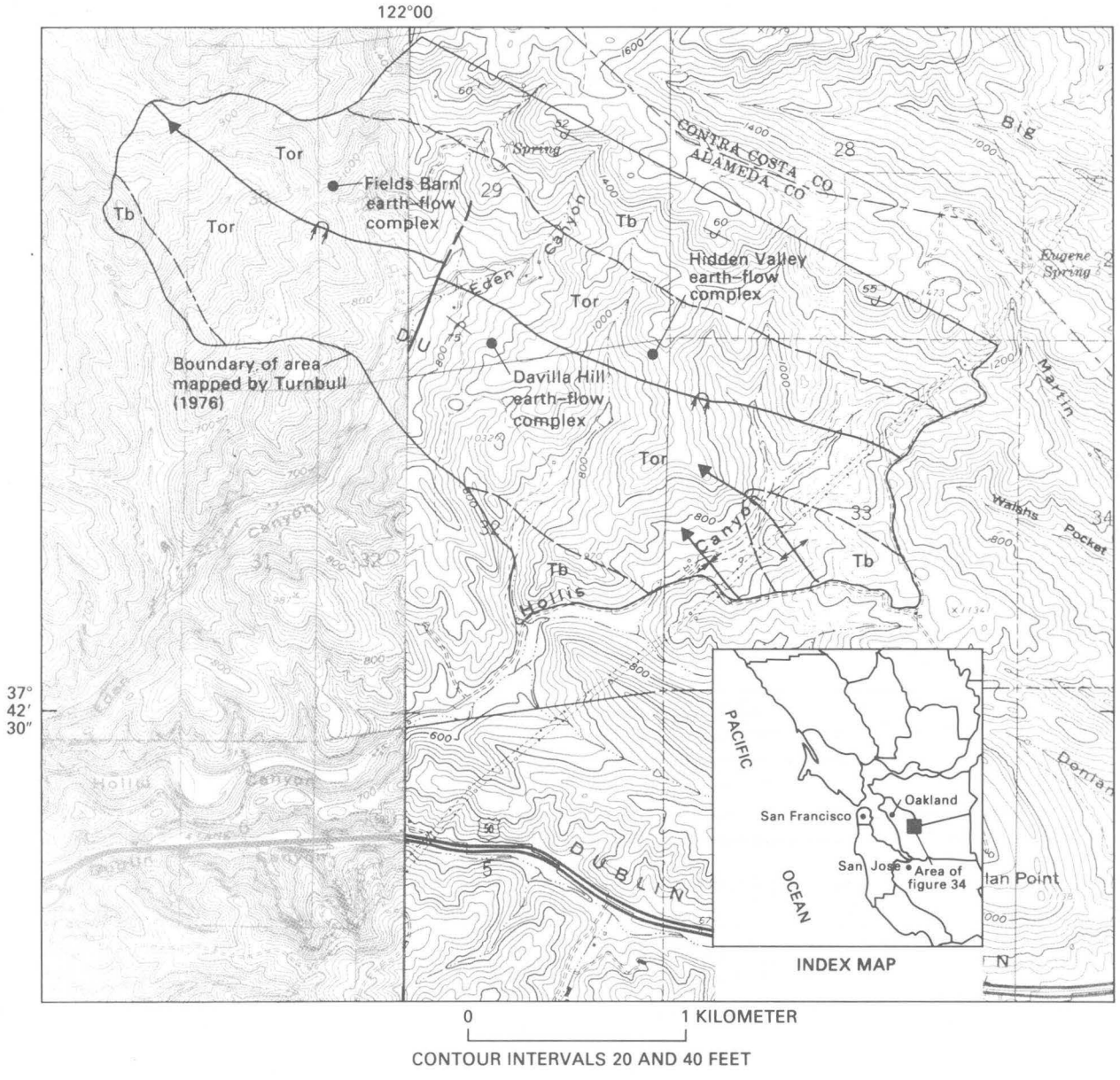

EXPLANATION

Tor — Orinda Formation (Miocene)—Nonmarine conglomerate, sandstone, siltstone, and shale containing minor limestone, tuff, and lignite

Tb — Briones Formation (Miocene)—Marine sandstone and shell reefs

Contact—Dashed where indefinite

D / U — Fault—Dashed where indefinite. U, upthrown side; D, downthrown side

Folds—Showing axial trace and direction of plunge

Anticline

Syncline

Overturned syncline

Strike and dip of bedding

60 — Inclined

75 — Overturned

FIGURE 24.—Geologic map of Eden Canyon area (from Turnbull, 1976), showing location of Davilla Hill earth-flow complex. Base from U.S. Geological Survey, Dublin and Hayward quadrangles, 1:24,000.

Calif., area (pl. 1; figs. 1, 24). In Eden Canyon, earth flows are more abundant than any other type of mass-movement phenomenon; an area of about 6 km^2 contains several hundred earth-flow complexes (pl. 1).

These earth-flow complexes are in colluvial and residual soils that mantle long northeast-trending ridges; the soils are silty clay, clayey silt, and sandy silt, generally 0.5 to 1.5 m thick but more than 4 m thick in the larger hillside reentrants and valleys tributary to Eden Canyon. Topography on the ridges is rounded, subdued, and hummocky owing to the pervasive degradation of slopes by earth flows. The earth flows occur on slopes with inclinations ranging from 8° to 45° (fig. 3*B*).

Bedrock underlying the area containing abundant earth flows belongs to the Orinda Formation, a sequence of Miocene freshwater conglomerate, sandstone, siltstone, and shale, and minor amounts of volcanic tuff, limestone, and lignite (Hall, 1956; Robinson, 1956; Turnbull, 1976). The rocks are soft, poorly consolidated, and closely jointed, and all the clastic rocks contain a matrix of clay (Turnbull, 1976).

Orinda Formation that crops out in a gully a few meters south of the Davilla Hill earth-flow complex is a medium-gray calcareous shale containing scattered egg-size concretions and ocher staining on the joints. The shale is soft, highly fractured, and highly weathered; bedding is lenticular and deformed by small-scale folding. In a bulldozer cut about 100 m west of the complex, the rocks are thin-interbedded shale, siltstone, and very fine grained to fine-grained sandstone. All these rocks are poorly consolidated, broken by closely spaced orthogonal joints, and weakly cemented by calcite.

Auger borings indicate that the rock beneath most of the earth-flow complex consists of interbedded mudstone and shale and small amounts of fine-grained sandstone. Auger borings on the steep slopes a few meters east and north of the complex indicate that the rock there contains more sandstone than the rock underlying the complex.

As in the rest of the San Francisco Bay region, the climate at the Davilla Hill site is characterized by cool rainy winters and warm dry summers. Temperatures rarely fall below freezing in the winter; in the summer, temperatures occasionally exceed 38°C (100°F). Nearly all precipitation falls during the months October through April. A private rain gage, maintained by Mr. and Mrs. A. A. Fields, is located 0.7 km southwest of the Davilla Hill earth-flow complex. During the period 1967-77, the average annual precipitation there was 59.9 cm.[9] The minimum annual precipitation during this period was 29.4 cm in 1975-76; the maximum was 94.8 cm in 1972-73. Figure 25 shows precipitation records for the time during which field studies were carried out at Davilla Hill.

MORPHOLOGY AND HISTORY OF MOVEMENT

Morphologic features of the Davilla Hill earth-flow complex were mapped using a planetable and alidade (pl. 3). From the planetable map, an interpretative map was made outlining individual earth-flow deposits within the complex (pl. 3). The following description refers to the earth-flow complex as it appeared in June and July 1975.

The earth-flow complex occupies a bowl-shaped reentrant in the ridge that forms the east wall of Eden Canyon. The slopes above the earth-flow complex have an average inclination of 27°. These slopes are cut by two gullies, one of which contains an earth-flow deposit (C3, pl. 3). The reentrant narrows in the reach occupied by the earth-flow complex. The average inclination of the surface of the complex is 15°. Downslope from the complex, the reentrant empties out onto a more gently sloping apron of colluvial material. After major storms, intermittent streams carry runoff across the surface of the complex, through a gully in the colluvial apron, and into the creek in Eden Canyon. A wire fence crosses the complex about midway along its length (pl. 3). On both sides of this fence a mixture of grasses and thistles is present on the earth-flow deposits. Upslope from the fence, vegetation on slopes undisturbed by mass movement consists mainly of grasses (fig. 26*A*). Downslope from the fence, most of the complex is shaded by eucalyptus, bay laurel, and oak trees (fig. 26*B*).

The Davilla Hill earth-flow complex is approximately 140 m long and 25 m wide and has 45 m of topographic relief from the uppermost scarp to the lowermost earth-flow toe. In plan view, the complex is shaped like a map of Italy with a broad crown region formed by earth-slide[10] features and a "boot" formed by two earth-flow toes (pl. 3). The earth-slide features consist of scarps as high as 1 m, scars as deep as 1 m, and deposits that form ridges and hummocks as high as 1 m. Immediately downslope from these deposits, the slope inclination decreases from 27° to 11°. The gently sloping area is underlain by a partially preserved earth-flow deposit (C2a, pl. 3), the distal boundary of which is a linear scarp connecting with extension cracks at either end. Downslope from the scarp, two earth-flow deposits (B7a and B8, pl. 3) occupy a channel bounded by two inward-

[9]Annual precipitation is measured from July 1 of one calendar year to June 30 of the next year.

[10]An *earth slide* is a landslide involving fine soil that moves rapidly and with much internal deformation along a planar shear surface.

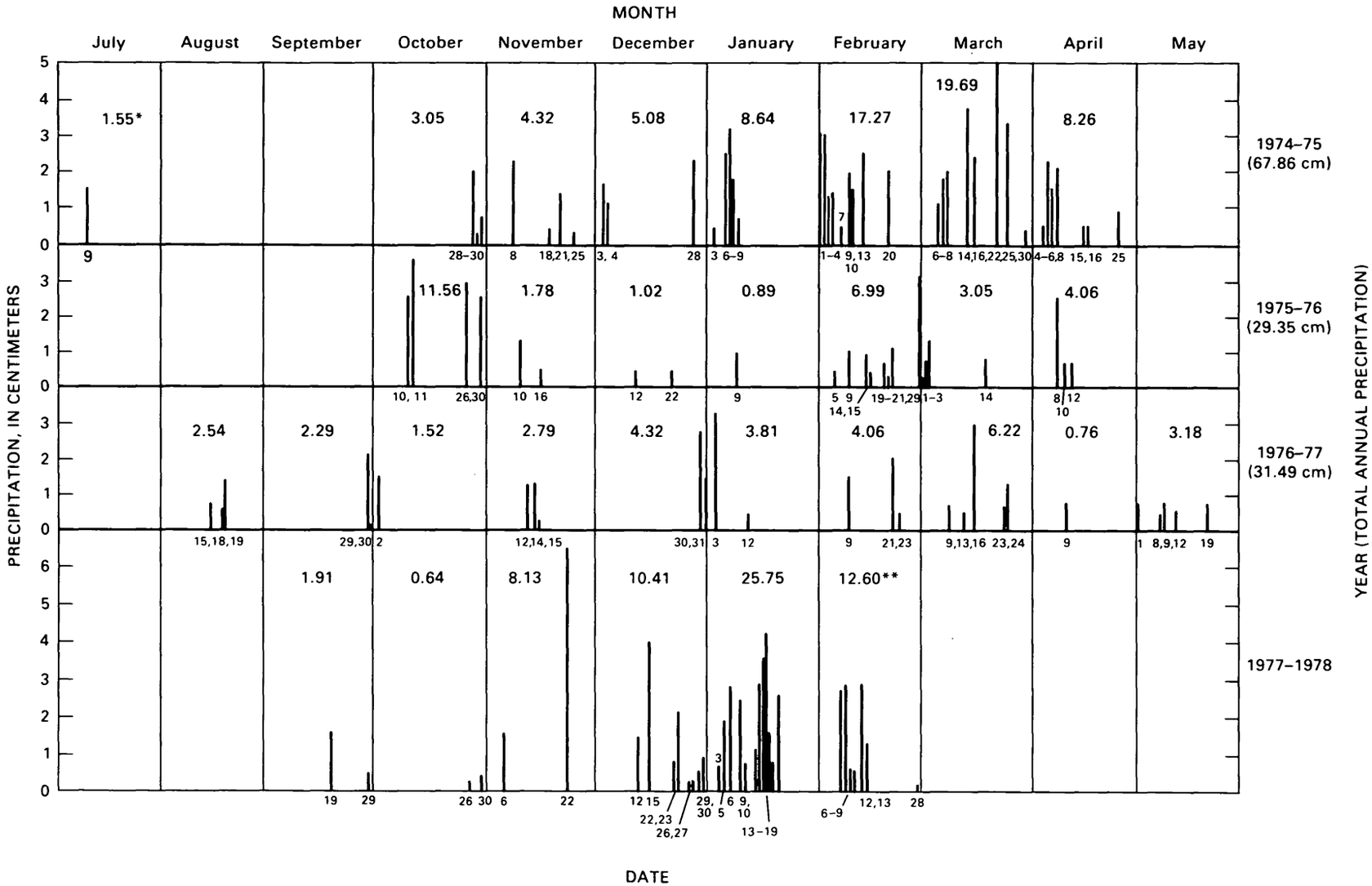

FIGURE 25.—Records of daily precipitation from rain gage in Eden Canyon, tabulated through February 28, 1978. Data courtesy of Mr. and Mrs. A. A. Fields. *, total precipitation for month (in centimeters); **, data from Hayward 4ESE weather station, 8 km south of Davilla Hill complex (National Oceanic and Atmospheric Administration, 1978).

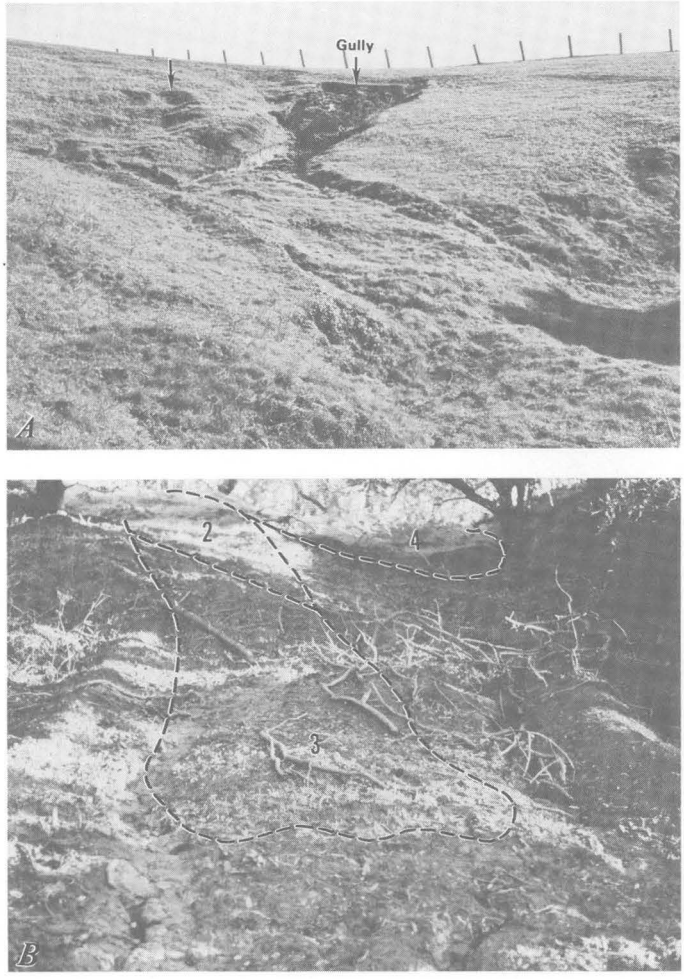

FIGURE 26.—Davilla Hill earth-flow complex. *A*, Upslope from wire fence. Surface of slump deposit is visible in foreground. Arrows point to area of earth-slide features in crown region and to gully containing earth-flow deposit C3 (see pl. 3). Much of complex upslope from slump deposit was mobilized by earth flows in January 1978. *B*, Downslope from fence. Prominent lateral ridges as high as 0.6 m flank this part of complex. In foreground, complex is 4 m wide. Parts of earth flows 2, 3, and 4, active in 1975, are outlined by dashed lines.

facing scarps capped by lateral ridges. These lateral ridges are remnants of an earth flow (C1, pl. 3), larger than any of the preserved deposits, that had its source in the area currently covered by earth-slide scars. The two earth-flow deposits in the channel spill out onto the surface of a slump deposit (pl. 3; fig. 26*A*).

The slump deposit has a surface slope that is relatively gentle and locally reversed. On the left flank[11] of the deposit is an inward-facing scarp covered with striations plunging downslope at angles of 30° to 36° (pl. 3); to the right of the deposit is a long narrow depression containing two earth-flow deposits (B6 and B7b, pl. 3). The distal boundary of the slump deposit, a jumbled mass of scarps and small landslide blocks, was the crown of one earth flow active in 1975; the other three earth flows active in 1975 mobilized within old earth-flow material farther downslope.

The slump deposit and much of the earth-flow complex downslope from it are contained in a channel bounded by a combination of inward-facing scarps and lateral ridges (fig. 26*A*). Flanking the slump deposit itself, however, are several earth-flow deposits that lie outside this main channel (A1, A2, A3, A5, A6, B1, B2a, B3b, and B4, pl. 3). The two largest of these (A1 and B4, pl. 3) have piled up behind obstructions consisting of the wire fence, a large eucalyptus tree, and a clump of shrubs. All these deposits are older than the inward-facing scarps bounding the main channel.

Downslope from the slump deposit, the complex is composed entirely of material transported by earth flows. The earth-flow deposits that are completely preserved are long and narrow; they are bounded by distinct main scarps, lateral shear surfaces, and bulging toes. Whereas their boundaries are locally irregular, most deposits are tongue or teardrop shaped. Many deposits, however, are only partially preserved; these remnants are highly irregular in shape.

The earth-flow deposits as well as the active earth flows observed in 1975 and 1978 contain numerous internal scarps, desiccation cracks, and cracks caused by differential movement; the larger cracks are several centimeters wide and about 1 m deep. Some scarps and cracks in active earth flows existed before the movement began; other scarps and cracks formed while the earth flows were moving.

Lateral ridges bordering the lower reaches of the complex are composite features, formed by numerous earth flows. These ridges, as high as 0.6 m, with steep flanks and rounded crests (pl. 3; fig. 26*B*), were formed by overflow of earth-flow material out of the main channel. In one locality (A7, pl. 3), the body of overflowing material divided and flowed around a tree. In another locality (intersection of A1 and fence, pl. 3), a bend of 70° in a lateral ridge indicates an abrupt change in the movement direction of the earth flow that formed the ridge. Downslope from this bend, a lateral shear surface was formed only a few centimeters inside the margin of an older earth-flow deposit (A4, pl. 3). Thus, even though the earth flow bounded by this lateral shear surface (A6, pl. 3) remobilized nearly all the older deposit, the boundaries of the younger earth flow do not coincide with those of the older deposit.

On the right flank of the complex, three lateral-ridge segments (A6, A7, and A9, pl. 3) form an echelon. These segments were formed by a series of three earth

[11] Right and left flanks are relative to an observer facing downslope.

flows, each of which came to rest progressively farther downslope, as illustrated in figure 10. At the downslope boundary of the earth-flow complex, a completely preserved earth-flow deposit—the fourth in this sequence (A10, pl. 3)—cuts off the third lateral-ridge segment. The downslope boundary of the earth-flow complex consists of two distinct earth-flow toes, 0.6 to 1.0 m high, with steep frontal slopes.

Earth-flow movements have been taking place intermittently in the Davilla Hill earth-flow complex for more than a decade (Russell Ferguson, oral commun., 1975); at least 34 individual earth flows have occurred (pl. 3), transporting and reworking the soil in the reentrant.

We have interpreted the relative ages of the earth-flow deposits from crosscutting or overlapping relations and by matching lateral-ridge segments across the complex. The deposits are grouped into three sequences identified by different capital letters because the absence of crosscutting or overlapping relations in some places within the complex precluded the grouping of all deposits into a single chronologic sequence. Deposits within each of the three sequences have been dated relative to each other. Each number or combination of number and lower-case letter designates a single earth-flow deposit; numbers increase from the oldest deposit to the youngest. Lower-case letters refer to earth-flow deposits that were bracketed in age relative to some deposits but which could not be dated relative to other deposits with the same number. For example, deposits C2a, C2b, and C2c are younger than deposit C1 and older than deposit C3, whereas the ages of deposits C2a, C2b, and C2c relative to each other are unknown.

MATERIAL

Material in the Davilla Hill earth-flow complex is a slightly overconsolidated clayey silt of low sensitivity (table 3), containing varying amounts of organic matter and minor amounts (less than 5 weight percent) of pebble-size bedrock fragments. The color, consistency, and organic matter content vary throughout the complex; however, the grain-size distribution and plasticity of the material are relatively uniform (Keefer, 1976, 1977a). The material contains 44 percent clay- (less than 2 μm), 51 percent silt-, and 5 percent sand-size and larger grains. Atterberg plastic and liquid limits are 30 and 56 percent, respectively. In the Unified Soil Classification System, the material is a silt with high plasticity (MH). Predominant colors are gray, yellowish brown, reddish brown, and black.

The material is pervasively fissured. Open cracks caused by desiccation and differential movement break the upper 1 m of soil into blocks smaller than 1 m on a side. Finer, hairline cracks further divide the soil into lumps a few millimeters on a side.

During most of the study period, the material was desiccated. Some desiccated material was so stiff that it could only be penetrated by a sharp blow from a pick; other desiccated material crumbled readily into pebble-size lumps along closely spaced fissures. Lumps of desiccated material, however, disintegrated within a few minutes when exposed to water; after even a small amount of precipitation, a layer a few millimeters thick on the surface of the earth-flow complex became soft and sticky, and the material slaked when immersed in water in the laboratory. In active earth flows, the material became so soft throughout that it would not support a person's weight.

Peak and remolded undrained strengths of the material in active earth flows, measured with a field vane, were 11 and 4.9 kN/m^2, respectively; the average sensitivity, therefore, is 2.2. In an undrained constant-volume simple-shear test on this material in the laboratory (Keefer, 1977a), the sensitivity was determined to be 1.3, in close agreement with the low value determined in the field. The material has an overconsolidation ratio (OCR) of 3.1 (Keefer, 1977a); this overconsolidation is probably due to desiccation.

Clay mineralogy was determined on seven samples from the site, using the X-ray diffraction techniques described by Hein and others (1975). In the six samples of earth-flow material, the clay contains an average of 49.3 percent illite, 26.2 percent chlorite, 20.1 percent kaolinite, and 4.4 percent montmorillonite (table 4). Clay in a bedrock sample contains 41.5 percent illite, 33.8 percent chlorite, 21.5 percent kaolinite, and 3.2 percent montmorillonite (table 4).

SUBSURFACE GEOMETRY

Data from hand-augered borings were used to construct a longitudinal cross section through the reentrant containing the earth-flow complex (pl. 3). On the steep slopes at the head of the reentrant, the soil is silty sand; elsewhere in the reentrant the soil is a clayey silt identical in appearance to the material in mapped earth-flow deposits. Soil thickness increases from a few centimeters on the steep slopes above the earth-flow complex to more than 4 m beneath parts of the complex itself; three borings drilled into bedrock beneath the complex encountered the bedrock surface at depths ranging from 1.7 to 4.2 m (pl. 3). Depths to basal shear surfaces of the active earth flows, however, were all less than 1.0 m; these basal shear surfaces were all several meters above the soil-bedrock contact (pl. 3).

Several auger borings not located on mapped earth-flow deposits revealed layers containing abundant or-

TABLE 4.—*Clay-mineral content of materials from the Davilla Hill earth-flow complex*

Sample	Location (pl. 3)		Clay-mineral content (percent)			
	Boring	Depth (m)	Kaolinite	Chlorite	Illite	Montmorillonite
Bedrock------	XIII	1.2	21.5	33.8	41.5	3.2
Earth-flow material 1.	VII	.2	23.3	36.4	40.3	0
Earth-flow material 2.	IV	.3	23.5	27.6	45.5	3.4
Earth-flow material 3.	IV	.8	20.3	26.9	51.2	1.6
Earth-flow material 4.	Pit 1	.4	17.3	20.7	52.3	9.7
Earth-flow material 5.	I	.3	20.8	20.4	55.3	3.5
Earth-flow material 6.	I	2.4	15.7	25.2	51.4	7.9
Average for earth-flow materials.		--	20.1	26.2	49.3	4.4

ganic material; these layers are interpreted as old topsoil horizons buried by earth flows. The presence of these buried topsoil layers, and the similarity between material outside and inside the mapped earth-flow deposits, suggest that most of the material outside the mapped deposits has also been deposited by earth flows.

STUDIES OF ACTIVE EARTH FLOWS AND GROUND-WATER CONDITIONS, 1974-78

SURFACE DISPLACEMENTS

Beginning in October 1974, lines of survey stakes were placed across the Davilla Hill earth-flow complex to monitor surface displacements (pl. 3). End points of the lines were placed outside the boundaries of the complex on ground that appeared to be stable. To measure displacements, a surveyor's tape was anchored between the two end stakes in each line, and the position of each stake in the horizontal plane relative to the tape was measured with a plumb bob and folding ruler. On the basis of repeated measurements made before earth-flow movements began, measurement errors were judged to be less than 3 cm, except where the distance from the stakes to the surveyor's tape exceeded 1 m, where errors may have been as large as 15 cm.

Surface displacements on earth flows within the complex were first recorded on February 21, 1975; on that date three earth flows (1, 2, 3, pl. 3) were active. Movement began between February 4 and 21; a survey on February 4 showed that no earth flows were active. A fourth earth flow (4, pl. 3) became active between March 8 and 15.

Neither the locations, shapes, nor boundaries of the active earth flows could have been predicted in advance, even from a careful examination of the complex. Only one earth flow (2, pl. 3) was bounded entirely by existing scarps and lateral shear surfaces; the other earth flows were bounded by lateral shear surfaces that cut across the boundaries of older earth-flow deposits.

On February 21, we noted that material in the active earth flows had softened markedly. This material remained soft as long as the earth flows were moving, whereas material making up the rest of the earth-flow complex remained stiff. The boundaries of active earth flows could, in fact, be mapped in a general way simply by testing the firmness of the surface. In spite of this softening, uncased auger holes in the active earth flows remained open and relatively undeformed while being transported several centimeters downslope.

The earth flows were active during a period of high precipitation, when the earth-flow complex was much

wetter than at other times. In the active earth flows, cracks were generally filled or nearly filled with water; elsewhere in the complex, the surficial material was wet, although the cracks generally did not contain so much water. A network of small streams carried runoff across the ground surface.

Figure 27 plots the displacements of all survey stakes on the active earth flows as a function of time. The calculated velocities of the earth flows (slopes of lines in fig. 27) varied over time and ranged from 1 to 39 cm/d. These velocities, however, were calculated from measurements taken several days apart and may not represent the true maximum or minimum velocities.

Surface movements on earth flow 1 were monitored by stake lines 2 and 2A[12]. The distribution of displacements indicated that most movement took place by shear on lateral shear surfaces or by differential displacement near the lateral shear surfaces; less than a third of the total displacement was due to internal deformation away from these boundary zones (fig. 28*A*). Surface displacements on earth flow 2 were monitored with a single survey stake (fig. 27), and so the spatial distribution of displacements was not determined. Although displacements of stakes were not measured in the vertical plane, observation of displacements of objects near the lateral shear surfaces indicated that movement of earth flows 1 and 2 was translational. Movement on earth flows 1 and 2 ceased between April 23 and June 19, 1975.

Surface displacements on earth flow 3, monitored by lines 3 and 3A (figs. 27, 28*B*, 28*C*), indicated that somewhat more internal deformation was taking place in this earth flow than in earth flow 1 (fig. 28), probably owing in part to differences in boundary conditions. Earth flow 1 had subparallel flanks where the survey line crossed it and was completely confined by flanking scarps; earth flow 3 had flanks that flared outward in the downslope direction, and material overflowed along the left flank in the zone of accumulation. Downslope from the point where this overflow occurred, forward tilting of the survey stakes during movement indicated that material was being rolled forward as if it were part of a caterpillar tractor tread. Two stakes were eventually washed away by an intermittent stream eroding the left flank of the earth flow (fig. 28*B*).

During movement, the main scarp of earth flow 3 grew in height from a few centimeters to slightly more than 2 m, owing to subsidence of the earth-flow surface in the zone of depletion. Striations near the top of one lateral shear surface, however, had plunges parallel to the surface slope; these features indicated that the initial movement was translational. Earth flow 3 stopped moving between March 21 and 31, 1975. Between these two dates, a gully was cut through the earth flow, and the drainage it provided probably caused the cessation of movement.

Material in earth flow 4 softened significantly between March 8 and 15, 1975; from this softening we inferred that the earth flow had begun to move. No survey stakes were placed on this earth flow to confirm its activity, however, and any movement that did occur could not be detected by visual inspection.

Fresh striations on the scarp on the left flank of the slump deposit (pl. 3) indicated that this landslide, too, moved during the winter of 1974-75, although its displacement was not surveyed, and so neither the amount nor the rate of displacement is known.

CORRELATIONS OF PRECIPITATION WITH MOBILIZATION AND RATE OF MOVEMENT

The interval of earth-flow activity in 1975 coincided with a period of high precipitation at Davilla Hill (fig. 25). Total precipitation during the winter of 1974-75 was above average, and more than two-thirds occurred in February, March, and April of 1975 (fig. 25), the months when most or all of the earth-flow movement took place.

Earlier in the winter, precipitation totaling 10.9 cm, between December 28, 1974, and January 9, 1975, did not cause any earth flows to mobilize. On the first 4 days of February 1975, an additional 8.8 cm of rain fell; yet no earth flows were active on February 4. However, 8.5 cm of additional precipitation occurred between February 4 and 21, and on February 21 three earth flows were active.

When the earth flows mobilized, the total precipitation after February 1 was between 8.8 and 17.3 cm, and the total annual precipitation between 29.9 and 38.4 cm. When earth flow 4 mobilized, the total precipitation after February 1 was between 22.1 and 24.1 cm, and the total annual precipitation between 43.2 and 45.2 cm. Once the earth flows mobilized, their velocities correlated with the amount of daily precipitation; that is, they moved rapidly during times when precipitation was high and relatively slowly during times when precipitation was low (fig. 27).

SUBSURFACE DISPLACEMENTS

In earth flow 1, subsurface displacements were measured by placing a stack of wooden disks in an augered borehole (borehole 10, pl. 3) and, later, excavating and measuring the displacement of each disk. On April 9, 1975, the disks, 3.33 cm in diameter and 1.27 cm

[12]Line 2A was installed after the stakes in line 2 were trampled by livestock.

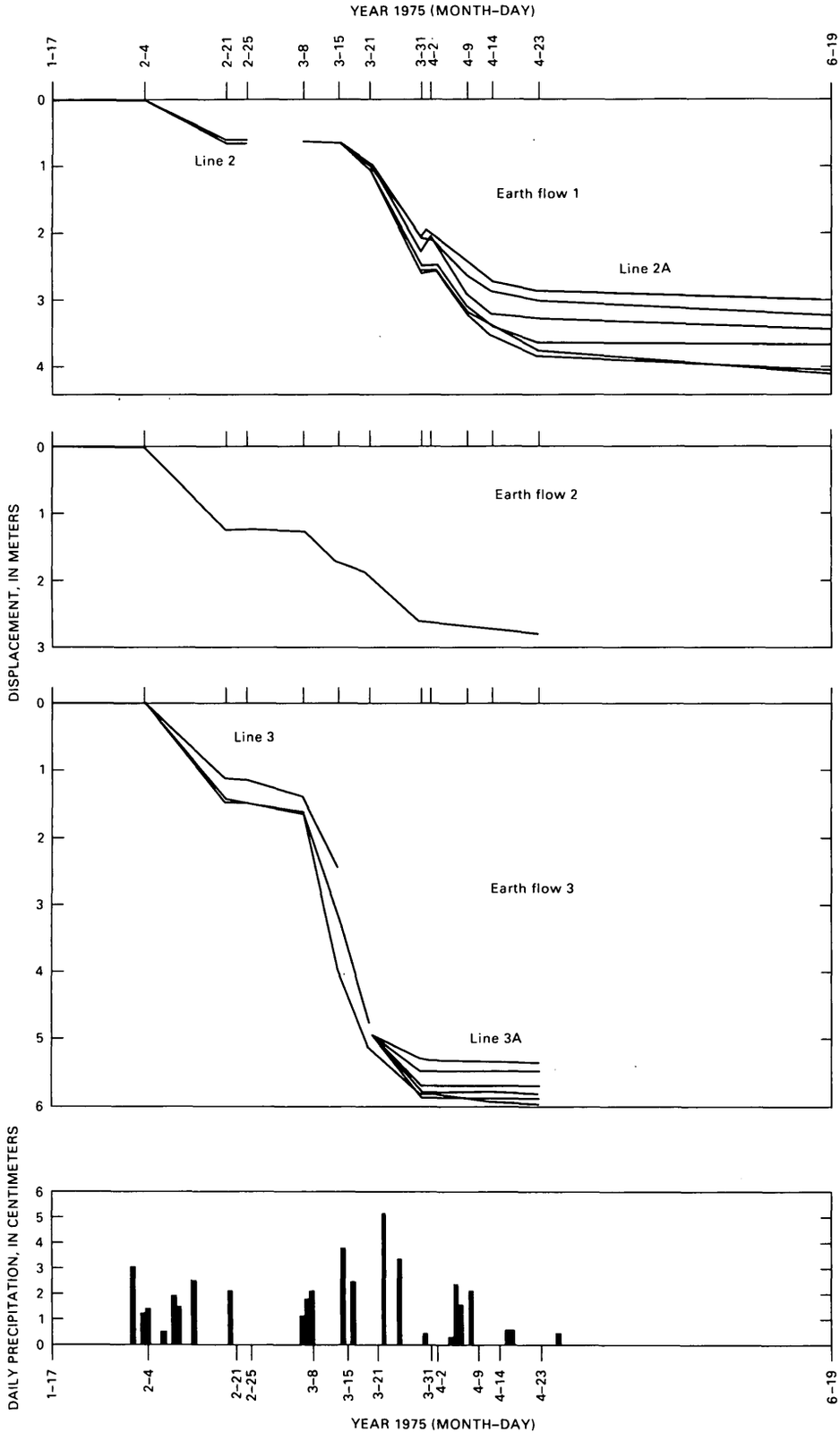

FIGURE 27.—Cumulative displacements of survey stakes on earth flows in Davilla Hill earth flow complex, January 17, 1975 to June 19, 1975. For stakes in lines 2A and 3A, previous displacements on surfaces of earth flows 1 and 3, respectively, were averaged to provide starting points for plots. See plate 3 for locations of stake lines.

thick, were placed in the borehole such that each was free to move independently. The disks were excavated on July 25, 1975, after earth flow 1 had stopped moving; figure 29*A* plots the measured displacements. A slickensided shear surface marked the base of the earth flow (fig. 29*B*). In all, 94 percent of the displacement observable at the ground surface occurred within 1.27 cm (the thickness of one disk) of the basal shear surface; little internal deformation had taken place.

Subsurface displacements were measured less

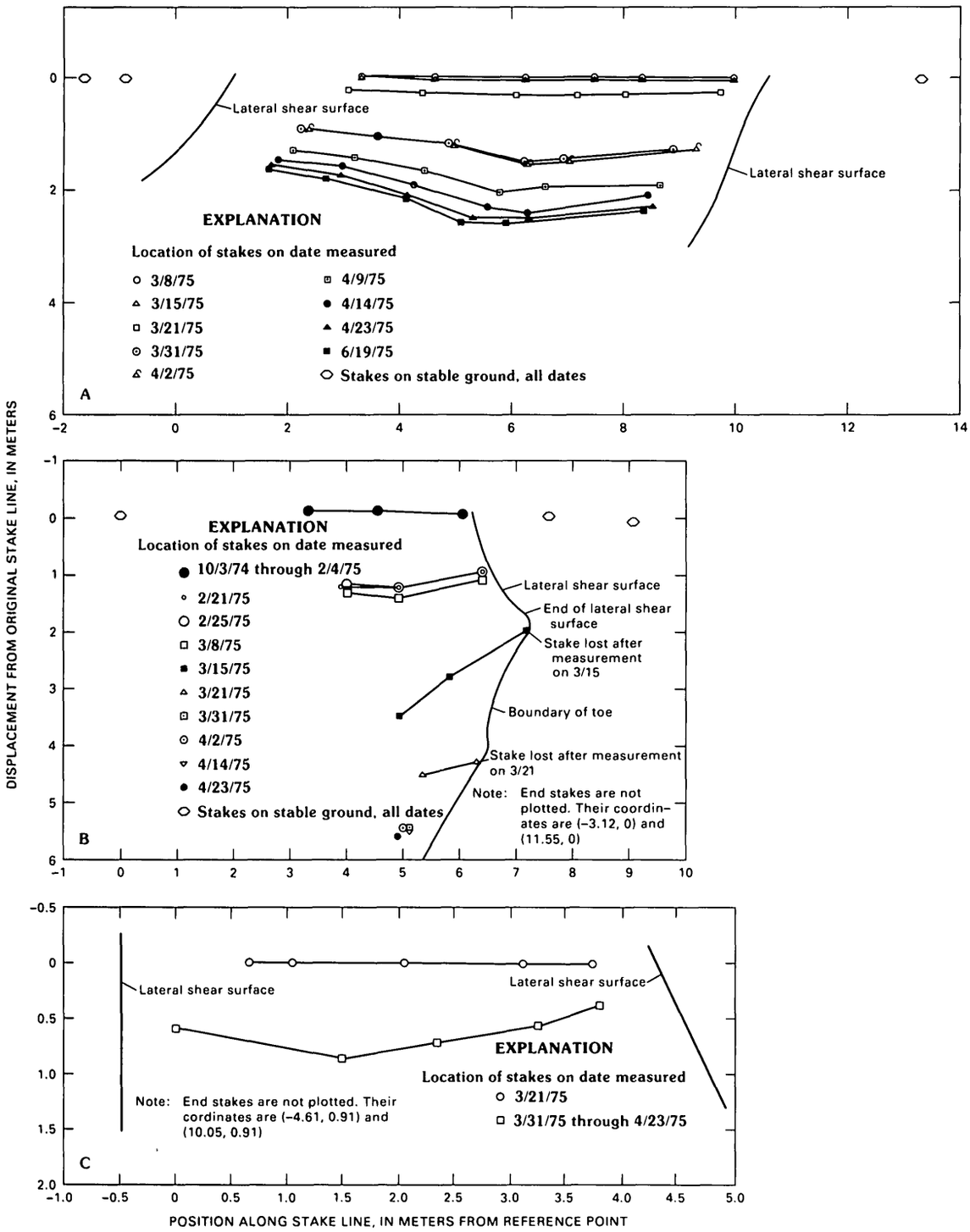

FIGURE 28.—Displacement of survey stakes on earth flows of the Davilla Hill earth-flow complex. See plate 3 for locations of stake lines. *A*, Line 2A of earth flow 1. *B*, Line 3 of earth flow 3. *C*, Line 3A of earth-flow 3.

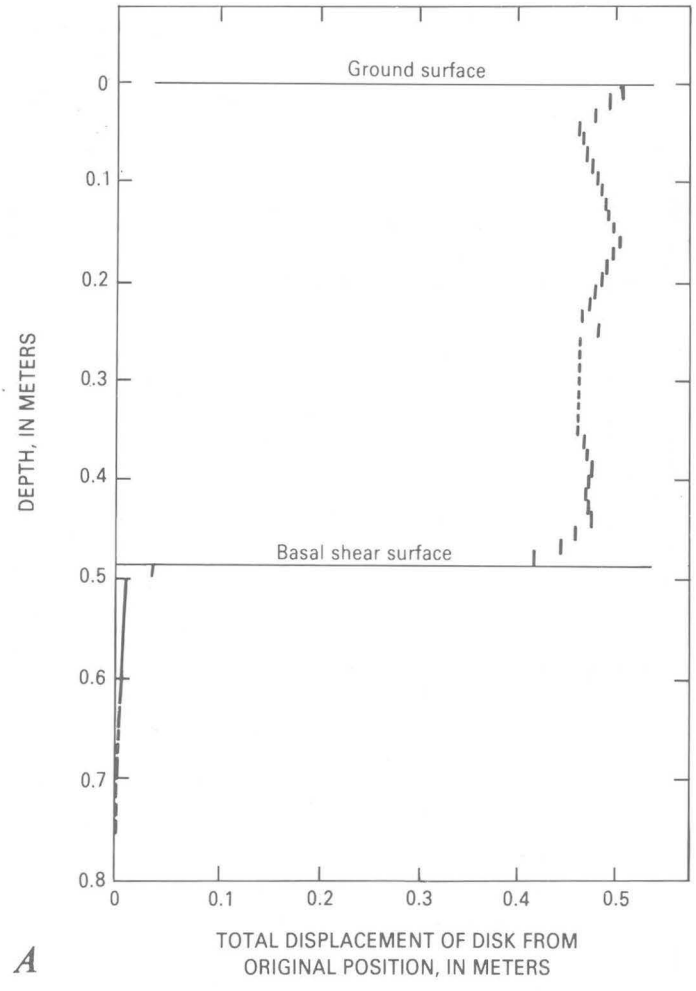

FIGURE 29.—Subsurface displacements measured by placing a stack of wooden disks in an augered borehole (borehole 10, pl. 3) on earth flow 1 of Davilla Hill complex. Disks emplaced on April 9, 1975; disks excavated and displacements measured on July 25, 1975. *A*, Subsurface displacement. Annular space created by difference between diameters of disks and borehole limited precision to ±1 cm. *B*, Slickensided basal shear surface is visible to left of stack of 3.33-cm-diameter disks. Below basal shear surface, annular space around disks remained open during earth-flow movement. View obliquely downward.

quantitatively in earth flow 3 by driving five stakes to different depths (15, 30, 46, 71, and 91 cm) in the zone of accumulation; spacings between stakes ranged from 17 to 56 cm. The stakes were emplaced on February 25, 1975. Between February 25 and March 15, 1975, the shortest stake toppled owing to softness of the surficial material, the stakes driven to 30 and 46 cm tilted downslope slightly, and the two longest stakes tilted downslope until they were buried by earth-flow material and were nearly horizontal. We concluded that the two longest stakes had penetrated below the basal shear surface and that their bases were being held in place while the stakes were rotated by earth-flow movement. Thus, the depth of the basal shear surface under the stake array was between 46 and 71 cm.

WATER LEVELS

During the interval when earth flows were active, water levels in the complex were measured in uncased boreholes (fig. 30). With one exception[13], water levels measured on active earth flows were within 23 cm of the ground surface. Except for borehole 1, water levels in inactive parts of the complex were lower than those in active earth flows. A striking difference between the water levels in boreholes 4 and 5 was noted on March 8, 1975. On that date, the water level in borehole 5, on an active earth flow, was at the ground surface, whereas that in borehole 4, 5 m away on an inactive part of the complex, was at a depth of 95 cm. The two boreholes had both been drilled on the same date (February 26, 1975) and to approximately the same depth.

Water-level measurements in open boreholes in fine soils give only approximate indications of the true ground-water level (Terzaghi and Peck, 1967; Hanna, 1973). The water-level measurements at Davilla Hill, however, conform to the more general observations in that the active earth flows appeared wet throughout and that water was standing at or near the surface in cracks on the active earth flows but not on inactive parts of the earth-flow complex.

WATER CONTENTS

The softening of the material that occurred when earth flows mobilized was accompanied by an increase in water content. From December 31, 1974, to April 9, 1975, water-content samples were taken at depths ranging from 0.05 to 2.0 m from 10 auger holes on the earth-flow complex (boreholes 1-10, pl. 3). Water contents were measured using standard laboratory techniques

[13]This exception—borehole 3 on February 26 (fig. 30)—was probably due to lack of sufficient time for equilibration of the water level; the measurement was made 4 days after the hole was drilled.

(Lambe, 1951); figure 31 shows the water-content profiles obtained. Excluding samples with high contents of organic matter, the average water content for soil in moving earth flows was 38.4 percent[14], the average for soil in inactive earth-flow deposits was 31.4 percent. Earth-flow mobilization, therefore, was accompanied by an average water-content increase of 7.0 percent.

Lateral shear surfaces formed sharp boundaries between the soft, wet material of the active earth flows and the stiffer, drier material in inactive earth-flow deposits. On February 26, 1975, for example, water-content samples were taken a few millimeters apart on either side of a lateral shear surface of earth flow 2 at a depth of a few centimeters. The soft sample in the active earth flow had a water content of 38.3 percent; the stiffer sample from the immobile material had a water content of 33.7 percent.

The existence of similar sharp boundaries beneath earth flows was suggested by distinct increases in resistance to augering felt when auger borings penetrated basal shear surfaces. Because the augering disturbed the structure of the earth-flow material, it prevented a precise determination of water-content distribution near the basal shear surfaces of active earth flows. However, measurements in a pit (1, pl. 3) excavated through earth flow 1 after movement had stopped showed that soil within a few millimeters of the basal shear surface had an elevated water content (fig. 32). This result suggests that thin zones surrounding the basal shear surfaces had elevated water contents while the earth flows were active. Similar basal zones of elevated water content were described by Hutchinson (1970).

UNIT WEIGHTS, VOID RATIOS, AND SATURATION

Table 5 lists the unit weights, void ratios, and saturations of one sample from earth flow 2 and of two samples from earth flow 3. Samples were obtained by pushing thin-walled aluminum cylinders, 9.8 cm in diameter and 10.5 cm high, into the soil and trimming the ends of the samples flush with the ends of the cylinders. The samples were placed in airtight containers, and total weights were measured in the laboratory. Water contents were calculated from measurements made on material trimmed off the samples in the field and placed in separate airtight containers.[15]

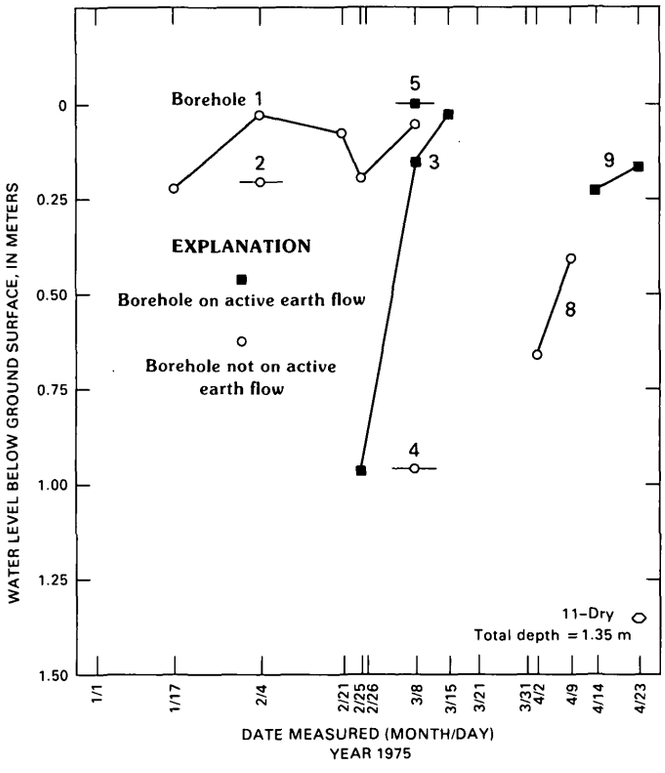

Borehole	Date drilled	Borehole depth (m)
1	12/31/74	0.75
2	1/17/75	1.60
3	2/21/75	1.30
4	2/26/75	1.42
5	2/26/75	1.24
8	3/31/75	1.12
9	4/09/75	1.12
11	4/14/75	1.32

FIGURE 30.—Water levels in boreholes on Davilla Hill earth-flow complex, January 17, 1975 to April 23, 1975. See plate 3 for locations of boreholes (numbers 1-5, 8, 9, 11).

LABORATORY SWELL TESTS

Laboratory swell tests were performed to determine whether the increase in water content that accompanied earth-flow mobilization was due to an increase in saturation, in void ratio, or both. To perform these tests, two naturally desiccated samples of material from inactive earth-flow deposits were placed in standard fixed-ring consolidometer cells, 7.6 cm in diameter. Water was added to the samples, and they were allowed to swell or consolidate under conditions of low vertical stress (0.20 kN/m^2). These conditions of low vertical stress simulated the conditions of low overburden stress in the earth flows. In the consolidation cells, the samples were prevented from expanding laterally; vertical expansion or consolidation was measured with dial

[14]Water content $w_n = 100$(weight of water)/(weight of dried soil).

[15]Although the samples from earth flow 3 were obtained several days after movement had stopped, water contents of the samples were in the same range as those of material in active earth flows. This result indicated that only minor desiccation of the material had taken place after cessation of movement.

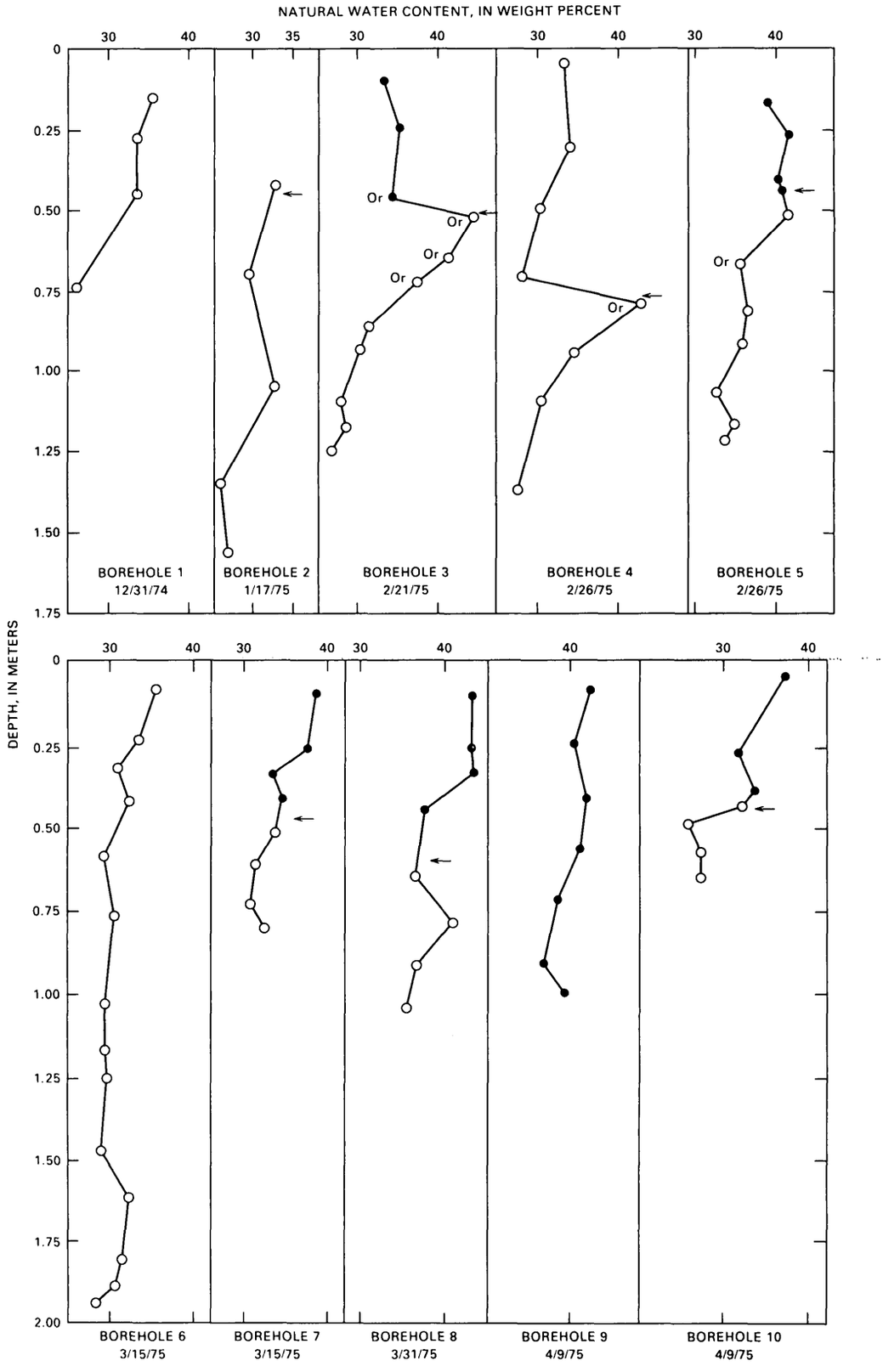

FIGURE 31.—Natural water contents in Davilla Hill earth-flow complex, December 31, 1974, to April 9, 1975. Dots indicate determinations in active earth flows; circles, determinations in immobile earth-flow material; arrow, basal shear surface; Or, sample rich in organic matter. Date below borehole indicates date drilled and sampled. See plate 3 for locations of boreholes.

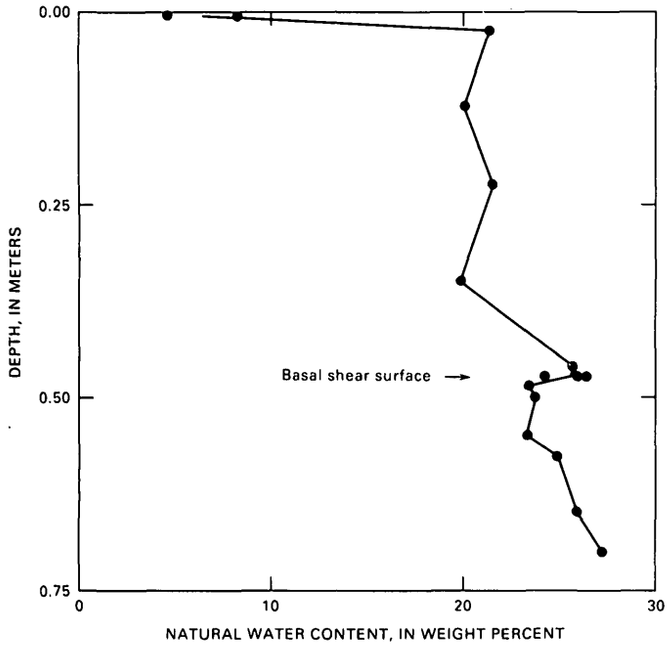

FIGURE 32.—Natural water contents in pit 1 of Davilla Hill earth-flow complex, July 25, 1975, showing elevated water content near basal shear surface.

gages. The tests were run for 118 hours (sample 1) and 115 hours (sample 2); however, 90 percent of the volumetric expansion occurred during the first hour. Water contents, void ratios, and saturations were calculated at the beginning and end of each test.

Table 6 lists the results of these swell tests. The average water-content increase was 7.2 percent, an amount that corresponded closely to the 7.0-percent average increase measured in the field. Thus, addition of water to immobile earth-flow material was sufficient, by itself, to bring about the water-content increase that accompanied earth-flow mobilization; no remolding or other disturbance of the internal structure of the soil was necessary.

The final void ratios and saturations of the samples also corresponded closely to values measured in the field (tables 5, 6). During the tests, the average saturation increased by 14.5 percent whereas the average volumetric increase was only 1.6 percent. Thus, the increase in water content was due primarily to an increase in saturation with little accompanying volume change.

TABLE 5.—*Unit weights, void ratios, and saturation of Davilla Hill earth-flow material*

[Natural water content = 100(weight of water)/(weight of solids). Total unit weight = (total weight)/(total volume). Dry unit weight = (weight of solids)/(total volume). Void ratio = (volume of pore spaces)/(volume of solids). Saturation = 100(volume of water)/(volume of pore spaces)]

Earth flow	Sample depth (m)	Natural water content (percent)	Total unit weight (kN/m^3)	Dry unit weight (kN/m^3)	Specific gravity of solids	Void ratio	Saturation (percent)
2	0.18	38.9	17.1	12.3	2.75	1.20	89.3
3	.05	34.1	17.5	13.0	2.75	1.07	87.4
3	.23	37.4	17.7	12.9	2.75	1.10	93.7
Average----------		36.8	17.4	12.7	2.75	1.12	90.1

TABLE 6.—*Laboratory swell tests on Davilla Hill earth-flow material*

[Volumetric expansion = 100(final volume - initial volume)/initial volume]

Sample	Water content (percent)			Saturation (percent)			Void ratio		Volumetric expansion (percent)
	Initial	Final	Increase	Initial	Final	Increase	Initial	Final	
1	32.7	39.5	6.8	76.5	90.0	13.5	1.15	1.18	1.5
2	31.9	39.4	7.5	80.8	96.3	15.5	1.07	1.10	1.6
Average--	32.3	39.5	7.2	78.7	93.2	14.5	1.11	1.14	1.6

A

Piezometer	Date drilled	Borehole depth (m)	Depth of basal shear surface (m)	Bedrock depth (m)	Depth of piezometer tip (m)	Remarks
I	10/23/75	2.82	0.84	2.24	2.13 - 2.74	—
II	10/25/75	0.46	—	—	0.32 - 0.37	Destroyed between 4/27/76 and 5/20/76
III	10/15/75	1.52	—	—	1.32 - 1.37	—
IV	10/22/75	.77	—	—	.61 - .66	Destroyed between 4/27/76 and 5/20/76
V	10/22/75	2.06	—	—	1.88 - 1.93	Destroyed between 11/16/75 and 12/31/76
VI	10/20/75	2.67	—	2.54	1.93 - 2.57	—
VII	10/20/75	1.28	.99	—	1.17 - 1.22	—
VIII	10/16/75	.99	—	—	.84 - .89	—
IX	10/16/75	4.37	—	4.22	3.58-4.19	—
X	11/04/75	2.74	—	—	2.01 - 2.62	—
XI	11/04/75	1.75	—	1.73	1.52 - 1.57	Destroyed between 1/6/78 and 1/30/78
XII	11/04/75	2.77	—	Surface	2.64 -2.69	—
XIII	10/16/75	1.83	—	Surface	1.70 - 1.75	—
IVA	1/14/77	approx .9	—	—	.79 - .84	—
VA	1/14/77	approx 1.3	—	—	1.17 - 1.22	—
VIIA	1/14/77	approx 1.5	—	—	1.40 - 1.45	—
VIIIA	1/14/77	approx 1.0	—	—	.86 - .91	—

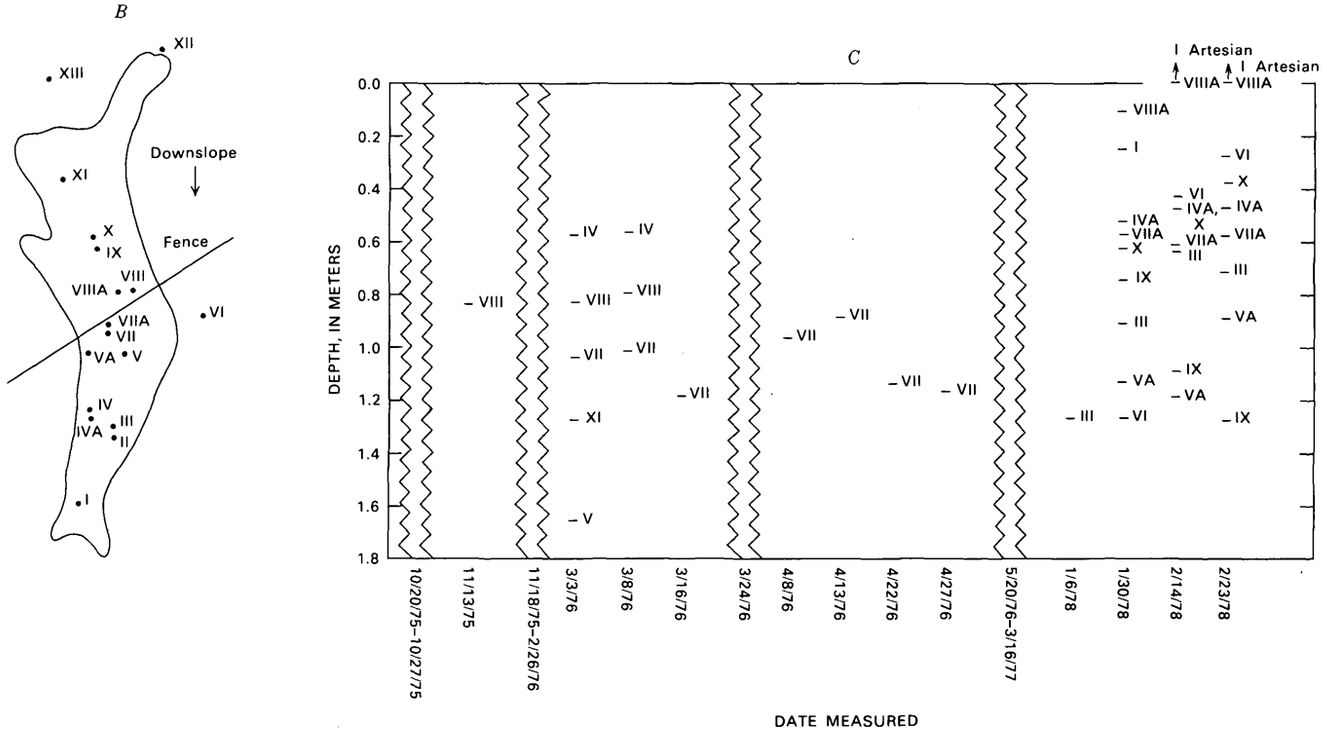

FIGURE 33.—Piezometric measurements on Davilla Hill earth-flow complex. *A*, Piezometer depths, dates of installation, and dates of destruction. *B*, Sketch map showing piezometer locations. See plate 3 for detail. *C*, Water levels in piezometers. *D*, Dates of piezometer measurements and precipitation data for observation period. Circles indicate that all piezometers were dry; dots indicate water in one or more piezometers.

PIEZOMETRIC AND TENSIOMETRIC MEASUREMENTS: AUGUST 1975-FEBRUARY 1978

From August 1975 through February 1978, groundwater levels and pore-water pressures were measured using portable tensiometers and open-standpipe piezometers (fig. 33). Piezometers I, VI, IX, and X (pl. 3) had standard, Casagrande-type porous stone tips, 60 cm long and 4 cm in diameter; all other piezometers had porous ceramic tips, 6 cm long and 2 cm in diameter, that were specifically designed for use in unsaturated soils. The tensiometers, manufactured by Soilmoisture, Inc., of Santa Barbara, Calif., measured both positive and negative pore-water pressures at depths as great as

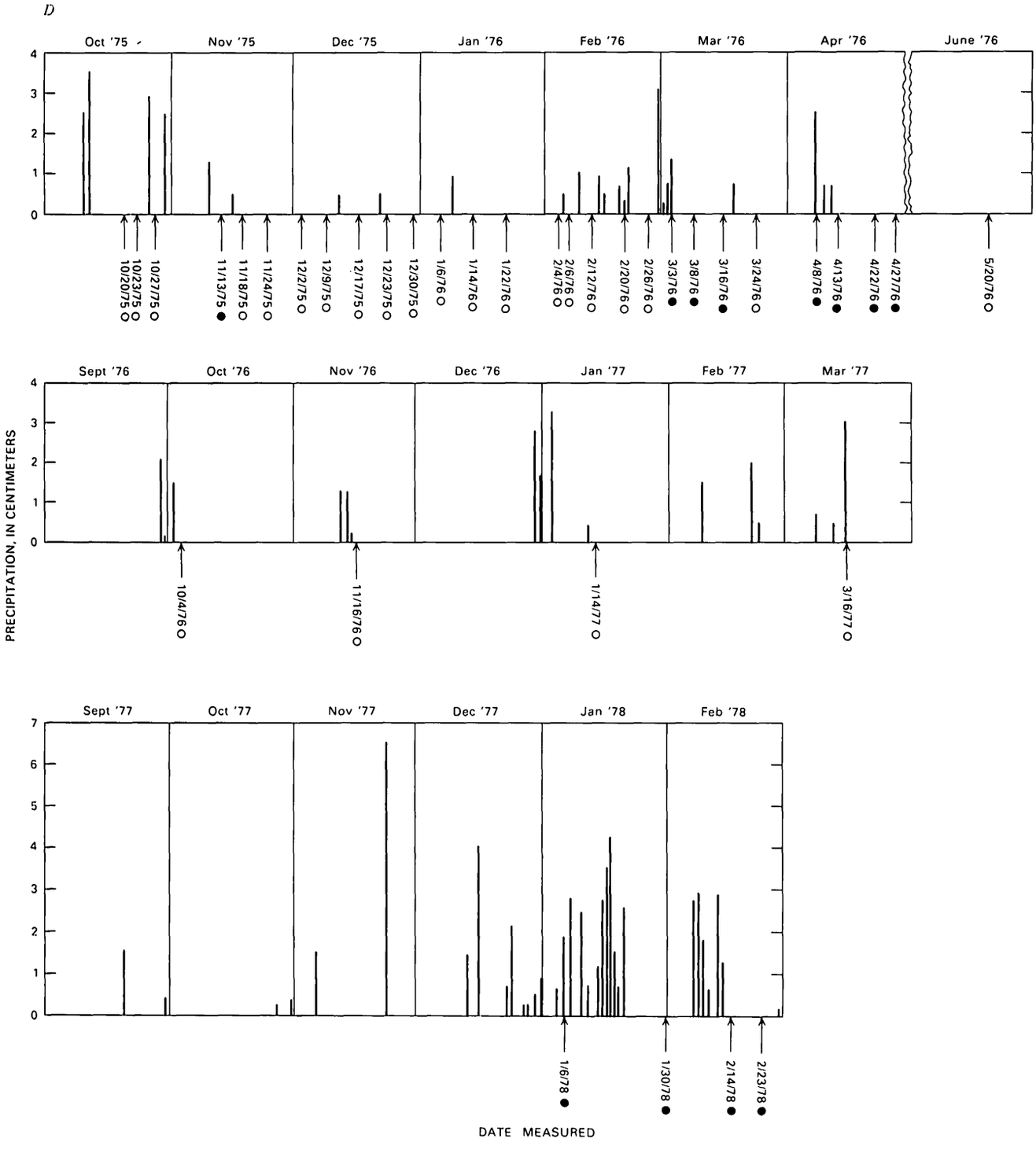

61 cm. The tensiometers and piezometers were installed according to manufacturers' instructions and the procedures described by Keefer (1977a).

No earth flows were active at Davilla Hill during the period July 1975 through December 1977; the winter of 1975-76 was the driest ever recorded in the San Francisco Bay area (San Francisco Chronicle, 1976, p. 1), and the subsequent winter was almost as dry.[16] On most

[16]Total annual precipitation at Davilla Hill was 29.45 cm in 1975-76 and 31.59 cm in 1976-77. These values are 49 and 53 percent, respectively, of the 10-year average annual precipitation.

survey dates during this period, all the open-standpipe piezometers were dry (fig. 33), an observation indicating that no ground water was present in or adjacent to the earth-flow material.

The shallow piezometers did contain water during four brief periods after moderate-size storms (fig. 33); water levels in these piezometers ranged from 0.57 to 1.66 m below the ground surface (fig. 33). During these four periods, several other piezometers, including all those with tips deeper than 1.8 m, remained dry. The absence of water in the deep piezometers at times when water was recorded in some of the shallow piezometers suggests that localized bodies of perched ground water were formed in parts of the complex after moderate rainfall. Rapid response of the piezometers after storms (apparently within 8 hours in the case of the April 8, 1976, measurement) indicated that rainfall infiltrates rapidly into shallow layers of the earth-flow complex.

Two earth flows became active near the head of the reentrant between January 6 and January 30, 1978 (pl. 3); activity may have continued into February, although this observation could not be ascertained because no displacement measurements were made. Piezometric measurements on January 30, February 14, and February 23 showed free water in all the piezometers within the earth-flow complex; water levels ranged from 1.28 m below the ground surface to slightly artesian (fig. 33). Water levels in the two active earth flows were not measured because earth-flow movement destroyed the one appropriately placed piezometer (XI, pl. 3). The piezometric measurements, however, confirm observations in 1975 that ground-water levels in the complex were near the surface when earth flows were active. Earth-flow activity in 1978 also occurred during a period of high precipitation; precipitation in Eden Canyon totaled 10.4 cm in December 1977, 25.8 cm in January 1980, and 12.6 cm in February 1980. Total annual precipation when the earth flows began moving was between 26.4 and 46.2 cm.

All but three of the 68 tensiometric measurements made on 21 different dates from August 1975 through February 1978 showed that pore-water pressures 61 cm below the ground surface were negative. This result conformed to observations and piezometric measurements showing that ground-water levels were generally deeper than 61 cm during times when earth flows were inactive (fig. 33). Pore-water pressures were generally less negative after rainstorms than at other times. Slightly positive pore-water pressures (at least 4.2 kPa) were recorded on November 18, 1975, and on February 23, 1978. Owing to instrument failure, no tensiometric measurements were made on January 30, 1978, or February 14, 1978, two of the three dates on which the water levels in piezometers were highest.

ANALYSIS OF MOBILIZATION

The earth flows at Davilla Hill moved primarily by shear along slickensided boundary shear surfaces. The predominance of boundary shear at Davilla Hill, as well as the work of previous investigators (Hutchinson, 1970; Hutchinson and Bhandari, 1971; Chandler, 1972; Hutchinson and others, 1974; Dunkerley, 1976; Fussgänger and Jadroň, 1977; Prior, 1977), indicates that a method of slope-stability analysis can be applied to the earth-flow mobilization at Davilla Hill. Slope-stability analysis combines the principles of equilibrium mechanics, the Coulomb failure criterion for soils, and Terzaghi's theory of effective stress to analyze the potential for initiation of movement along a discrete shear surface in a soil slope.

Figure 34 illustrates this method of analysis for the simplified case of a block on a uniformly inclined plane.

According to the principles of equilibrium mechanics, the block will begin to move when the driving force L exceeds the resisting force T by an infinitesimal amount. L is the component of the block's weight acting in the downslope direction; that is,

$$L = \gamma_t V sin\Theta,$$

where γ_t = the unit weight of material in the block,
V = the total volume of the block,
and Θ = the angle of slope inclination.

In the case of a soil body, T is the product of the area of the base of the block and the shear resistance of the soil, which is defined by the Coulomb failure criterion as modified by Terzaghi's theory of effective stress. Thus,

$$T = \int_A \tau \cdot dA$$

where τ = the shear resistance of the soil
and A = the area of the base of the block.
The shear resistance is defined by

$$\tau = (\sigma_n - u) \tan \bar{\phi} + \bar{c}, \quad (1)$$

where σ_n = the normal stress at a point on the base of the block,
u = the pore-water pressure at a point on the base of the block,
$\bar{\phi}$ = the effective angle of internal friction,
and $\bar{c}$ = the effective cohesion.
The quantity $(\sigma_n - u)$ is the effective stress, as defined by Terzaghi (1924). The result of a slope-stability analysis is expressed as a factor of safety F, where $F = T/L$. A condition $F = 1$ corresponds to the initiation of movement; if $F > 1$, no movement can occur.

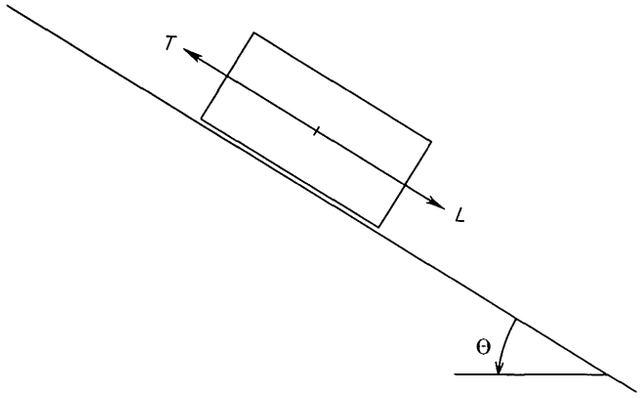

FIGURE 34.—Stability of block on inclined plane. T, resisting force; L, driving force; Θ, angle of slope inclination. See text for explanation of stability analysis.

Mobilization of earth flows at Davilla Hill was analyzed using a modified form of the slope-stability analysis developed by Morgenstern and Price (1965, 1967). This analysis treats the irregular geometries and nonuniform conditions in earth flows by dividing an earth flow into a finite number of slices with vertical sides, determining the differential equations governing the force and moment equilibrium of each slice, and numerically integrating the results along the basal shear surface. The modified Morgenstern-Price method, which was programmed on a PDP8 minicomputer, was described in more detail by Keefer (1977a).[17]

MEASUREMENT OF SHEAR-STRENGTH PARAMETERS, USING DIRECT-SHEAR TESTS

Soil shear-strength parameters $\bar{\phi}$ and $\bar{c}$, required for the analysis, were measured using laboratory direct-shear tests. The direct-shear test simulates field conditions of boundary shear on earth flows by forcing shear displacement on a sample to occur in a thin well-defined zone. A constant vertical load is applied to the sample during shear, and shear resistance of the soil in the horizontal plane is measured. By performing several tests under different vertical loads, a Mohr-Coulomb failure envelope and the shear strength parameters $\bar{\phi}$ and $\bar{c}$ can be determined. By cycling the direction of shear, the direct shear test can also simulate the effects of such large shearing displacements as occur along natural shear surfaces (Skempton and Hutchinson, 1969). A general discussion of the direct-shear testing method was given by Lambe (1951).

Two samples from the basal shear surface of earth flow 1 were tested on a Wykeham-Farrance direct-shear machine, which had a cylindrical shear box 6.35 cm in diameter. The samples were hand excavated from a pit (2, pl. 3) and were trimmed in the laboratory to fit the direct-shear apparatus. The basal shear surface was placed in the plane separating the two halves of the shear box, and the slickensides were alined parallel to the direction of shear displacement.

Samples were obtained from a depth of 69 cm, where the normal stress caused by the weight of material above the basal shear surface was $\sigma_n = 11.7$ kN/m^2. Assuming that maximum pore-water pressures were associated with a ground-water level at the ground surface, the minimum effective on site normal stress was $\sigma_n = 5.1$ kN/m^2. Each sample was sheared under four different normal (vertical) stresses ranging from 5.3 to 19.1 kN/m^2. Thus, values of $\bar{\phi}$ and $\bar{c}$ were measured over approximately the same range of effective normal stresses as those encountered on site as the ground-water table rose from the basal shear surface to the ground surface. Samples were sheared at a displacement rate of 9.75×10^3 mm/min, a rate assumed to be slow enough to allow for complete dissipation of shear-induced pore-water pressures.[18]

Samples were consolidated under each normal load for 12 to 24 hours before being sheared. Under the first increment of normal load, each sample was sheared through a distance of 3.5 mm for each of 12 cycles (6 forward and 6 reverse); under subsequent loads, the samples were sheared for 8 cycles. Decreases in strength were observed on successive cycles under many normal loads, but the strength loss was generally small after the first two cycles under each load.

Mohr-Coulomb failure envelopes were determined from straight-line fits of shear resistances measured during the final forward and final reverse cycles under each vertical load for each sample (fig. 35). Results from tests on the two samples agree closely with each other: for sample 1, $\bar{\phi} = 15.8°$ and $\bar{c} = 0.50$ kN/m^2; and for sample 2, $\bar{\phi} = 15.2°$ and $\bar{c} = 0.55$ kN/m^2. The average effective shear-strength parameters, therefore, were $\bar{\phi} = 15.5°$ and $\bar{c} = 0.525$ kN/m^2.

During shear, the samples generally consolidated slightly, although on many cycles this general trend was interrupted by one or more periods of dilatation; dilatation was greatest under the lowest vertical loads. The shear surfaces in the samples were not perfectly planar, and so we concluded that this intermittent dilatation was due to riding up of the top half of the sample over asperities.

[17] A preliminary analysis, described by Keefer (1977a), showed that the lateral shear surfaces of the earth flows contribute negligibly to the total shear resistance. Therefore, the contribution of the lateral shear surfaces was ignored, and a two-dimensional analysis was used.

[18] A later test, in fact, showed that increasing the displacement rate to as high as 1.2 mm/min causes only minor changes in shear resistance (see fig. 40).

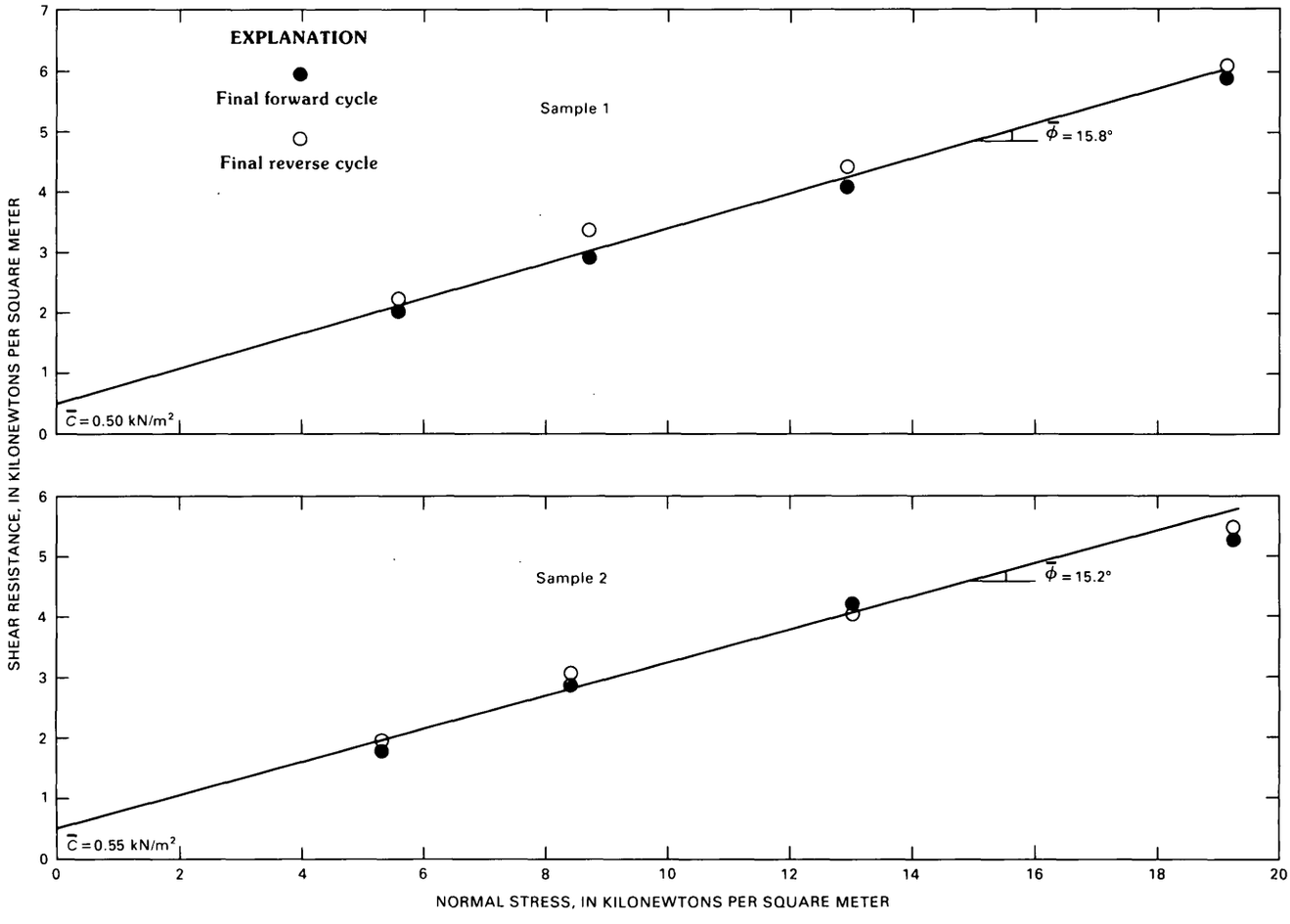

FIGURE 35.—Mohr-Coulomb failure envelopes for direct-shear tests on basal-shear-surface material in earth flow 1 of Davilla Hill earth-flow complex. ϕ, effective angle of internal friction; c, effective cohesion.

For most soils containing a large portion of clay, $\bar{\phi}$ and $\bar{c}$ decrease with increasing shear displacements. At very large displacements, values of $\bar{\phi}$ and $\bar{c}$ approach lower bounds known as residual values, $\bar{\phi}_r$ and $\bar{c}_r$ (Skempton and Hutchinson, 1969). The direct-shear tests were performed on samples containing parts of the basal shear surface along which several meters of movement had already occurred; thus, the values of $\bar{\phi}$ and $\bar{c}$ measured in the tests were probably approximately equal to the residual values for this earth-flow material.

SLOPE-STABILITY ANALYSIS OF EARTH FLOWS

Slope-stability analysis was applied to the three earth flows shown by direct measurement of displacements to be active (1, 2, 3, pl. 3). Required for the analysis are: the shear-strength parameters $\bar{\phi}$ and $\bar{c}$, the configurations of the ground surface and basal shear surface of each earth flow (pl. 3), the total and dry unit weights of the soil (table 5), and the pore-water pressure at specified points on the basal shear surfaces.

Pore-water pressures were known only rather imprecisely. However, field observations and measurements indicated that the earth flows had mobilized when ground-water levels within them rose to levels intermediate between the basal shear surfaces and the ground surface (figs. 30, 33). A rise in the ground-water level in an earth flow would cause the shear resistance in the soil, as defined by equation 1, to decrease owing to increases in pore-water pressure. We hypothesized that increased pore-water pressure is the mechanism that mobilizes the earth flows.

To test our hypothesis, we analyzed earth flows 1, 2, and 3, and treated the pore-water pressure as variable. An initial analysis was performed on each earth flow for conditions of no pore-water pressure ($u = 0$) on the basal shear surface. Several subsequent analyses were then performed for various elevations of the water table in each earth flow. In all cases, pore-water pressures were computed on the assumptions that the slope of the water table was uniform and parallel to the average slope of the ground surface and that permeability

and ground-water flow in the soil were uniform. The factor of safety F for each earth flow was then plotted as a function of the average depth of the water table below the ground surface (fig. 36).

All three earth flows were immobile ($F>1$) for conditions of zero pore-water pressure on the basal shear surfaces; all three earth flows reached the condition of mobilization ($F=1$) when the water table was at some depth intermediate between the basal shear surface and the ground surface (fig. 36). Results of these analyses thus agree well with observational data on water levels (figs. 30, 33) and indicate that pore-water pressures induced by rising water tables did, indeed, mobilize the earth flows.

DISCUSSION

Field observations show that the earth flows at Davilla Hill are mobilized by addition of water to the soil; our combined field, laboratory, and analytical studies indicate the mechanism by which this mobilization takes place. During seasons when little rain falls at Davilla Hill, potential earth-flow material is unsaturated; the material is disrupted by a network of cracks and is subjected to negative pore-pressures. During periods of high precipitation, water infiltrates into the earth-flow complex, locally saturates the fissured near-surface material, and dissipates these negative pore-pressures. After moderate precipitation, local bodies of perched ground water form; with additional precipitation, a continuous body of ground water forms. As the water table associated with this body rises to near the ground surface, pore-water pressures increase on potential failure surfaces within the earth-flow material. When the pore-water pressures locally exceed threshold values, earth flows are mobilized.

Most movement on the earth flows at Davilla Hill takes place by boundary shear, and the water-content changes that accompany mobilization can be accounted for by addition of water without any internal disturbance or remolding. Internal disturbance and remolding, therefore, play only a minor role in the earth-flow process at Davilla Hill; the material is mobilized by the addition of water alone. The main effect of this addition of water is to increase the pore-water pressures.

Earth flows at Davilla Hill recur year after year in the same materials. This recurrence is due, in part, to the moderate velocities at which the earth flows move; because of these moderate velocities, the earth flows move only a few meters during a single winter. Thus, many years and many remobilizations are required before the earth-flow material reaches the gentle slopes near the present downslope boundary of the complex.

Slope-stability analysis indicates that rising pore-water pressure is the mechanism mobilizing earth flows out of the older earth-flow materials. The question remains, how were earth flows originally mobilized at Davilla Hill? Using upper-bound, peak values of shear-strength parameters measured in a Geonor simple-shear apparatus ($\bar{\phi}_p=25.4°$, $\bar{c}_p=5.0$ kN/m^2), Keefer (1977a) reported that earth flows cannot mobilize out of soil at peak shear resistance on the slopes presently existing at Davilla Hill, even with a water table at the ground surface. The near-surface soil at Davilla Hill, however, is pervasively fissured, and this fissuring reduces the shear resistance of the soil mass below its peak value. If the soil were sufficiently weakened by these fissures, then pore-water pressures caused by a water table at the ground surface could mobilize earth flows out of previously undisturbed material in the same way that earth flows were mobilized out of older earth-flow material during the study period.

Two field observations indicated that fissures significantly reduce the shear resistance of the soil mass. First, the maximum depth of the earth flows that mobilized in 1975 and 1978 coincides with the depths of the deepest extension and desiccation fissures. This coincidence, due partly to the way in which the network of fissures facilitates the infiltration of water, is also probably due partly to a reduction in soil-mass shear strength. Second, boundaries of active earth flows consistently cut across boundaries of older earth-flow deposits, rather than utilizing existing lateral shear surfaces. This observation suggests that the shear resistance of the fissured soil mass is not significantly higher than that along the shear surfaces.

Even without weakening of the soil by fissuring, earth flows could be mobilized at Davilla Hill out of material previously undisturbed by mass movement, if artesian conditions were to raise pore-water pressures sufficiently above those due to a water table at the ground surface. Artesian conditions do sometimes exist in some parts of the complex (fig. 33).

Because the geometries of and ground-water conditions within the earth flows that originally formed at Davilla Hill are unknown, a rigorous slope-stability analysis is not possible. However, the weakening of the near-surface soil by fissures and the presence of local artesian ground-water levels suggest that earth flows can be mobilized out of previously undisturbed material in the same way that earth flows are mobilized out of older earth-flow deposits.

A MODEL FOR EARTH FLOW

Analysis of the earth flows at Davilla Hill and at sites in England (Hutchinson, 1970; Hutchinson and Bhandari, 1971), northern Ireland (Hutchinson and

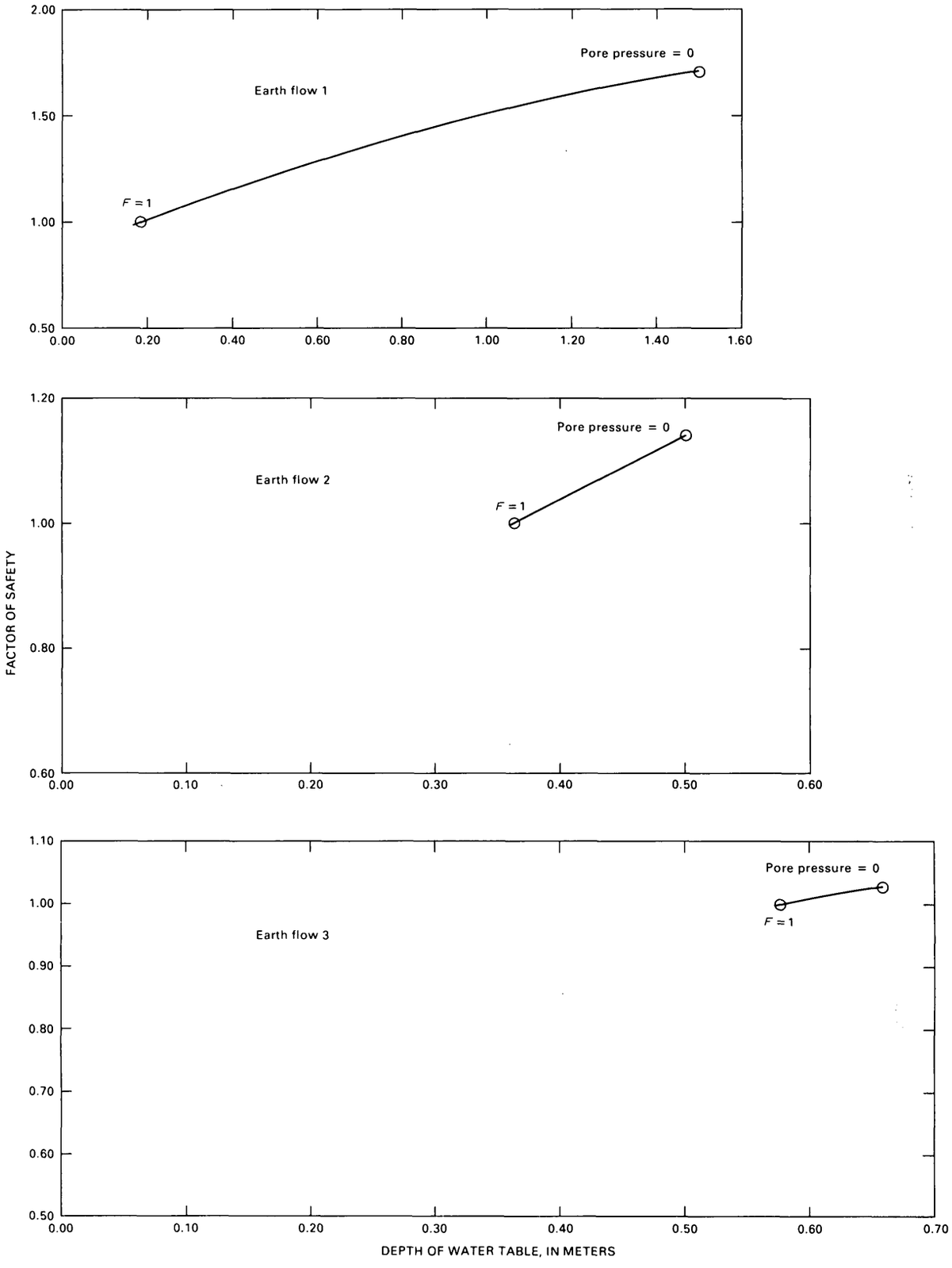

FIGURE 36.—Mobilization of earth flows in Davilla Hill earth-flow complex, showing factor of safety F as a function of water-table depth. Mobilization occurs when $F = 1$.

others, 1974), and Czechoslovakia (Fussgänger and Jadroň, 1977) indicate that earth-flow mobilization, in general, can be explained by a slope-stability model of soil mechanics that incorporates the effects of pore-water pressure. This model is also useful as a starting point for analyzing how the velocity of a moving earth flow is governed; this aspect of earth-flow behavior, however, requires additional analysis. The main purposes of this section are to discuss mobilization and to propose a model to explain the behavior of moving earth flows.

EARTH-FLOW MOBILIZATION

The slope-stability model explains earth-flow mobilization and several other characteristics of earth flows. In every active earth flow to which this analysis has been applied, rising pore-water pressure was shown to be capable of causing mobilization (Hutchinson, 1970; Hutchinson and Bhandari, 1971; Hutchinson and others, 1974; Fussgänger and Jadroň, 1977; Keefer, 1977a, b, c; Keefer and Johnson, 1978). At Davilla Hill and at most other earth-flow sites, pore-water pressures necessary for mobilization were generated by infiltration of water. In a few earth flows, necessary pore-water pressures were created by rapid loading of the zones of depletion by material from other earth flows. This rapid loading created pore-water pressures in excess of those that would result from a water table at the ground surface. At sites where these excess pore-water pressures were generated, earth flows were observed to move on slopes as gentle as 4° (Hutchinson and Bhandari, 1971; Hutchinson and others, 1974), and Hutchinson and Bhandari calculated that this mechanism could allow earth flows to move on even gentler slopes.

Two more general observations support the conclusion that rising pore-water pressure is, in general, the cause of earth-flow mobilization. First, earth flows throughout the world commonly mobilize during times of high precipitation or seasonal snowmelt (Rapp, 1960; Radbruch and Weiler, 1963; Campbell, 1966; Prior and others, 1968, 1971; Hutchinson, 1970; Hutchinson and others, 1974; Nilsen and Turner, 1975; Oberste-Lehn, 1976; Keefer, 1976, 1977a; Kelsey, 1977, 1978; Swanson and Swanston, 1977; Harden and others, 1978; Nolan and others, 1979; Janda and others, 1980). During such times, infiltration of water into hillside materials causes pore-water pressures to rise. Second, many earth flows occur on hillsides underlain by impermeable rock or soil layers that have dips parallel to the ground surface (Sharpe and Dosch, 1942; Kachadoorian, 1956; Prior and others, 1968; Záruba and Mencl, 1969); such geologic settings are conducive to the formation of perched water tables with resulting high pore-water pressures.

Nothing fundamental in the slope-stability model requires a minimum, threshold slope for earth-flow occurrence, and, where excess pore-water pressures are generated, earth flows can move on very gentle slopes (Hutchinson and Bhandari, 1971; Hutchinson and others, 1974). However, in most areas where systematic studies have been carried out, earth flows originate only on slopes with inclinations greater than some threshold value (Radbruch and Weiler, 1963; Dunkerley, 1976; Turnbull, 1976; Harden and others, 1978; fig. 3). The minimum slope inclination on which an earth flow can mobilize, according to the slope-stability model, depends on the unit weight and shear-strength parameters of the soil, the maximum pore-water pressure generated, and the geometry of the mass that is mobilized. Earth flows exhibit a limited range of shapes, and the unit weights of soil materials, in general, vary only within a limited range. Thus, the threshold slope angle in a given area is primarily determined by a combination of the minimum soil shear resistance and maximum pore-water pressure generated at sites in that area.

The slope-stability model also explains what causes movement on an earth flow to cease. All the parameters in the model (unit weight, configurations of basal shear surface and ground surface, shear-strength parameters, and pore-water pressure) are interrelated; changes in one parameter affect the values of the other parameters that are necessary for continued movement. Thus, if all the other parameters remain constant, an earth flow will stop moving if the slope inclination decreases. This interdependency explains why few earth flows move beyond the bases of the hillsides on which they originate. The model also explains why many earth flows stop moving part way down apparently uniform slopes; if pore-water pressures decrease below the threshold value, owing to drainage or evaporation, an earth flow will stop moving even if the slope is uniform.

MODEL OF A MOVING EARTH FLOW

Whereas the slope-stability model explains how earth flows mobilize and some other aspects of earth-flow behavior, an explanation of what controls the velocity of an earth flow once it has been mobilized requires the consideration of several additional factors. In particular, a satisfactory model of a moving earth flow must be consistent with measurements of earth-flow velocities, observations of the morphology of shear surfaces and of associated zones of disturbance, and measurements of the distribution of displacements within earth flows.

VELOCITY MEASUREMENTS

Earth flows exhibit two basically different patterns of velocity behavior. The more common pattern is one of slow movement that persists for several days, months,

TABLE 7.—*Earth-flow velocities*

Site	Average surface slope (degrees)	Period of measurement (method)	Velocity (m/d)		Reference
			Average	Maximum	
Panama Canal Zone					
Cucaracha 1		2 weeks	4.2	--	Cross (1924).
		1 week(?)	1.2	--	
		6 months	.76	--	
Cucaracha 2		10 days	4.2	--	Do.
Cucaracha 3		20 minutes	--	1.6×10^{3}	Do.
Ames, Colo	25-30	1 month	.3	--	Varnes (1949).
Slumgullion, Colo	7.5	13 years (trees)	4.9×10^{-3}-1.3×10^{-2}	--	Crandell and Varnes (1961).
		2 years (survey stakes)	2.1×10^{-3}-1.7×10^{-2}	--	
		6 months (camera)	1.2×10^{-2}	--	
Kirkwood, Mont	6-10	1 month	.9	--	Hadley (1964).
Waerenga-o-kuri, New Zealand.	--	26 months	8.8×10^{-3}	8.2×10^{-3}	Campbell (1966).
Stoss, Switzerland	7.5	1 year	1.9×10^{-2}	--	Skempton and Hutchinson (1969).
Mount Chausu, Japan	8.5	20 years	6.7×10^{-2}	.24	Do.
Stonebarrow Down, England.	9.0	2.5 years	4.9×10^{-2}	.46	Do.
Handlová, Czechoslovakia.	9.0	5.25 months	.40-1.5	6.4	Záruba and Mencl (1969).
Beltinge, England	7.0	51 months	4.0×10^{-2}	2.0	Hutchinson (1970).
Minnis North, northern Ireland.	--	11 months	3.6×10^{-2}	.13	Prior and others (1968).
	20	--	--	67	Prior and Stephens (1972).
	--	5 minutes(?)	--	1.2×10^{4}	Hutchinson and others (1974).
Davilla Hill					
Earth flow 1	13	40 days	6.8×10^{-2}	.16	Keefer (1977a).
Earth flow 2	17	47 days	3.2×10^{-2}	7.0×10^{-2}	Do.
Earth flow 3	20	39 days	12×10^{-2}	.39	Do.
Cycle Park[1]	12	26 days	5.9×10^{-2}	.19	Do.
Melendy Ranch[1]					
Stake line B		43 days	3.4×10^{-2}	4.9×10^{-2}	Do.
Stake line C		43 days	3.7×10^{-2}	4.9×10^{-2}	Do.
Sochi, Black Sea coast, U.S.S.R.					
Earth flow P	14	7 years	3.6×10^{-5}	--	Ter-Stepanian and Ter-Stepanian (1971).
Earth flow Q		7 years	4.2×10^{-5}	--	Do.
"Y" Earth flow, Lomerías Muertas area[1].	--	85 days (Jan.-Apr. 1974)	.50	2.07	Oberste-Lehn (1976).
	--	23 days (Feb. 26-Mar. 20, 1975)	.33	--	
	--	7 days (Mar. 20-27, 1975)	1.49	2.26	
Van Duzen River basin, Calif.					
Halloween earth flow.	--	3 years	6.5×10^{-2}	--	Kelsey (1977, 1978).

TABLE 7.—*Earth-flow velocities*—Continued

Site	Average surface slope (degrees)	Period of measurement (method)	Velocity (m/d)		Reference
			Average	Maximum	
Donaker earth flow----------		1 year	1.6×10^{-3}	--	Kelsey (1977, 1978).
Cashla Pooda earth flow					
(west tongue)----------		1 year	4.7×10^{-3}	--	Do.
(east tongue)----------		1 year	4.7×10^{-3}	--	
Broken Road earth flow					
(west tongue)----------		1 year	4.7×10^{-3}	--	Do.
(east tongue)----------		1 year	3.3×10^{-3}	--	
Chimney Rock earth flow.	--	1 year	1.5×10^{-2}	--	Do.
Falling Tree earth flow.	--	1 year	7.4×10^{-3}	--	Do.
Lookout Creek earth flow, H. J. Andrews Experimental Forest, Oreg.[2]	14	1.4 years (Dec. 12, 1974-May 18, 1976)	3.8×10^{-4}	--	Swanson and Swanston (1977).
	--	5 years (1974-79)	2.4×10^{-4}	--	Swanson and others (1980).
Redwood Creek basin, Calif.[2,3]					
Poison Oak Prairie earth flow.	--	2.4 years	9.1×10^{-5}-1.2×10^{-2}	--	Harden and others (1979).
Minor Creek earth flow.	--	2.4 years	7.4×10^{-5}-1.5×10^{-2}	--	Do.
Rain Gage earth flow.	--	1.7 years	5.9×10^{-5}-8.4×10^{-3}	--	Do.
Devils Creek earth flow.	--	2.1 years	8.4×10^{-4}-2.3×10^{-3}	--	Do.
Counts Hill Prairie earth flow.	--	3.1 years	3.5×10^{-5}-4.9×10^{-3}	--	Do.

[1]See figure 1 for location.

[2]Velocities are based on survey measurements several months apart; these intervals may include some periods of inactivity, and so actual velocities may be greater than those calculated from survey measurements.

[3]Given range of velocities was derived from Harden and others (1978, table 8) by determining the average velocity of each line of survey stakes between each of two successive survey dates.

or years; the less common pattern is a surge of rapid movement that lasts a few minutes. Surges have been observed only on few earth flows, and it is not known whether all earth flows are capable of surging. However, the available data show that all earth flows, including those that surge, move in a slow, persistent manner most of the time. Measured velocities during slow, persistent movement range from less than 1 mm/d to several meters per day (table 7). Velocities vary from day to day, minute to minute, or second to second, but continuous acceleration leading to high velocities does not generally occur.

One of the earliest and clearest accounts of slow, persistent earth-flow movement was provided by Blackwelder (1912, p. 489-490), who described movements within the Gros Ventre earth-flow complex in northwestern Wyoming as follows:

"According to residents of the district, the [earth-flow complex] first came into action in May, 1908. So far as I am able to learn, no one actually saw it begin; but it is believed by some that the initial movement was fairly rapid if not indeed precipitate. When first observed, the disturbance was manifested only at the head of the gulch, where large masses of the slippery Morrison and Sundance (Jurassic) clays had slumped down along the steeper slopes, overturning trees and leaving a general wreck. Either quickly or slowly, the impulse from this upper mass was then communicated to the old landslide debris farther down the valley, and that in turn began to press forward, bulge, and crack. The novel thing about this case is that the movement of at least the lower part was very slow and yet continuous, like that of a glacier * * *.

"Whether or not motion continued during the winter of 1908-1909 I have not learned; but in the spring of 1909 the material in the lower part of the valley slowly pushed forward and its surface bulged into low irregular domes fretted with open crevasses, many of which were several feet wide * * *.

"So far as observed, the motion of the slide was not at any time rapid enough to be actually seen. The evidence of it, however, was plain enough. It was found impossible to keep the Forest Service telephone line in repair more than a few days, for the poles would slowly move down hill or be overturned and thus snap the wire. The wagon road soon became so hopelessly twisted and broken that it was almost impossible for wagons to follow it without capsizing, and it was no easy task to cross it even on a saddle horse. Attempts to repair the damage were almost futile, because in a few days the road would be rendered again impassable by folds of earth several yards in height or by gaping crevasses with vertical walls * * *.

"According to members of the United States Forest Service, the slide did not move as one mass, but rather in sections; the disturbance began on the east side and manifested itself week by week at new places. Changes progressed most rapidly in the wet spring months and declined noticeably toward autumn. The slow but apparently incessant movement continued through the years 1908, 1909, and 1910, but in 1911 had practically ceased."

Significant aspects of this description that illustrate the behavior of earth flows in general are: the slow movement at varying velocities over a period of several years, the acceleration during wet periods, and the progressive mode of failure in which failure began near the crown of the complex and proceeded downslope.

Blackwelder also noted that an initial surge of rapid movement may have occurred on the Gros Ventre earthflow complex. Such initial surges of rapid movement have been observed on other earth flows; for example, Cross (1924, p. 25) stated: "The motion of [an earth flow] is apt to be rapid at first, but it soon becomes slow and resembles that of a glacier." The initial surge of rapid movement of an earth flow in the San Francisco Bay region was described in a similar way by Krauskopf and others (1939, p. 630-631): "The principal movement * * * was sufficiently rapid and noisy to cause a near-panic in the surrounding countryside. During several days the motion subsided * * *." Study of aerial photographs flown in 1974 showed that movements were, in fact, still taking place 35 years after the original description.

Most earth flows move faster during periods of high precipitation or snowmelt than during drier periods (Campbell, 1966; Prior and others, 1968, 1971; Hutchinson, 1970; Hutchinson and others, 1974; Oberste-Lehn, 1976; Keefer, 1977a; Kelsey, 1977, 1978; Swanson and Swanston, 1977; Harden and others, 1978; Nolan and others, 1979; Janda and others, 1980; Swanson and others, 1980).[19] Correlations between precipitation and velocity are complex, however, and the velocity of an earth flow also appears to depend on several other factors.

A few earth flows have been monitored with devices that record movement continuously; velocities of these earth flows vary according to three distinct patterns (fig. 37). In the first and most common pattern, earth flows move at constant velocities for several days at a time (figs. 37*A*, 37*B*); these periods are commonly interrupted by shorter periods of acceleration or deceleration (fig. 37*A*). The second movement pattern is one of stick- slip, in which earth flows advance at relatively low velocities for several hours and then abruptly surge forward a few millimeters or centimeters at relatively high velocities (fig. 37*C*). The average velocities of earth flows exhibiting stick-slip behavior are determined by the number of small surges within a given period. Both the first and second patterns result in generally slow and persistent movement.

The continuous-recording devices also registered a third and basically different movement pattern—that of a major surge, in which an earth flow advances several meters at a velocity of several meters per minute (fig. 37*D*). At the Minnis North site in northern Ireland, where such surges were recorded, they are most common on earth flows being rapidly loaded under conditions generating excess pore-water pressures. The surges commonly occur during or shortly after rainstorms (Prior and Stephens, 1971, 1972; Hutchinson and others, 1974); most surges begin suddenly and are followed by periods of smooth, gradual deceleration. One surge was described by an eyewitness as follows (Hutchinson and others, 1974, p. 371):

"(a) At 4.15 pm there was heavy rainfall while surveying was in progress, and considerable noise from surface water which ran down the feeder slides [earth flows with relatively steep surface slopes] and across the accumulation slide [earth flow with relatively gentle surface slope] * * * There was no sign of any movement in the accumulation slide at this time.* * *

(b) At 4.25 pm a sudden cessation of the noise of running water was observed even though it was still raining heavily * * *. As the noise ceased, a layer of mud was observed to move rapidly down the feeder slides, where previously nothing moved except water. This mud overrode the two electrical piezometer positions and deep-seated movements of the accumulation slide commenced simultaneously. These movements were largely confined to a well-defined channel, bounded by shear surfaces, except where overflow produced miniature levees. The material accelerated perceptibly on the accumulation slope and again on the steeper front slope, eventually spilling across the road as a great lobe of wet mud.

(c) By 4.30 pm all movements of mud had ceased and a lobe 0.5 metres thick and about 400 square metres in area was completely blocking the road. The noise of running water was heard again, and the water was seen to be following the much deepened [earth flow] channel."

SHEAR SURFACES AND ADJACENT ZONES OF DISTURBANCE

All earth flows are bounded by slickensided shear surfaces (figs. 15, 17, 19, 29*B*); their ubiquity indicates

[19]One exception to this generalization was observed on the Slumgullion earth flow in the San Juan Mountains of Colorado, which moved at a nearly constant velocity during an observation period of 13 years (table 7).

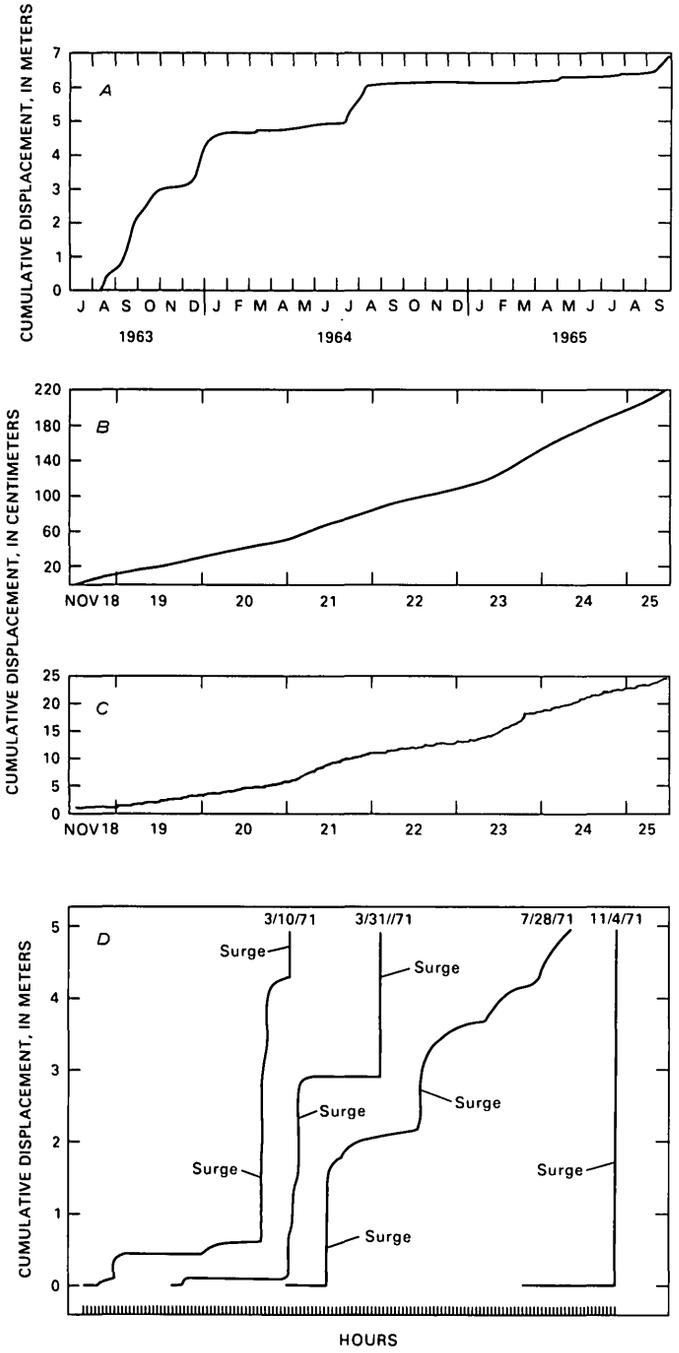

FIGURE 37.—Patterns of movement of earth flows monitored with continuous-recording devices. *A*, Example of movement at relatively constant velocity with short periods of acceleration and deceleration. Waerenga-o-kuri earth flow, New Zealand (from Campbell, 1966). Reprinted with permission from the National Water and Soil Conservation Authority, New Zealand. *B*, Movement at relatively constant velocity. Earth flow 1, Minnis North, northern Ireland (from Prior and Stephens, 1972). Reprinted with permission from the Geological Society of America and D. B. Prior. *C*, Slip-stick movement. Earth flow 2, Minnis North, northern Ireland (from Prior and Stephens, 1972). Reprinted with permission from the Geological Society of America and D. B. Prior. *D*, Major surges. Earth flow 1, Minnis North, northern Ireland (from Hutchinson and others, 1974). Reprinted with permission from the Geological Society of London and J. N. Hutchinson.

that boundary shear is an important component of earth-flow movement. In overall form, shear surfaces are planar or gently curved, although they also contain local asperities (fig. 17). Adjacent to some basal shear surfaces, zones of disturbed material are also present (fig. 18); disturbed zones examined by us ranged from 0.2 to 30 cm in thickness (figs. 17, 19). Zones of disturbed material, a few centimeters or tens of centimeters wide, also adjoin many lateral shear surfaces. The disturbance is manifested by sets of echelon cracks trending oblique to the shear surfaces (fig. 14*B*).

DISTRIBUTION OF DISPLACEMENTS

Measurements of surface and subsurface displacements confirm that most movement on earth flows takes place by boundary shear or by displacement in thin zones adjacent to the boundary. The predominance of displacements in boundary zones is particularly striking in subsurface-displacement profiles. In Davilla Hill earth flow 1, 94 percent of the total displacement measured at the ground surface took place on or within 1.3 cm of the basal shear surface (fig. 29*A*). Similarly, in an earth flow at Beltinge, England, 89 to 95 percent of the displacement measured at the ground surface took place on or within 20 cm of the basal shear surface (fig. 38). Analogous results were obtained by Prior and Stephens (1972), who measured the deformation of flexible plastic tubes in an earth flow at Minnis North, northern Ireland, and concluded that most displacement took place by slip on the basal shear surface.

Measurements of surface displacements also show that, whereas some internal deformation occurs, displacements on and adjacent to lateral shear surfaces predominate (fig. 39). Many surface-displacement profiles show little internal deformation (figs. 39*A*-39*C*); other profiles are irregular and show abrupt discontinuities in displacement due to shear on discrete internal shear surfaces (figs. 39*C*, 39*D*); in still other profiles, more uniform distribution of differential displacements across the earth flows indicates that some distributed internal shear or flow is taking place (figs. 39*E*, 39*F*).

SURGES

The surges of rapid movement that occur on some earth flows can be explained by using the above data and slope-stability analysis. According to slope-stability analysis, an earth flow is mobilized when pore-water pressures on the shear surfaces increase to values at which the resisting shear force is smaller than the driving force. If pore-water pressures were to rise even higher, as they commonly do because of additional precipitation and infiltration, then the resisting shear force

would decrease still further. According to Newton's third law, as long as the driving force exceeds the resisting force, the earth flow will accelerate; this acceleration would, if continued, lead to movement at high velocity, which is apparently what happens in a surge.

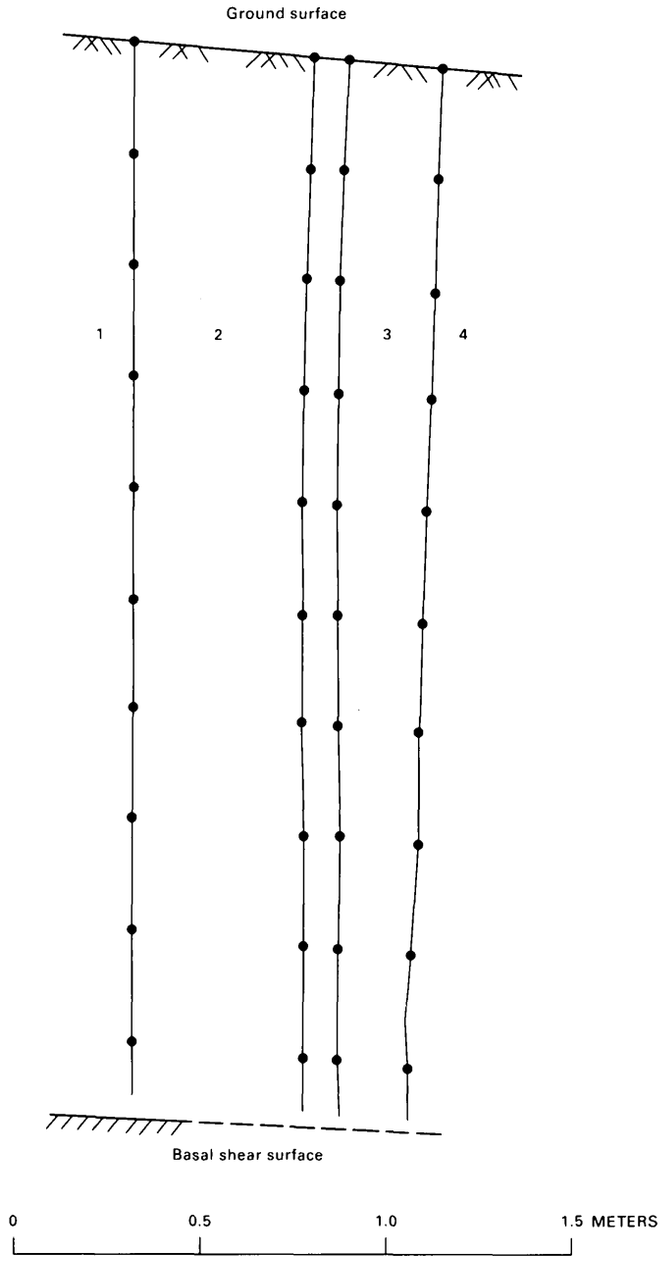

FIGURE 38.—Subsurface-displacement profile of earth flow at Beltinge, England. From 89 to 95 percent of total displacement took place on or within 20 cm of basal shear surface. Measurements were made with borehole inclinometer (from Hutchinson, 1970). 1, initial position of inclinometer tube, on April 15, 1964; 2, position on April 22, 1964; 3, position on April 28, 1964; 4, position on June 11, 1964. Lines 1 to 4 are corrected for initial deviations from vertical. Reprinted with permission from J. N. Hutchinson.

In a published eyewitness account (Hutchinson and others, 1974) of a major surge, the beginning of the surge was preceded by rapid loading in the zone of accumulation that, in turn, caused an increase in pore-water pressure. The surge began abruptly, and acceleration led to high velocities within a few minutes. The surge continued until the earth flow reached the base of the hill on which it originated and encountered a gentler slope; this decrease in slope restored the force balance by decreasing the driving force. Association of other surges on this same group of earth flows with periods of high precipitation (Prior and Stephens, 1971, 1972; Hutchinson and others, 1974), indicated that increased pore-water pressure, in general, caused the surges.

Slope-stability analysis can be similarly used to explain the small surges that are part of the stick-slip movement of some earth flows (fig. 37*C*). These small surges may occur when pore-water pressure briefly exceeds the threshold value required for mobilization.

VELOCITY, BOUNDARY SLIP, AND BOUNDARY ROUGHNESS

Surges occur relatively infrequently and have been recorded on only a few earth flows. More commonly, earth flows move at relatively constant velocities for long periods. Although these periods of constant velocity are interrupted by periods of acceleration or deceleration, sustained acceleration leading to very high velocities does not generally occur. Slope-stability analysis, however, predicts that an earth flow will accelerate as long as the pore-water pressure exceeds the threshold value required for mobilization.

To explain these long periods of constant velocity, using an unmodified slope-stability analysis, it is necessary to assume that pore-water pressures are maintained at, but not above, threshold values over long periods. We infer that such maintenance of pore-water pressures is unlikely because of the variations in precipitation, infiltration, drainage, and evaporation to which all active earth flows are subjected. Even if the pore-water pressure were to remain constant over time in some cases, there is no apparent physical reason to expect that the constant pore-water pressure would exactly equal the threshold value. Hence, slope-stability analysis must be modified to explain the absence of sustained acceleration. This modified analysis must then address conditions on and adjacent to the shear surfaces, because the largest component of movement occurs there.

One possible mechanism for preventing sustained acceleration when pore-water pressures rise above threshold values assumes the existence of a velocity-dependent component of shear resistance. If, for example, the shear resistance of the material along the shear surfaces were given by the equations

$$[\tau - (\sigma_n - u)\tan\bar{\phi} - \bar{c}]^n = A\dot{E}_s; \quad \tau > (\sigma_n - u)\tan\bar{\phi} + \bar{c} \quad (2a)$$

and

$$0 = A\dot{E}_s; \quad \tau \leq (\sigma_n - u)\tan\bar{\phi} + \bar{c} \quad (2b)$$

where $\dot{E}_s$ is the deformation rate, A and n are constants, and τ, σ_n, u, $\bar{\phi}$, and $\bar{c}$ are defined as in equation 1, then the shear resistance would increase as the velocity[20] increased, and this increased resistance would retard the movement. This rheologic model is a combination of the Mohr-Coulomb and the power-law models, and equation 2a reduces to equation 1 when $\dot{E}_s = 0$. A form of equations 2 with $n = 1$ was suggested as a rheologic model for soils by several investigators (Terzaghi, 1931; Stroganov, 1961; Ter-Stepanian, 1963; Yen, 1969; Johnson, 1970).

To determine whether shear resistance along earth-flow shear surfaces does, in fact, increase with increasing velocity, we performed an experiment, using material from Davilla Hill earth flow 1. In this experiment, a sample containing part of the basal shear surface was placed in the direct-shear apparatus, consolidated, and then sheared at several velocities ranging from 1.5×10^{-3} mm/min (0.21 cm/d) to 1.2 mm/min (180 cm/d). The range of velocities used in the experiment included the full range of velocities measured on the earth flow in the field. At the lower velocities, conditions were probably drained; at the higher velocities, conditions probably were partially drained or undrained. The sample was initially sheared for 12 cycles at a velocity of 37×10^{-3} mm/min (5.3 cm/d); the decrease in shear resistance associated with increasing displacement was thus significantly diminished before velocity of shear was varied. The sample was consolidated between tests at different velocities. The vertical load remained constant during the experiment (σ_n = 5.3 kN/m^2); total shear resistance in the horizontal plane was measured during one forward and one reverse cycle at each velocity, and the two values of shear resistance obtained were averaged to plot the results in figure 40.

A linear-regression-line fit to the data in figure 40 yields the relation:

$$\tau = 1.800 + 0.046 \log_{10} v,$$

where τ = the shear resistance (in kN/m^2)
and v = the velocity (in cm/d).

The near-constancy of shear resistance over the range of velocities tested indicates that material along the shear surfaces does not exhibit any significant velocity-dependent component of shear resistance. This result conforms to results from direct-shear tests on other fine soils (Kenney, 1967; Ramiah and Purushothamaraj, 1971).

Another possible mechanism for retarding movement is boundary roughness. This mechanism, believed to be important in retarding basal slip in temperate glaciers (Kamb and LaChapelle, 1964; Weertman, 1964; Paterson, 1969), may also operate on earth flows. Though not verified by experiment, this mechanism conforms to the data on earth-flow velocity, displacement distribution, and shear-surface morphology.

We hypothesize that boundary roughness retards movement as follows. Asperities on the boundaries of earth flows force material adjacent to the shear surfaces to deform around the asperities or to shear through them. The asperities themselves contribute a component of shear resistance that varies over time as the earth flow deforms and advances over different parts of the bounding channel. In addition, the properties of the material thus forced to deform around the asperities may differ significantly from those of the material along the shear surfaces. In particular, soil that does not contain discrete shear surfaces commonly exhibits a velocity-dependent component of shear resistance (Fleming and Johnson, 1975; Mitchell, 1976). Therefore, deformations in this material could retard earth-flow movement.

Field observations show that asperities occur on earth-flow shear surfaces (fig. 17) and that the material in zones adjacent to shear surfaces has been deformed (figs. 18, 19). Even parts of basal shear surfaces that appear planar, such as the basal shear surface of Davilla Hill earth flow 1, contain small asperities, a few millimeters high. Traces of most lateral surfaces are also irregular, and internal shear adjacent to lateral shear surfaces has been directly observed (Hutchinson, 1970).

These observations show that, in detail, earth-flow boundaries are rough and that material adjacent to the shear surfaces deforms and shears. In glaciers that slip on their beds, the velocity of basal slip depends on the shape, size, and spacing of asperities and on the rheologic properties of the ice (Paterson, 1969). Similar factors may also control the velocity of slip in earth flows, although neither the mechanism by which deformation near asperities takes place nor the rheologic properties of the earth-flow material are yet well enough known to analyze the boundary shear and associated deformations quantitatively.

[20]The velocity is obtained by integrating the deformation rate $\dot{E}_s$ over the thickness of the zone in which deformation occurs.

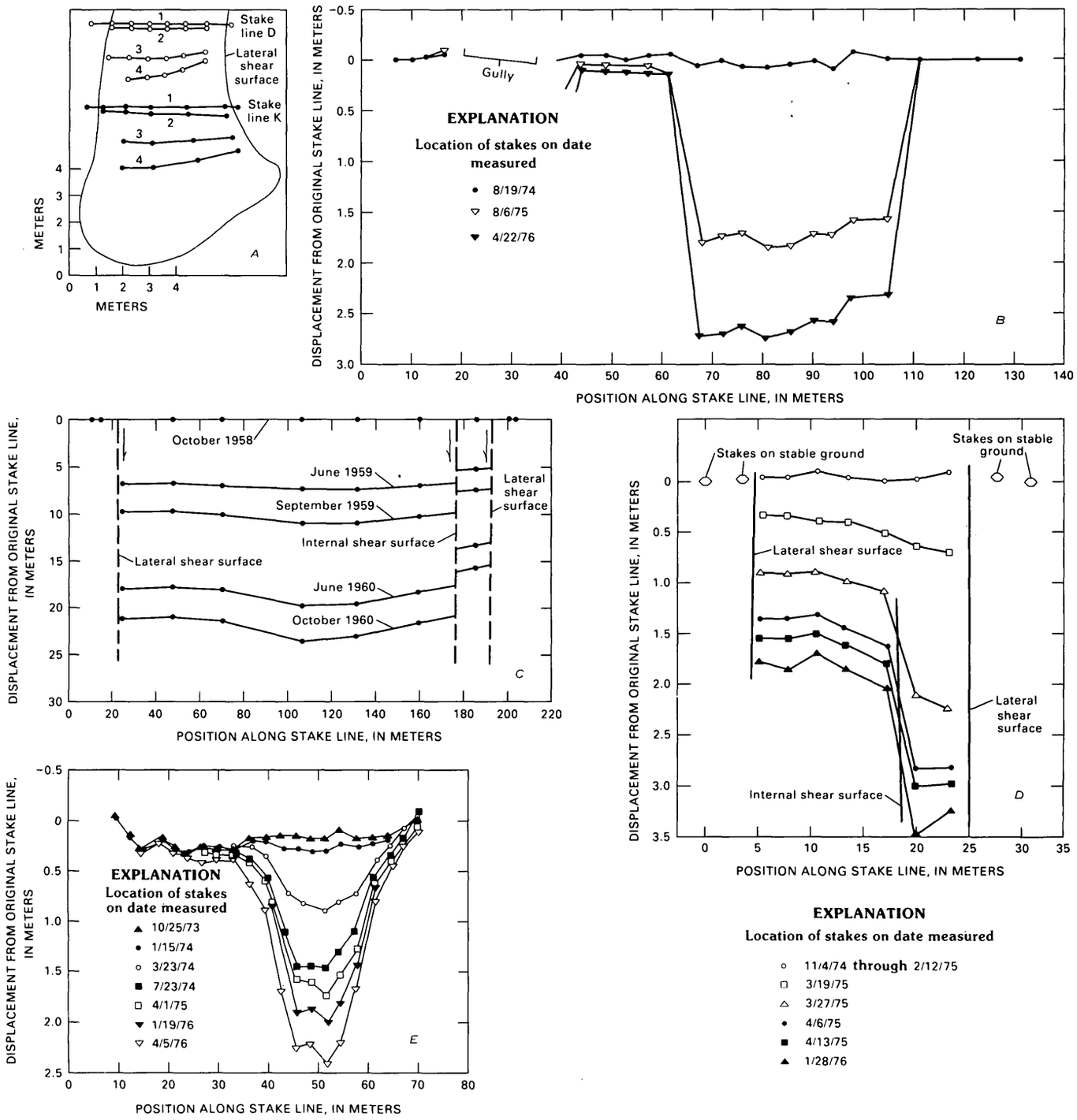

FIGURE 39.—Surface-displacement profiles of earth flows as indicated by displacements of lines of survey stakes. *A*, Most movement occurs on or adjacent to lateral shear surfaces. Earth flow at Beltinge, England (from Hutchinson, 1970). Dates of measurement: 1, November 14, 1962; 2, March 27, 1963; 3, April 16, 1963; 4, June 7, 1963. Reprinted with permission from J. N. Hutchinson. *B*, Most movement occurs on or adjacent to lateral shear surfaces. Stake line 3, Devil's Creek earth flow, Redwood Creek basin, Calif. (from Harden and others, 1978). *C* Large component of movement at boundary and small component of differential movement on a discrete internal shear surface. Earth flow at Slumgullion, Colo. (from Crandell and Varnes, 1961). *D*, Large components due to movement at boundary and to differential movement on a discrete internal shear surface. Earth flow at Cycle Park, Calif. (from Keefer, 1977a). *E*, Significant component of distributed internal shear or flow. Stake line 1, Poison Oak Prairie earth flow, Redwood Creek basin, Calif. (from Harden and others, 1978). *F*, Significant component of distributed internal

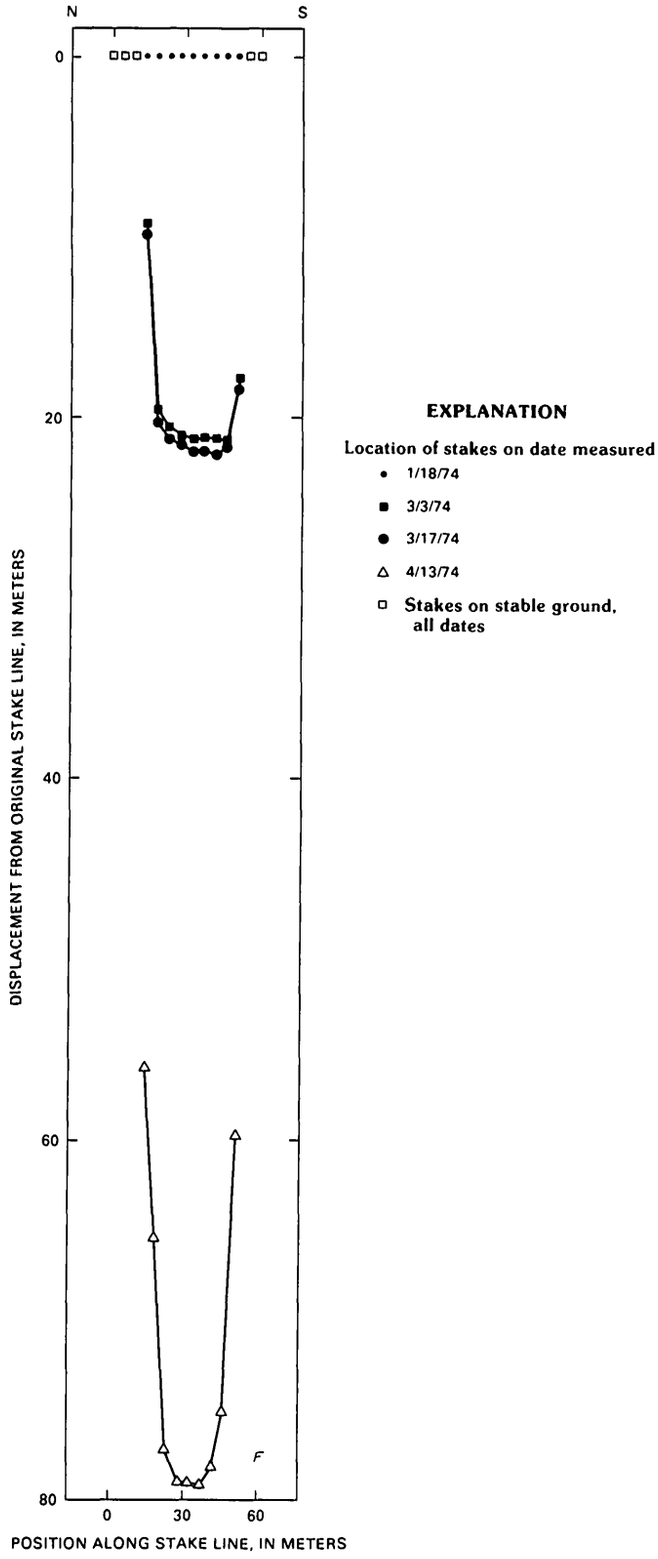

shear or flow; boundary slip, however, is largest component of movement. "Y-slide" earth flow, Lomerias Muertas area, Calif. (after Oberste-Lehn, 1976). Reprinted with permission from Deane Oberste-Lehn.

INTERNAL DEFORMATION

Surveyed displacement profiles indicate that some internal deformation also occurs in earth flows (fig. 39). Some of this deformation is due to shear on discrete internal shear surfaces; the mechanism controlling this shear probably resembles that controlling shear at the boundaries. However, some distributed internal deformation, which may be due to flow within the material, also occurs.

Displacement profiles of material flowing in a channel have been calculated by several previous investigators using various rheologic models for soils (Yano and Daido, 1965; Paterson, 1969; Johnson, 1970; Cunningham, 1972; Keefer, 1977a). For channels of uniform cross section and for uniform material properties, these calculations show that the material moves faster near the centers of channels than near the boundaries, a result in general agreement with velocity profiles measured on earth flows (fig. 39). The exact shapes of these theoretical velocity profiles depend on the rheologic model used, the properties of the material, and the geometry of the channel.

Assuming that equations 2 apply to material in the interior of an earth flow, even though they do not apply to material disrupted by discrete shear surfaces, velocity profiles due to internal flow in infinitely wide and semicircular channels were derived by Keefer (1977a). According to these derivations, a rigid plug with no internal deformation exists in the center of the channel. Between this plug and the channel boundary is a zone where internal deformation takes place; the velocity profile in this zone is curved. The thickness of this zone of deformation and its degree of curvature depend on the shear-strength parameters and unit weight of the material, the surface slope, the values of constants A and n in equation 2a, and the pore-water pressure.

The detailed field and laboratory measurements needed to quantitatively compare theoretical profiles with profiles surveyed in earth flows have not been made. However, the shape of the theoretical velocity profile generally agrees with the shapes of profiles surveyed on earth flows that exhibit significant distributed internal deformation (figs. 39*E*, 39*F*). In addition, the analysis for an infinitely wide channel, in which pore-water pressure was treated as a variable, shows that the maximum velocity within an earth flow increases with the pore-water pressure. This result also agrees with field observations.

COMPOSITE MODEL

Earth flows move primarily by boundary shear, and the velocity appears to be controlled primarily by a

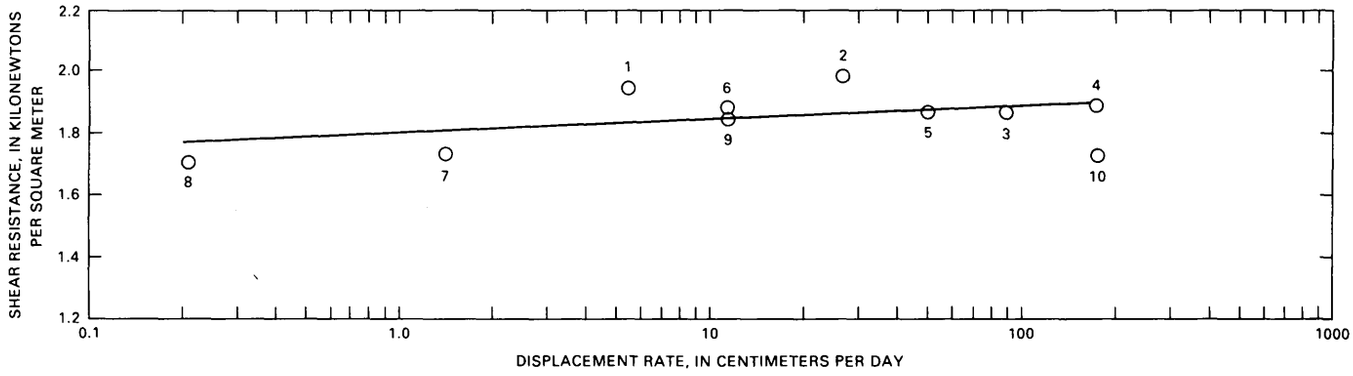

FIGURE 40.—Shear resistance as a function of velocity in direct-shear tests on basal-shear-surface material in earth flow 1 of Davilla Hill earth-flow complex. Numbers indicate order in which tests were run. Line indicates linear-regression fit of data.

mechanism involving boundary roughness and complex deformations in thin zones near the boundary shear surfaces. Added to this major boundary-shear component of displacement are smaller contributions from distributed internal deformation and from shear on discrete internal shear surfaces.

CONCLUSIONS

Earth flows differ from other types of mass movement on the bases of morphology, materials, and rate and kind of movement. Characteristic morphologic features are: a tongue or teardrop shape; a rounded, bulging toe; a sinusoidal longitudinal profile, concave upward near the head and convex upward near the toe; a pair of flanking lateral ridges; and a set of discrete boundary shear surfaces.

Many earth flows occur in large complexes made up of myriad individual earth-flow deposits. Within these complexes, earth flows mobilize from material in older earth-flow deposits and from material in other types of mass-movement deposits, as well as from material not previously involved in mass movement. The boundaries of earth flows that remobilize older earth-flow material commonly cut across those of older earth-flow deposits. The common remobilization of earth-flow deposits indicates that no significant irreversible changes take place in the soil when an earth flow stops moving. Therefore, material in earth-flow deposits is highly susceptible to renewed movement.

In many zones of depletion are deposits of slumps or of other types of mass movement. This relation has led many previous investigators to suggest that earth flows are derived from slumps or other types of mass movement by progressive disruption of internal structure. Observations during this study, however, indicate that this mechanism is not generally valid. In many zones of depletion, mass-movement deposits are derived from failure of the steep scarps left behind by earth-flow movement; thus, these mass-movement deposits are younger than the associated earth flows, and the earth flows are not derived from them. In addition, some earth flows mobilize out of materials not previously transported by mass movements, and other earth flows mobilize directly out of older earth-flow material in the absence of any other mass-movement process.

Material in earth flows consists of fine soil containing a significant amount of entrained water. The proportions of clay, silt, sand, and coarser material vary from earth flow to earth flow, although silt- and (or) clay-size grains predominate in most earth flows. Clay-mineral composition also varies from site to site; earth flows form in clays containing abundant kaolinite, illite, or chlorite as well as in clays containing abundant montmorillonite. Earth-flow materials are pervasively fissured; these fissures create planes of weakness and facilitate infiltration of water.

At two sites where appropriate measurements have been made, earth-flow materials have low sensitivities. A low sensitivity may distinguish earth-flow materials from materials in other types of mass movement—particularly, "rapid earth flow" or "quick clay flow"—although more measurements at other sites are needed to confirm or disprove this hypothesis.

Mobilization of earth flows is accompanied by an increase in water content. Measurements at one site indicate that this water-content increase is due to in-place saturation of the material without significant volume change, remolding, or other disturbance.

Although some internal deformation occurs within earth flows, most movement takes place on or immediately adjacent to their boundaries. Conditions at the boundaries, therefore, are of primary importance in

determining how earth flows are mobilized and how they move. Slope-stability analysis of soil mechanics explains how earth flows are mobilized. In this analysis, the shear resistance of the soil is given by the Coulomb failure criterion modified by Terzaghi's theory of effective stress, which accounts for the effects of pore-water pressure. Earth flows are mobilized by increases in pore-water pressure along shear surfaces. At most sites, the pore-water pressures necessary for mobilization are generated by infiltration of water into the soil. At a few sites, necessary pore-water pressures are created by rapid loading in zones of depletion. This rapid loading, which creates an undrained condition, generates high pore-water pressures that allow earth flows to move on slopes with inclinations of only a few degrees. Movement of earth flows commonly ceases when they encounter decreases in slope or when drainage or evaporation decreases pore-water pressure.

Earth flows are characterized by slow, persistent movement; they generally move with velocities of a few meters per day or less, and they remain active for several days, months, or years. During this slow, persistent movement, velocities vary over time; many earth flows move faster during periods of high precipitation than during drier periods. However, correlations between precipitation and velocity are complex, and earth-flow velocity depends on several other factors, including local boundary conditions.

In addition to slow, persistent movement, surges occur on some earth flows. During these surges, which last for a few minutes, velocities as high as 8 m/min have been measured. The surges are caused by increases in pore-water pressure that lower shear resistance below the point at which an earth flow originally mobilizes. The resulting imbalance between the driving force and the available shear resistance causes an earth flow to accelerate and leads to a high-velocity surge. Surges are relatively infrequent, however, and most earth flows do not accelerate continuously, even when pore-water pressures rise above those required for mobilization. Thus, in the general case, some mechanism acts to retard earth-flow movement.

A retarding mechanism consistent with the available data involves boundary roughness and deformation in thin zones adjacent to the boundaries. We hypothesize this mechanism to work as follows. Asperities on boundary shear surfaces force material in zones adjacent to the shear surfaces to deform; these asperities provide a shear-resistance component that varies over time. In addition, material deforming around the asperities may exhibit a component of shear resistance that increases as the velocity increases. Thus, both the asperities themselves and deformations in the adjacent material retard the movement of an earth flow. According to this boundary-roughness model, the velocity of an earth flow is complexly controlled by several factors, including the number, shape, and spacing of asperities on the shear surfaces, the rheologic properties of the material that deforms around asperities, and the shear-strength parameters and pore-water pressure on shear surfaces.

A retarding mechanism consistent with the available data involves boundary roughness and deformation in thin zones adjacent to the boundaries. We hypothesize this mechanism to work as follows. Asperities on boundary shear surfaces force material in zones adjacent to the shear surfaces to deform; these asperities provide a shear-resistance component that varies over time. In addition, material deforming around the asperities may exhibit a component of shear resistance that increases as the velocity increases. Thus, both the asperities themselves and deformations in the adjacent material retard the movement of an earth flow. According to this boundary-roughness model, the velocity of an earth flow is complexly controlled by several factors, including the number, shape, and spacing of asperities on the shear surfaces, the rheologic properties of the material that deforms around asperities, and the shear-strength parameters and pore-water pressure on shear surfaces.

REFERENCES CITED

Aboim-Costa, Carlos, and Stein, R. S., 1976, A landslide in Eden Canyon, California: Stanford, Calif., Stanford University, student project.

Bailey, R. G., 1972, Landslide hazards related to land use planning in Teton National Forest, northwest Wyoming: Ogden, Utah, U.S. Department of Agriculture, Forest Service, Intermountain Region, 131 p.

Barton, M. E., 1973, The degradation of the Barton clay cliffs of Hampshire [England]: Quarterly Journal of Engineering Geology, v. 6, no. 3-4, p. 423-440.

Benson, W. N., 1940, Landslides and allied features in the Dunedin district [New Zealand] in relation to geological structure, topography, and engineering: Royal Society of New Zealand Transactions and Proceedings, v. 70, no. 3, p. 249-263.

Blackwelder, Eliot, 1912, The Gros Ventre slide, an active earth-flow: Geological Society of America Bulletin, v. 23, p. 487-492.

Blake, M. C., Jr., Bartow, J. A., Frizzell, V. A., Jr., Schlocker, Julius, Sorg, D. H., Wentworth, C. M., and Wright, R. H., 1974, Preliminary geologic map of Marin and San Francisco counties and parts of Alameda, Contra Costa and Sonoma counties, California: U.S. Geological Survey Miscellaneous Field Studies Map MF-574, scale 1:62,500, 2 sheets.

Bromhead, E. N., 1978, Large landslides in London clay at Herne Bay, Kent [England]: Quarterly Journal of Engineering Geology, v. 11, no. 4, p. 291-304.

Brunsden, Denys, and Jones, D. K. C., 1976, The evolution of landslide slopes in Dorset [England]: Royal Society of London Philosophical Transactions, ser. A, v. 283, no. 1315, p. 605-631.

Campbell, A. P., 1966, Measurement of movement of an earthflow: Soil and Water, v. 2, no. 3, p. 23-24.

Chandler, R. J., 1972, Periglacial mudslides in Vestspitsbergen and their bearing on the origin of fossil "solifluction" shears in low angled clay slopes: Quarterly Journal of Engineering Geology, v. 5, no. 3, p. 223-241.

Cooksley, J. W., Jr., 1964, Geophysical investigation of a landslide employing seismic exploration technique: Engineering Geology and Soils Engineering Symposium, 2d, Pocatello, Idaho, 1964, Proceedings, p. 97-103.

Crandell, D. R., and Varnes, D. J., 1961, Movement of the Slumgullion earthflow near Lake City, Colorado, art. 57 *in* Short papers in the geologic and hydrologic sciences: U.S. Geological Survey Professional Paper 424-B, p. B136-B139.

Cross, Whitman, 1924, Historical sketch of the landslides of Gaillard cut, app. A *of* Report of the Committee of the National Academy of Sciences on Panama Canal slides: National Academy of Sciences Memoir 18, p. 23-43.

Cunningham, M. J., 1972, A mathematical model of the physical processes of an earthflow: New Zealand Hydrological Society Journal of Hydrology, v. 11, no. 1, p. 47-54.

Dibblee, T. W., Jr., compiler, 1975, Geologic map of the Hollister quadrangle, California: U.S. Geological Survey Open-File Map 75-394, scale 1:62,500.

Dunkerley, D. S., 1976, A study of long-term slope stability in the Sydney Basin, Australia: Engineering Geology, v. 10, no. 1, p. 1-12.

Ellen, Stephen, Peterson, D. M., Reid, G. O., and Savina, M. E., 1979, Hillslope forms and landslide processes in erosional terrain on Franciscan rocks of the Marin peninsula, California [abs]: Geological Society of America Abstracts with Programs, v. 11, no. 3, p. 77.

Fleming, R. W., and Johnson, A. M., 1975, Rates of seasonal creep of silty clay soil: Quarterly Journal of Engineering Geology, v. 8, no. 1, p. 1-29.

Fraser, G. D., Waldrop, H. A., and Hyden, H. J., 1969, Geology of the Gardiner area, Park County, Montana: U.S. Geological Survey Bulletin 1277, 118 p.

Fussgänger, E., and Jadroň, D., 1977, Engineering-geological investigation of the Okoličné landslide using measurement of stresses existing in soil mass: International Association of Engineering Geology Bulletin, no. 16, p. 203-209.

Geological Society of America, 1963, Rock-color chart: New York.

Hadley, J. B., 1964, Landslides and related phenomena accompanying the Hebgen Lake earthquake of August 17, 1959: U.S. Geological Survey Professional Paper 435-K, p. 107-138.

Hall, C. A., Jr., 1956, The geology of the Pleasanton area, Alameda County, California: Stanford, Calif., Stanford University, Ph. D. thesis, 269 p.

Ham, C. K., 1952, Geology of Las Trampas Ridge, Berkeley Hills, California: California Division of Mines Special Report 22, 26 p.

Hanna, T. H., 1973, Foundation instrumentation: Cleveland, Ohio, Trans Tech Publications, 372 p.

Harden, D. R., Janda, R. J., and Nolan, K. M., 1978, Mass movement and storms in the drainage basin of Redwood Creek, Humboldt County, California—a progress report: U.S. Geological Survey Open-File Report 78-486, 161 p.

Hawkins, A. B., 1973, The geology and slopes of the Bristol region [England]: Quarterly Journal of Engineering Geology, v. 6, no. 3-4, p. 185-205.

Hein, J. R., Scholl, D. W., and Gutmacher, C. E., 1975, Neogene clay minerals of the far NW Pacific and southern Bering Sea: International Clay Conference, Mexico City, 1975, Proceedings, p. 71-80.

Howe, Ernest, 1909, Landslides in the San Juan Mountains, Colorado: U.S. Geological Survey Professional Paper 67, 58 p.

Hutchinson, J. N., 1970, A coastal mudflow on the London clay cliffs at Beltinge, north Kent [England]: Geotechnique, v. 20, no. 4, p. 412-438.

Hutchinson, J. N., and Bhandari, R. K., 1971, Undrained loading, a fundamental mechanism of mudflows and other mass movements: Geotechnique, v. 21, no. 4, p. 353-358.

Hutchinson, J. N., Prior, D. B., and Stephens, Nicholas, 1974, Potentially dangerous surges in an Antrim [Ireland] mudslide: Quarterly Journal of Engineering Geology, v. 7, no. 4, p. 363-376.

Janda, R. J., Nolan, K. M., and Stephens, T. A., 1980, Styles and rates of landslide movement in slump-earthflow-sculpted terrane, northwestern California [abs.]: Geological Society of America Abstracts with Programs, v. 12, no. 3, p. 113.

Johnson, A. M., 1965, A model for debris flow: University Park, Pennsylvania State University, Ph. D. thesis, 248 p.

Johnson, A. M., 1970, Physical processes in geology: San Francisco, Freeman, Cooper & Co., 577 p.

Kachadoorian, Reuben, 1956, Engineering geology of the Warford Mesa subdivision, Orinda, California: U.S. Geological Survey open-file report, 13 p.

Kamb, Barclay, and LaChapelle, E., 1964, Direct observation of the mechanism of glacier sliding over bedrock: Journal of Glaciology, v. 5, no. 38, p. 159-172.

Keefer, D. K., 1976, Earthflows in the Coast Ranges of central California: Preliminary report: U.S. Geological Survey Open-File Report 76-734, 58 p.

———1977a, Earthflow: Stanford, Calif., Stanford University, Ph. D. thesis, 317 p.

———1977b, Earthflows at Davilla Hill, Alameda County, California [abs.]: Association of Engineering Geologists Annual Meeting, 20th, Seattle, Wash., 1977, abstracts, p. 29.

———1977c, A model for earthflow [abs.]: Geological Society of America Abstracts with Programs, v. 9, no. 7, p. 1045-1046.

Keefer, D. K., and Johnson, A. M., 1978, Mobilization and movement mechanics of earthflows, *in* Sierakowski, R. L., ed., Recent advances in engineering science: Society of Engineering Science Annual Meeting, 15th, Gainesville, Fla., 1978, Proceedings, p. 223-226.

Kelsey, H. M., 1977, Landsliding, channel changes, sediment yield, and land use in the Van Duzen River basin, north coastal California, 1941-1975: Santa Cruz, University of California, Ph. D. thesis, 370 p.

———1978, Earthflows in Franciscan melange, Van Duzen River basin, California: Geology, v. 6, no. 6, p. 361-364.

Kenney, T. C., 1967, The influence of mineral composition on the residual strength of natural soils: Geotechnical Conference, Oslo, Norway, 1967, Proceedings, v. 1, p. 123-129.

Krauskopf, K. B., Feitler, S., and Griggs, A. B., 1939, Structural features of a landslide near Gilroy, California: Journal of Geology, v. 47, no. 6, p. 630-648.

Lambe, T. W., 1951, Soil testing for engineers: New York, John Wiley & Sons, 165 p.

Lambe, T. W., and Whitman, R. V., 1969, Soil mechanics: New York, John Wiley & Sons, 553 p.

Mitchell, J. K., 1976, Fundamentals of soil behavior: New York, John Wiley & Sons, 422 p.

Morgenstern, N. R., and Price, V. E., 1965, The analysis of the stability of general slip surfaces: Geotechnique, v. 15, p. 79-93.

———1967, A numerical method for solving the equations of stability

of general slip surfaces: Computer Journal, v. 9, p. 388-393.
National Oceanic and Atmospheric Administration, 1978, Hourly precipitation data [California]: v. 28, no. 2, 54 p.
Nilsen, T. L., and Turner, B. L., 1975, Influence of rainfall and ancient landslide deposits on recent landslides (1950-71) in urban areas of Contra Costa County, California: U.S. Geological Survey Bulletin 1388, 18 p.
Nolan, K. M., Janda, R. J., and Duls, J. M., 1979, Recent history of the surface morphology of two earthflows adjacent to Redwood Creek, *in* Guidebook for a field trip to observe natural and management-related erosion in Franciscan terrane of northern California: Geological Society of America, Cordilleran Section, p. XI-1 to XI-10.
Oberste-Lehn, Deane, 1976, Slope stability of the Lomerias Muertas area, San Benito County, California: Stanford, Calif., Stanford University, Ph. D. thesis, 216 p.
Paterson, W. S. B., 1969, The physics of glaciers: Oxford, Pergamon Press, 250 p.
Peck, R. B., Hanson, W. E., and Thornburn, T. H., 1974, Foundation engineering: New York, John Wiley & Sons, 514 p.
Peterson, D. M., 1979, Hillslope erosional processes related to bedrock, soils, and topography in the Three Peaks area, Marin County, California [abs.]: Geological Society of America Abstracts with Programs, v. 11, no. 3, p. 121.
Pilgrim, A. T., and Conacher, A. J., 1974, Causes of earthflows in the southern Chittering Valley, Western Australia: Australian Geographical Studies, v. 12, no. 1, p. 38-56.
Prior, D. B., 1977, Coastal mudslide morphology and processes on Eocene clays in Denmark: Geografisk Tidsskrift, v. 76, p. 14-33.
Prior, D. B., and Ho, C., 1972, Coastal and mountain slope instability on the islands of St. Lucia and Barbados, West Indies: Engineering Geology, v. 6, no. 1, p. 1-18.
Prior, D. B., and Stephens, Nicholas, 1971, A method of monitoring mudflow movements: Engineering Geology, v. 5, no. 3, p. 239-246.
———1972, Some movement patterns of temperate mudflows: Examples from northeastern Ireland: Geological Society of America Bulletin, v. 83, no. 8, p. 2533-2543.
Prior, D. B., Stephens, Nicholas, and Archer, D. R., 1968, Composite mudflows on the Antrim coast of north-east Ireland: Geografiska Annaler, ser. A, v. 50, no. 2, p. 65-78.
Prior, D. B., Stephens, Nicholas, and Douglas, G. R., 1971, Some examples of mudflow and rockfall activity in north-east Ireland, *in* Brunsden, Denys, compiler, Slopes: Form and process: Institute of British Geographers Special Publication 3, p. 129-140.
Radbruch, D. H., and Weiler, L. M., 1963, Preliminary report on landslides in a part of the Orinda Formation, Contra Costa County, California: U.S. Geological Survey open-file report, 35 p.
Ramiah, B. K., and Purushothamaraj, P., 1971, Influence of strain rate on the residual strength of a kaolinitic clay: Geotechnical Engineering, v. 2, no. 2, p. 151-158.
Rantz, S. E., 1971, Precipitation depth-duration-frequency relations for the San Francisco Bay region, California, *in* Geological Survey research 1971: U.S. Geological Survey Professional Paper 750-C, p. C237-C241.
Rapp, Anders, 1960, Recent development of mountain slopes in Karkevagge and surroundings, northern Scandanavia: Geografiska Annaler, v. 42, no. 2-3, p. 65-200.
Reiner, Markus, 1960, Deformation, strain, and flow: New York, Interscience, 347 p.
Robinson, G. D. V., 1956, Geology of the Hayward quadrangle, California: U.S. Geological Survey Geologic Quadrangle Map GQ-88, scale 1:24,000.
San Francisco Chronicle, 1976: v. 112, no. 143, p. 1.
Sharpe, C. F. S., 1938, Landslides and related phenomena; a study of mass-movements of soil and rock: New York, Columbia University Press, 136 p.
Sharpe, C. F. S., and Dosch, E. F., 1942, Relation of soil-creep to earthflow in the Appalachian Plateaus: Journal of Geomorphology, v. 5, no. 4, p. 312-324.
Sims, J. D., Fox, K. F., Jr., Bartow, J. A., and Helley, E. F., 1973, Preliminary geologic map of Solano County and parts of Napa, Contra Costa, Marin, and Yolo Counties, California: U.S. Geological Survey Miscellaneous Field Studies Map MF-484, scale 1:62,500, 5 sheets.
Skempton, A. W., and Hutchinson, J. N., 1969, Stability of natural slopes and embankment foundations: International Conference on Soil Mechanics and Foundation Engineering, 7th, Mexico City, Proceedings, p. 291-340.
Spain, Steven, and Upp, Rex, 1976, Bull Ranch landslide, California: Stanford, Calif., Stanford University, student project.
Stroganov, A. S., 1961, Viscous-plastic flow of soils: International Conference on Soil Mechanics and Foundation Engineering, 5th, Paris, Proceedings, v. 2, p. 721-726.
Swanson, F. J., Harr, R. D., and Fredriksen, R. L., 1980, Field trip guide: Geomorphology and hydrology in the H. J. Andrews Experimental Forest, western Cascades, *in* Geologic field trips in western Oregon and southwestern Washington: Oregon Department of Geology and Mineral Industries Bulletin 101, p. 217-232.
Swanson, F. J., and James, M. E., 1975, Geology and geomorphology of the H. J. Andrews Experimental Forest, western Cascades, Oregon: U.S. Department of Agriculture, Forest Service Research Paper PNW-188, 14 p.
Swanson, F. J., and Swanston, D. N., 1977, Complex mass-movement terrains in the western Cascade Range, Oregon, *in* Coates, D. R., ed., Landslides: Geological Society of America Reviews in Engineering Geology, v. 3, p. 113-124.
Swanston, D. N., 1980, Creep and earthflow erosion from undisturbed and management impacted slopes in the Coast Ranges and Cascade Mountains of the Pacific Northwest [abs.]: Geological Society of America Abstracts with Programs, v. 12, no. 3, p. 155.
Ter-Stepanian, George, 1963, On the long term stability of slopes: Norwegian Geotechnical Institute Publication 52, p. 1-13.
———1967, The use of observations of slope deformation for analysis of mechanism of landslides: Yerevan, [U.S.S.R.], Armenian Academy of Sciences, Problems of Geomechanics, no. 1, p. 32-51.
Ter-Stepanian, George, and Ter-Stepanian, Hasmic, 1971, Analysis of landslides, *in* Kézdi, Árpad, ed., Budapest Conference on Soil Mechanics and Foundation Engineering, 4th, 1971, Proceedings: p. 499-504.
Terzaghi, Karl, 1924, Die Theorie der hydrodynamischen Spannungserscheinungen und ihr erdbautechnisches Anwendungsgebiet: International Congress on Applied Mechanics, 1st, Delft, 1924, Proceedings, p. 288-294.
———1931, Static rigidity of plastic clays: Journal of Rheology, v. 2, p. 253-262.
Terzaghi, Karl, and Peck, R. B., 1967, Soil mechanics in engineering practice: New York, John Wiley & Sons, 729 p.
Turnbull, R. W., 1976, Engineering geology of the Eden Canyon area near Castro Valley, Alameda County, California: Stanford, Calif., Stanford University, M.S. thesis, 107 p.
Varnes, D. J., 1958, Landslide types and processes, *in* Eckel, E. B., ed., Landslides and engineering practice: Highway Research Board Special Report 29 (National Academy of Sciences-National Research Council Publication 554), p. 20-47.
———1978, Slope movement types and processes, chap. 2 *of* Schuster,

R. L., and Krizek, R. S., eds., Landslides: Analysis and control: U.S. National Academy of Sciences, Transportation Research Board Special Report 176, p. 11-33.

Varnes, H. D., 1949, Landslide problems of southwestern Colorado: U.S. Geological Survey Circular 31, 13 p.

Waldrop, H. A., and Hyden, H. J., 1962, Landslides near Gardiner, Montana, *in* Geological Survey research 1962: U.S. Geological Survey Professional Paper 450-E, p. E11-E14.

Ward, B. H., 1948, A coastal landslip: International Conference on Soil Mechanics and Foundation Engineering, 2d, Rotterdam, 1948, Proceedings, v. 2, p. 33-38.

Weertman, Johannes, 1964, The theory of glacial sliding: Journal of Glaciology, v. 5, no. 39, p. 287-303.

Wilson, I. F., 1943, Geology of the San Benito quadrangle, California: California Journal of Mines and Geology, v. 39, no. 2, p. 183-270.

Yano, K., and Daido, A., 1965, Fundamental study on mud-flow: Kyoto, Japan, Kyoto University, Disaster Prevention Research Institute Bulletin, v. 14, pt. 2, p. 69-83.

Yen, B. C., 1969, Stability of slopes undergoing creep deformation: American Society of Civil Engineers Proceedings, Soil Mechanics and Foundations Division Journal, v. 95, no. SM4, p. 1075-1096.

Záruba, Quido, and Mencl, Vojtěch, 1969, Landslides and their control: Prague, Elsevier, 214 p.

GPO 787-042/112